Biscay Gulf Western Interconnector

Metocean study

FINAL REPORT

ARTELIA Eau & Environnement
Activité MARITIME
6 rue de Lorraine
38130 - Echirolles
Tel. : +33 (0) 4 76 33 40 00
Fax : +33 (0) 4 76 33 43 33

DATE : MARCH 2018 **REF :** 8 71 3734 3

N°8713734 3 - Biscay Gulf Interconnector Project – Metocean study – Final report					
5	Final version	Florence Gandilhon	Sophie Ancel	Sophie Ancel	2018/03/29
4	Inclusion of additional analysis points S08 and S09	Franck Mazas	Sophie Ancel	Sophie Ancel	2018/02/14
3	Inclusion of INELFE comments	Florence Gandilhon	Sophie Ancel	Sophie Ancel	2018/02/07
2	Inclusion of INELFE comments on the hydrodynamic model (mails of the 22th and 26th September 2017) Integration of Properties of the sea water Integration of the wave calibration (Spanish model), water levels/currents exploitation	Florence Gandilhon Delphine Le Bris	Sophie Ancel Delphine Le Bris	Sophie Ancel	2017/11/16
1	Inclusion of INELFE comments on the wave propagation and wind along the French coast Integration of the preliminary results for the hydrodynamic phase	Florence Gandilhon Delphine Le Bris	Sophie Ancel Olivier Bertrand	Sophie Ancel	2017/08/31
0	Dradt report - First submission – Preliminary results - Wave propagation and wind along the French coast	Florence Gandilhon	Franck Mazas		2017/07/20
Version	Description	Redaction	Checked	Approved	Date

TABLE OF CONTENTS

TABLES

FIGURES

EXECUTIVE SUMMARY

The aim of the metocean study is to characterise the metocean conditions (operational and extreme conditions) at various locations along the probable route cable in the Gulf of Biscay.

WAVE MODELLING

Wave generation and propagation has been modelled using the SWAN (Simulating WAves Nearshore) software, a state-of-the-art and 3rd-generation model developed by the University of Delft, the Netherlands.

A set of 5 wave models were set up based on the methodology of "nested models". This number of models is necessary to achieve a suitable spatial resolution according to the bathymetry schemes, along the route cable and near the landfalls areas and the Capbreton canyon while keeping the computation time acceptable.

The nearshore models (canyon and landfalls) are nested to the offshore model: it means that the wave conditions imposed at the boundary of the nearchore model come from the results of the offshore model. At the nearshore boundary points, the wave spectrum are extracted from the offshore model outputs.

For the 2 offshore models, the forcing data come from the HOMERE wave database developed by Ifremer and which provides 2D wave spectrum, wind and water level from 1994 to 2012. The 3 nearshore models are nested to the offshore model: it means the wave boundary conditions are the output of one of the offshore model.

The French offshore model has been calibrated by comparison with a wave buoy located south of the Capbreton canyon.

The Spanish offshore model has been calibrated by comparison with 2 wave buoys located offshore Bilbao ("Vizcaya" buoy – 600m water depth) and nearshore Bilbao ("Bialbao" buoy).

The modelling period spans 19 years from 1 January 1994 to 31 December 2012. The results are analysed:

- at 7 points along the probable cable route (French side), in the nearshore area, on both sides of the canyon (points L03, N02, N05, N07, S04, S05, S06);
- at 4 points along the probable cable route (Spain side), offshore and in the nearshore area (points L11, Sp01, Sp02 and Sp03).

For each analysis point, operational statistics have been realised for key wave parameters (H_s,T_p, Dir_p):

- the **annual and monthly wave climate** files are directly provided in the Excel format;
- annual and monthly **wave roses**;
- some **colour maps** of the wave propagation are also proposed for specific dates;
- the **extreme wave analysis**.

The following conclusions have been drawn from the analyses along the **French coastline**:

- as regards the climate **offshore** (points L03, N02), the wave direction is mainly West/North-West for every month. The highest waves occur during the winter season (December to February) with H_s higher than 3 m more than 10 % of the time. It corresponds to long period waves (T_p > 12 s). During the summer season (May to September), the waves remain lower than 3 m most of the time and the periods are shorter.

The exceedance frequency of H_s and T_p confirms this. During the winter, the wave height H_s is mainly between 1.5 and 3 m (about 60% of the time for example in January) and is higher than 3 m (more than 25% of the time in January); the wave period exceeds 12 s. When the summer season approaches, the H_s and the T_p tends to decrease to reach the most frequent values between 0.5 and 1.5 m and 8 to 10 s.

- It is worth noting that the wave direction at the offshore point N02 in front of the landfall is oriented slightly more often from the West than at the point L03 located at the south of the landfall.
- In front of the French **landfalls** (points N02, N05, N07) the main directions are West/West-North-West with a narrower spread around the main direction near the coastline (point N05) due to refraction. Regarding the seasonal variation, the wave climates variability is consistent with the offshore one; the highest H_s and the longest periods (12-14 s) appear frequently during winter months whereas the summer season sees waves with lower H_s (0.5 to 1.5 m) and shorter period.
- The **canyon** has an important effect on wave propagation through the phenomena of **reflection** and **refraction**. Waves approaching the canyon obliquely (mainly from the north-west) will tend to be reflected on the northern side of the canyon because the depth stops decreasing and suddenly increases again. The longer the period is, the more important the effect on wave propagation is. This creates **areas of over-agitation north of the canyon** and **areas of under-agitation south of the canyon**.

  North of the canyon (point S09), the waves come from the West-North-West sector. During winter and spring, the main direction is N280° whereas the second direction N300° appears during summer and autumn.

  Closer to the coastline (point S04), the wave climate is mainly westerly from November to April. Then, the direction turns slightly and the waves come from the West-North-West sector. The values of H_s and T_p evolve depending on the season; they are consistent with those offshore .

  What is interesting to note is that the reflection of wave conditions with wave periods larger than ~10 - 12 s against the canyon leads to :

  - The more westerly incidence direction at point S04 compared to S09
  - Over-agitation at point S04 with respect to point S09 “until it breaks” as S04 is in shallower water than S09

  At the head of the canyon (point S06), the waves are clearly directed by the canyon shape with a narrow rose around the direction N280°/N290° and the wave propagation is attenuated especially in winter with H_s lower than 3.5 m all the time.

  South of the canyon (point S08, by -20 m MSL), the waves are still centered around the direction N300°/N310°.

  Closer to the coastline (point S05), the influence of the canyon on the wave propagation appears(reflection and refraction phenomena) with no waves coming from [280-300] . Hence, on the contrary of the previous points, the waves come clearly from 2 different directions: the West and the North-West (especially in summer).

  We can note that due to reflection/refraction phenomena, wave periods at S05 are shifted to longer periods with respect to S08.
- The wave height decreases as one gets closer to the coast. The wave direction changes slightly to be perpendicular near the coastline. As the wave comes from the W-NW sector most of the time, the north part of the canyon is the most exposed.
- Offshore (point L03), the 1-year significant wave height H_{m0} reaches 7 m and the 100-year significant wave height H_{m0} reaches 13.5 m with a large confidence interval (between 10.42 m at the lower bound of the interval and 17.9 m at the upper bound of the interval).

Obviously, the extreme sea states are lower near the coastline (point N05 – landfall area) where the values of the 1-year significant wave height (5.58 m) and the 100-year significant wave height (6.37 m) are closer because of wave refraction and depth-induced breaking.

South of the canyon (points S05 and S08), the extreme sea states evolve between 4.03 m and 6.98 m depending on the return period (1 to 100 years); it is lower than the values at the north of the canyon (point S04 and especially point S09 where the values are the highest of the canyon, between 7.21 and 13.08 m). At the head of the canyon (point S06), the extreme values are the lowest with 3.61 m for the 1-year significant wave height H_{m0} and 5.43 m for the 100-year significant wave height..

Along the **Spanish coast**, the analyses lead to the following conclusions:

- as regards the climate **offshore** (points L11), the wave direction is mainly North-West for every month. The highest waves occur during the winter season (November to March) with H_s higher than 3 m more than 12 % of the time. During the winter, the wave height H_s is mainly between 1.5 and 3 m (about 63% of the time for example in January). It corresponds to long period waves (T_p > 10 s). When the summer season approaches, the H_s and the T_p tends to decrease to reach the most frequent values between 0.5 and 1.5 m and 8 to 10 s. During the summer season (May to September), the waves remain lower than 3 m most of the time and the periods are shorter.
- In front of the **landfall** (points Sp02, Sp03), the wave climates are consistent with the offshore climate. The main directions are North-West with a narrower spread around the main direction near the coastline. Near the coastline (point Sp01), the direction change due to refraction, the wave come mainly from the North. The highest H_s (> 3 m) and the longest periods (12-18 s) appear frequently during winter months whereas the summer season sees waves with lower H_s (0.5 to 1.5 m) and shorter period.
- At the offshore, the 1-year significant wave height H_{m0} reaches 6.67 m and the 100-year significant wave height H_{m0} reaches 12.65 m with a large confidence interval (between 10.04 m at the lower bound of the interval and 16.18 m at the upper bound of the interval). The extreme values are less important than on the French side.
- Near the coastline, the 1-year significant wave heights are in the same order of magnitude (6.24 m at point Sp01 to 6.66 m at point Sp02). The 100-year significant wave heights are also consistent for the points Sp02 and Sp03 (12.

WIND

For each analysis points, operational statistics have been assessed for key wind parameters (W_s, W_{dir}):

- annual wave roses;
- correlogramm wind speed/wind direction;
- exceedance frequency plots of W_S.

The wind roses are quite spread along the French and Spanish coast; all the wind directions appear at least 4% of the time. However the direction North-West is slightly more present (around 5% / 6%) along the Spanish coastline.

More than 50% of the time, the wind speed varies between 3 and 7 m/s in front of the French and Spanish landfalls and offshore. At the point near the canyon, which is closer to the coast, the wind speed is mainly between 1 and 5 m/s.

HYDRODYNAMIC

The hydrodynamic model was developed on the basis of the software TELEMAC-2D, part of TELEMAC-MASCARET system, owned by EDF R&D and developed by a consortium of core organisations. The model provides water level and depth-averaged currents.

A single model was built. It is large enough to represent the proposed cable route, the landing areas and the CapBreton canyon. Its characteristic dimensions are more than 200 km northward and about 180 km westward.

The forcing data consist of tide, wind and atmosphere pressure. Daily global oceanic currents have been added to improve the quality of the results.

The model was calibrated by comparison with 3 tide gauges (Arcachon, Saint Jean de Luz, Bilbao) and nautical SHOM charts at the scale of the Biscay Gulf. The model is good and consistent with measured water levels and tidal currents.

The **extreme sea levels** are consistent along the probable cable route:

- between 2.46 and 2.52 m for the 1-year return period and 2.71 to 2.79 m for the 100-year return period along the French coast;
- around 2.42 m for the 1-year return period and 2.66 m for the 100-year return period along the spanish coast.

The conclusions about the extreme surges are similar with values slighly higher in front of the Lacanau landfall and offshore French coastline than around the canyon or along the Spanish coastline.

For each analysis point, the **currents** have been studied 1 m below the surface and 1 m above the seabed using a power law applied to the 2D-averaged velocity (Lewis Law - α=7, β = 0.32).

All the analyses lead to the followings remarks:

- Except in front of the Lacanau landfall, the tidal currents remain weak and the residual current generated by the wind, the atmospheric pressure and the broad-scale circulation patterns are predominant;
- **Offshore the French coast**, the total near surface currents does not exceed 0.3 m/s. Most of the time the total current remains lower than 0.15 m/s and the current directions are variable;
- In front of the **French landfall**, the influence of the tide is more visible with tidal current intensities higher than 0.15 m/s and total currents intensities higher than 0.35 m/s near surface. Offshore, the 2 main directions are North-north-east and South-south-west both near surface and sea bottom. As we approach the coastline, the main direction slightly changes to become North/South for the 2 studied depths.
- Around the **canyon**, the total directions are directed alternately towards North and South for the 3 studied points. The total current is less important at the head of the canyon than on both sides of the canyon. The flow coming from the west is deviated by the canyon features towards the south thus the total current is stronger in the south part of the canyon where it can be higher than 0.35 m/s.
- **Offshore the Spanish coast** the tidal currents are weak (less than 0.05 m/s near surface and less than 0.04 m/s above the seabed). Below the surface, the total currents remains higher than 0.3 m/s only 1% of the time. The main current direction is towards the South-East and less frequently towards the North-West.
- In front of the **Spain landfall**, offshore, the total direction (below surface and at 1m above the sea bed) is mainly directed towards the East. As one approaches the coast, the direction alternates between East-South-East and West-North-West. The intensity remains lower than 0.3 m/s near the seabed and can exceed 0.35 m/s punctually near the surface. The main part of the signal is due to residual currents.

PROPERTIES OF THE SEA WATER: TEMPERATURE AND SALINITY

The properties of the sea water are characterised by the sea temperature and salinity.

The sea temperature and the salinity values come from the global re-analyze GLORYS2V3 which provides 3D daily mean mean fields of temperature and salinity.

The sea temperature and salinity values are extracted at 5 locations along the possible cable route from 1993 to 2014:

- One point along the cable, about 10 km in front of the French landfall area (point TS01);
- One point along the cable between the French landfall area and the Capbreton canyon, 10 km offshore (point TS02);
- One point in the canyon area (point TS03);
- One point along the cable, about 10 km offshore from the Spanish coast (point TS04);
- One point along the cable, about 5 km in front of the Spanish landfall area (point TS05).

The **mean temperature** is quite homogeneous along the possible cable route (maximum of 1°C of difference between the points near the surface and 0.5°C at -36 m). Close to the surface, the mean temperature varies between 15.8°C (Point TS01 – French landfall) and 16.7°C (Point TS05 – Spanish landfall) whereas they are around 14°C at -36 m MSL;

The **minimum temperatures** are globally higher along the Spanish coast than along the French coast. Near the surface, they vary between 8.4°C (TS01 - French landfall) and 11.2°C (TS04 – Spanish cable route). The temperature profile remains homogeneous along the water column at point TS03 (10.5 / 11°C - canyon), TS04 (≈11 / 11.2°C – Spanish route) and TS05 (10.5 / 11.5 °C - Spanish landfall).

The **maximum temperature** profiles are heterogeneous for each point with a decrease of the temperature with the depth and a gap of more than 7°C between the surface and the bottom. Close to the surface, the maximum temperature evolves between 25.7°C (Point TS04 – Spanish route) and 26.8°C (Point TS03 - canyon) whereas they are between 19.8°C (TS02) and 21.7°C (TS04) at -36 m MSL.

The temperatures appear cooler along the French coast than along the Spanich coast.

The impact of the seasons appears in the **mean temperature** profiles for each point along the probable cable route:

- From November to February (winter), the temperature profiles are homogeneous throughout the water column with colder water in the bottom layers.
- From April (spring season), the temperature profile begins to change with an increase ot the near surface temperature; the top layers become warmer than those of the bottom. This trend increases until August. A strong vertical thermocline (layer of temperature gradient) is observed during this period.
- In September and October, the temperature becomes uniform on the top layers.

This trend appears also in the maximum and minimum profiles.

A decrease of the **minimum and mean salinity** in the upper layers of the water column (halocline) clearly appears for the point TS01 located between the Gironde estuary and the Bassin d'Arcachon and the point TS02 near the Bassin d'Arcachon. It is worth noting that the Gironde estuary and various rivers coming out in the bassin d'Arcachon can bring freshwater.

Close to the surface, the **mean salinity** varies between 33 (Point TS01) and 35.1 (Point TS04) whereas they are between 35.2 (TS01) and 35.4 (TS05) at -36 m MSL;

The **maximum salinity** profiles are homogeneous throughout the water column for each point and do not exceed 35.8;

The salinity appears higher along the Spanish coast (TS04 and TS05) where it is less affected by the fresh water influx, and where the water depth is deeper.

The water column can be divided into 2 parts: the top layers (mixing layer) where the **mean salinity** varies seasonally and the bottom layers where the mean salinity profiles remain consistent over time. The boundary between the two layers is located at -15m MSL. This trend is clearly evident along the French coast (points TS01, TS02) but is less visible along the Spanish coast (points TS04, TS05).

The impact of the seasons on **mean salinity** is particularly apparent along the French coast (Points TS01, TS02) due to freshwater inlfux:

- From September to January (autumn and beginning of winter), the mean salinity profiles are slightly heterogeneous throughout the water column with values between 33.7 and 34.5 near the surface and 35 to 35.1 in the bottom (-36 m MSL);
- From March to July (spring and beginning of the summer), the mean salinity profiles are impacted by a strong decrease of salinity in the surface layers (from the surface to around 10 m depth – presence of halocline). This decrease reaches 31.5 in May and July whereas near the bottom the values of salinity are around 35.1 / 35.2;
- February and August appear as “intermediate” months.

Near the canyon (point TS03), the behaviour of the mean salinity is different. The impact of the seasons is less clear and the profiles less contrasted according to the month:

- From November to February (winter), the profiles are homogeneous throughout the water column (35.1 to 35.2);
- From April to September, the decrease of salinity near the bottom appears (34 to 34.4) but it is less important than at point TS01 and TS02 whereas the bottom values remains similar to the other profiles;
- March and October are “intermediate” months.

oOo

DEFINITIONS, ABREVIATIONS AND NOTATIONS

MSL	Mean Sea Level
T_p	Peak wave period $T_p = 1/f_p$: the peak frequency is the frequency of the maximum value (peak) of the spectrum
Spectral Significant wave heigh H_{m0}, also referred to as H_s	Spectral definition - wave height derived from wave energy spectrum $= 4\sqrt{m_0}$, with m_0 the zeroth moment of the spectrum.
Wave Mean Direction	Propagation mean direction of the wave system. Direction FROM WHICH waves come

1. PURPOSE OF THE STUDY AND OBJECTIVES OF THE METOCEAN STUDIES

1.1. CONTEXT OF THE STUDY

RTE launched a consultation about metocean and hydrosedimentary studies in the frame of various projects concerning the interconnectors for the electricity supply (laying and protection of the submarine cables).

INELFE, a consortium between RTE and REE (Red de Eléctrica de España, its Spanish counterpart), has awarded ARTELIA for the studies of the Biscay Gulf Western Interconnector (BGWI) project (Figure 1).

Figure 1. Route of the interconnector

The length of the marine cable is approximately 280 km (180 km in French waters and 100 km in Spanish waters). The cable route is located between 10 and 20 km offshore from the coast, except at the landfalls and the Capbreton canyon crossing. The possible route position corresponding to the routes surveyed in 2016 is provided in APPENDIX 1.

The metocean and hydrosedimentary studies aim to:

- give input to define the best position of the cable (route and burying depth within de pre-defined corridor);
- optimise the laying of the cable (schedule, Weather Down Time to go on site…);
- inform the requirement for cable protection.

The present report deals with the metocean study. It describes the methodology used, the models developed and the results of the metocean study.

1.2. OBJECTIVES OF THE METOCEAN STUDY

The aim of the metocean study is to provide the metocean conditions (operational and extreme conditions) at various locations along the probable route cable. These conditions consist of:

- waves;
- wind;
- water levels;
- currents;
- physic-chemical parameters (i.e sea water temperature and salinity).

The present report describes the methodology used, the models developed and the results of the metocean study (wave propagation along the French coast).

oOo

2. DIGITAL ELEVATION MODEL

2.1. SYSTEM OF COORDINATES AND ALTIMETRIC REFERENCE

The geographic coordinates are referred to the following system: WGS84 UTM30 North.

Because of the large extent of the models, altimetry is defined relative to the Mean Sea Level (MSL).

2.2. BATHYMETRY

A preliminary analysis of the bathymetric data available for the study area has concluded that the following data have to be used to achieve an accurate and reliable Digital Elevation Model:

- SHOM HOMONIM database (100 m resolution);
- Local survey along the route provided by INELFE;
- Bathymetric data from AZTI and available on Basque Country Government website (Ref. [1]). These data consist in isobathic lines each meter.

Figure 2 below presents the final bathymetry which is used on the various models (wave and hydrodynamic) developed in the Bay of Biscay.

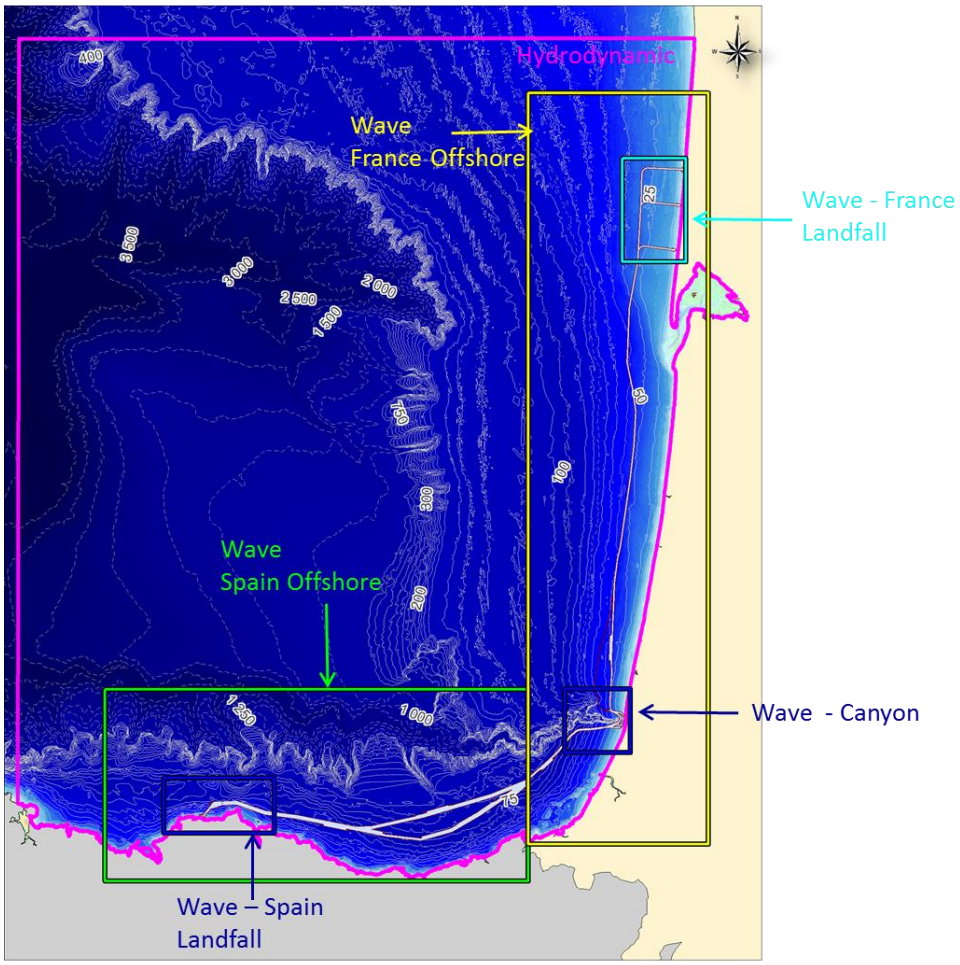

Figure 2. Digital Elevation and model areas on the study area

Along the main part of the French coast, the seabed is gently sloping and the isobathic lines are almost parallel to the coastline from the shore down to the - 200 m line (end of the continental shelf), located about 60 / 65 km offshore. Then, the bathymetry falls abruptly over a few kilometers (10 to 15) down to 800 m / 1000 m deep (continental slope). The seabed then lowers gently (continental rise) from 1000 m down to 3000 m depth where it reaches the ocean floor (abyssal plain).

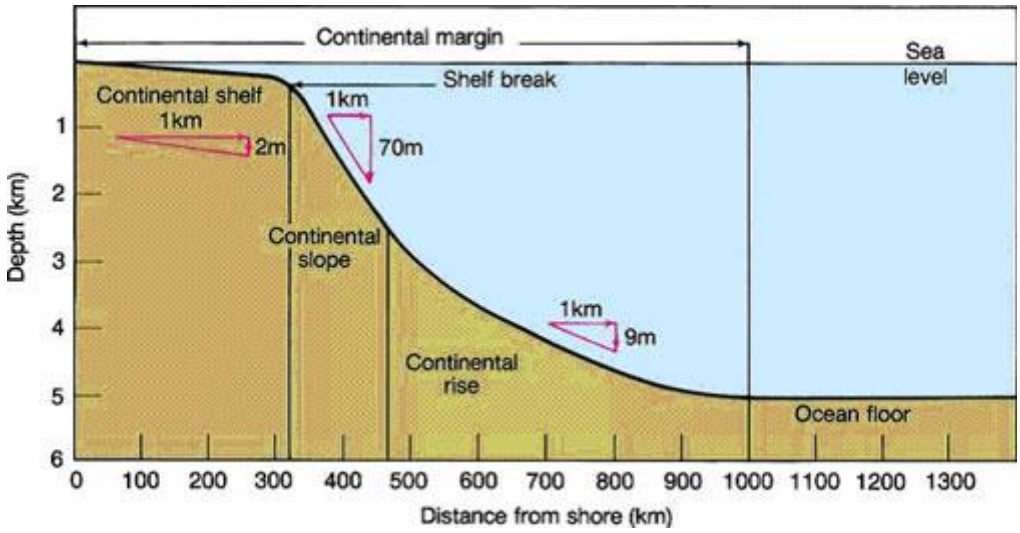

Figure 3. Sketch of the continental margin (Source: Ref. [2])

The Capbreton canyon is the geological feature which appears at the south of the French coast and marks an abrupt end to the regularity of the bathymetry by breaking the shelf up to the shoreline. The head of the canyon is located near the coastline (few hundred meters). The canyon is oriented west / east and extends over almost 300 km to the abyssal plain where it reaches depths around 2500 / 3000 m.

Along the Spanish coast, the continental shelf is narrower (10 to 20 km wide) and marginally shallower (the shelf break is about 150 to 200 m deep). The slope goes directly down to the Capbreton canyon.

oOo

3. WAVE MODELLING AND ANALYSIS

3.1. SOFTWARE

Wave generation and propagation is modelled using the SWAN (Simulating WAves Nearshore) software, a state-of-the-art and 3rd-generation model developed by the University of Delft, the Netherlands. It takes into account the main physical processes involved in the propagation of waves in coastal areas:

- propagation in time and space of the wave spectrum;
- depth-induced refraction;
- bottom friction;
- wave breaking due to depth and wave steepness;
- diffraction, transmission and reflection by obstacles.

3.2. MODEL SETUP

3.2.1. Model areas and computation grids

For this study, the SWAN modelling chain is based on regular grids (finite difference) to reduce the computation times.

A set of 5 wave models has been set up based on the methodology of “nested models”. This number of models is necessary to achieve a suitable spatial resolution according to the bathymetry schemes, along the probable cable route and near the landfalls areas and the Capbreton canyon while keeping the computation time acceptable.

2 offshore models and 3 nearshore models in dedicated areas (canyon, landfall) are built.

These 5 models are presented in Figure 4:

- on the French coast side:
  - an **offshore** model oriented N-S along the French Coast,
  - a **nearshore** model in the **landfall** area nested in the offshore model,
  - a **nearshore** model around the Capbreton **canyon**, nested in the offshore model,
- on the Spanish coast side:
  - an **offshore** model oriented E-W along the Spanish Coast,
  - a **nearshore** model in the **landfall** area nested in the offshore model.

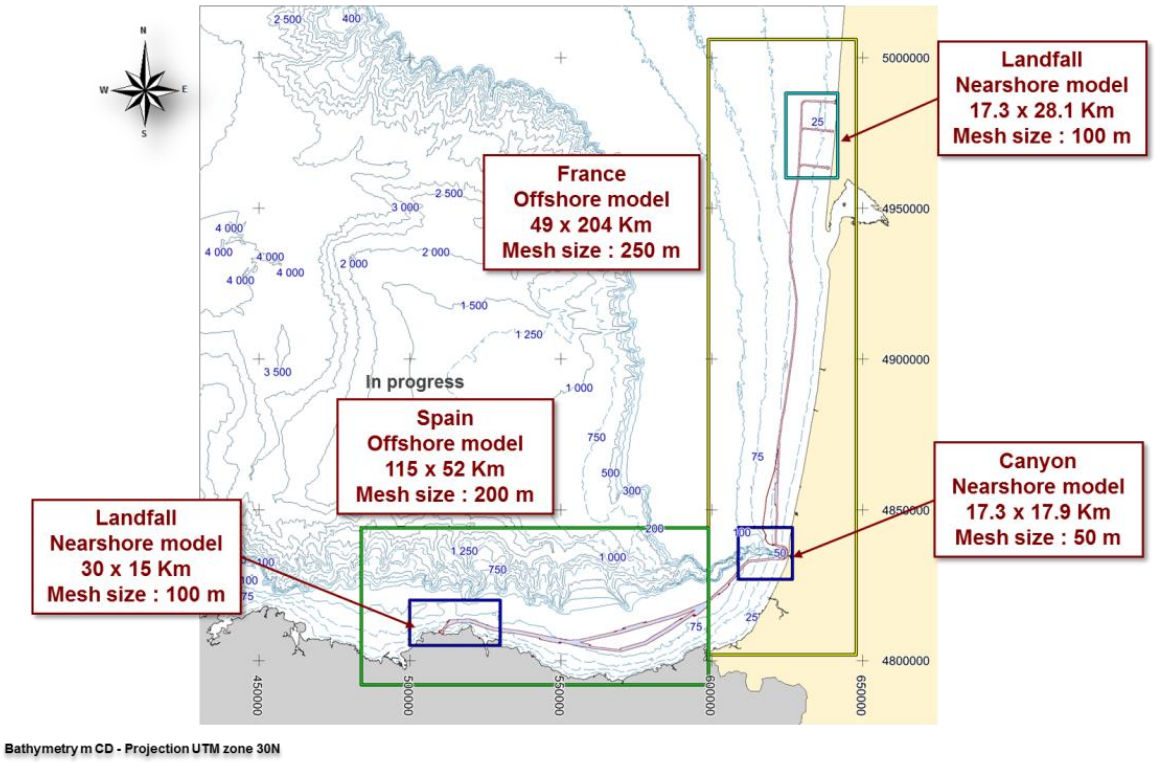

Figure 4. Wave models: areas and mesh size

The mesh sizes have been chosen:

- in relation with the accuracy of the bathymetric data and the width of the cable corridor (see Figure 5 and Figure 6);
- so as to propagate the wave around the probable cable route with enough accuracy;
- so as to have a computation time acceptable.

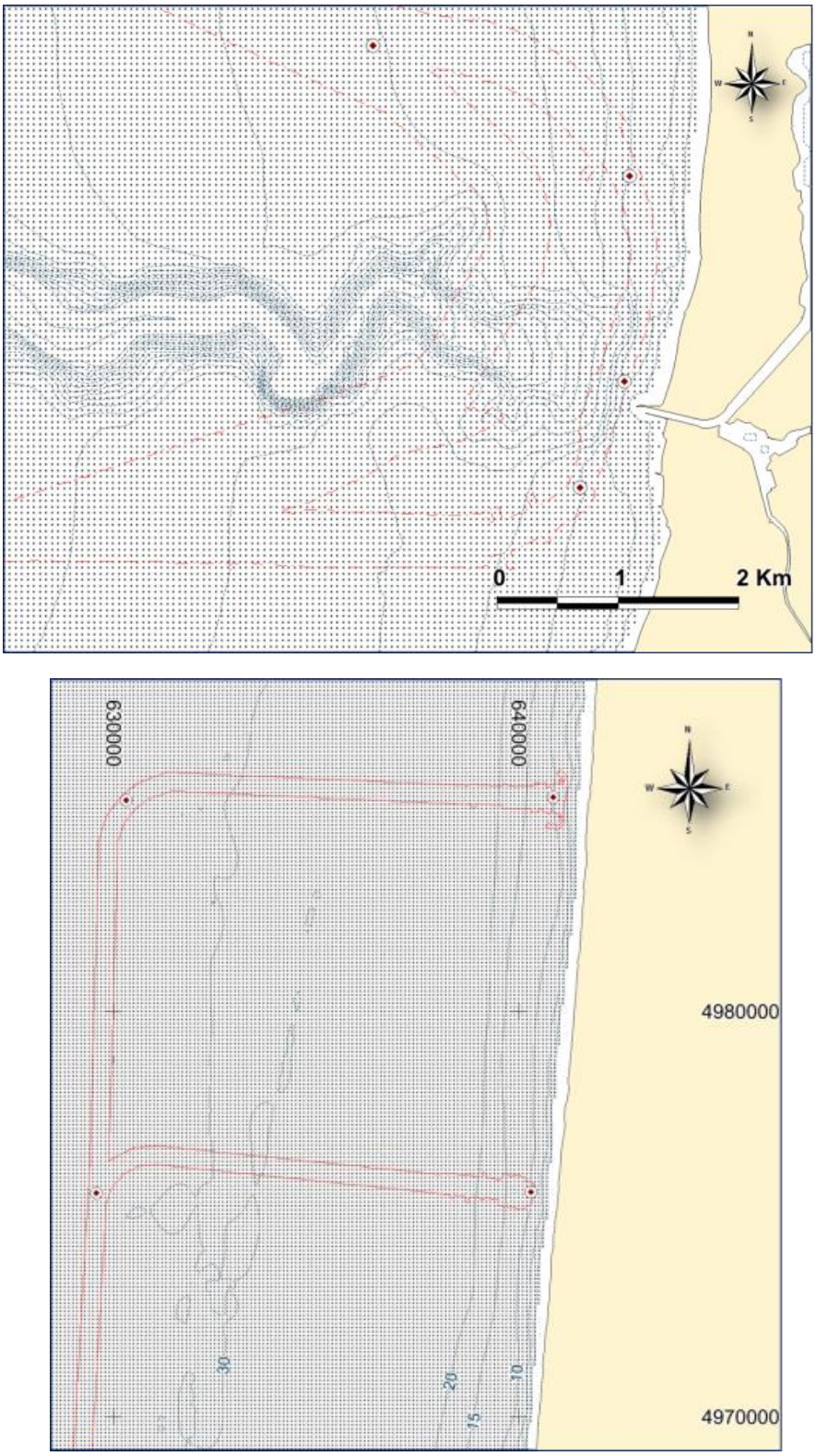

***Figure 5.** Computation grid vs cable and bathymetry (isolines) – French coast*

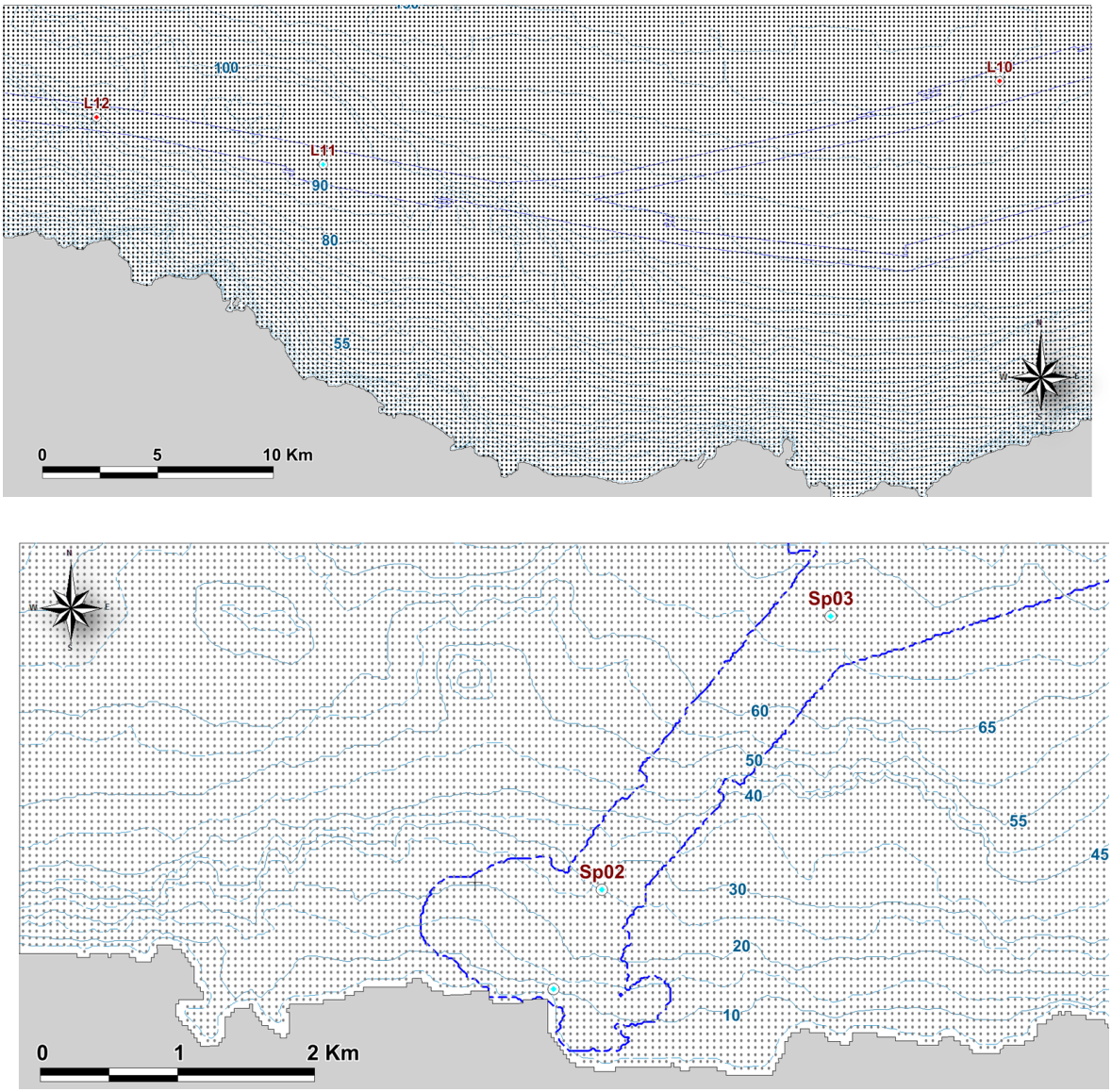

Figure 6. Computation grid vs cable and bathymetry (isolines) – Spanish coast

The mesh sizes are as follows:

- 250 m for the France offshore model;
- 100 m for the nearshore model in the French landfall area;
- 50 m for the nearshore model around the Capbreton canyon;
- 200 m for the offshore model oriented E-W along the Spanish Coast;
- 100 m for the nearshore model in the landfall area.

3.2.2. Forcing data

For the offshore model, the forcing data come from the HOMERE wave database developed by Ifremer and which provides wave data from 1994 to 2012. A detailed description of the HOMERE database is provided in APPENDIX 2.

The 2D wave spectrum has been extracted from HOMERE:

- at 9 points along the boundary of the French coast as shown in Figure 7;
- at 11 points along the boundary of the Spanish coast (Figure 8).

These data are used as boundary conditions along the maritime border. The density of input points is increased around the canyon.

The time evolution of the water level and the wind[1] coming from HOMERE is imposed at each grid point.

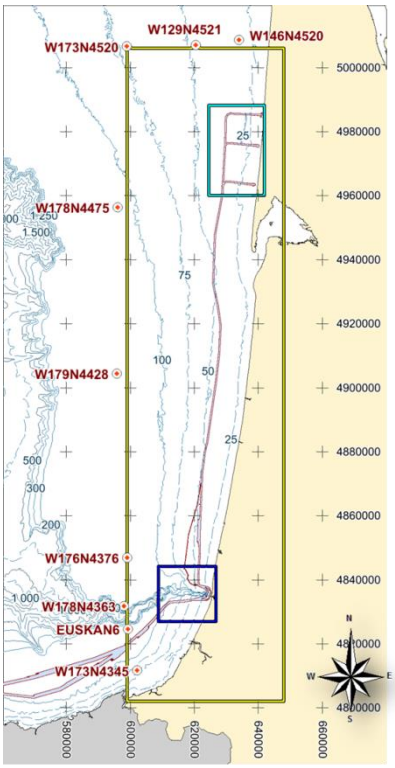

Figure 7. Points of extraction of the wave spectrum (HOMERE database) along the boundary of the French coast

[1] The wind fields in HOMERE come from the CFSR system (Climat Forecast System Reanalysis) developed by the NOAA.

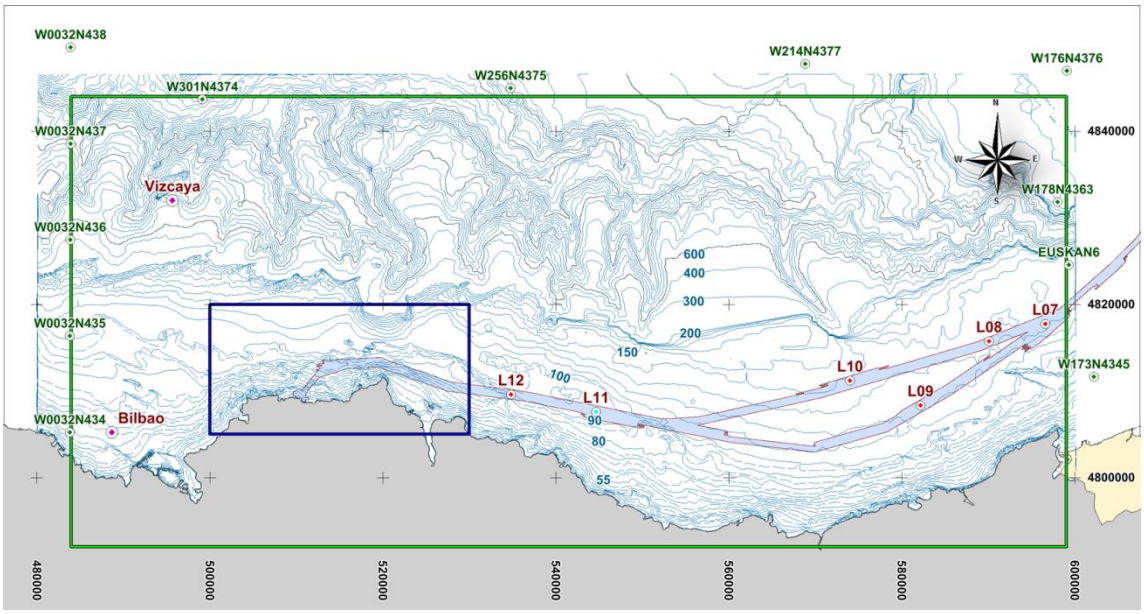

Figure 8. Points of extraction of the wave spectrum (HOMERE database) along the boundary of the French coast

The nearshore models (canyon and landfalls) are nested to the offshore model: it means that the wave conditions imposed at the boundary of the nearchore model come from the results of the offshore model. At the nearshore boundary points, the wave spectrum are extracted from the offshore model outputs.

3.3. MODEL CALIBRATION

3.3.1. French coast

3.3.1.1. Available data for wave calibration

The data available for the calibration of the models consist of the time series of the wave parameters (H_{m0}, T_p, Direction) at two buoys located in the south part of the offshore model (Figure 9). These buoys are part of the CANDHIS network run by the CEREMA (previously CETMEF - French Government).

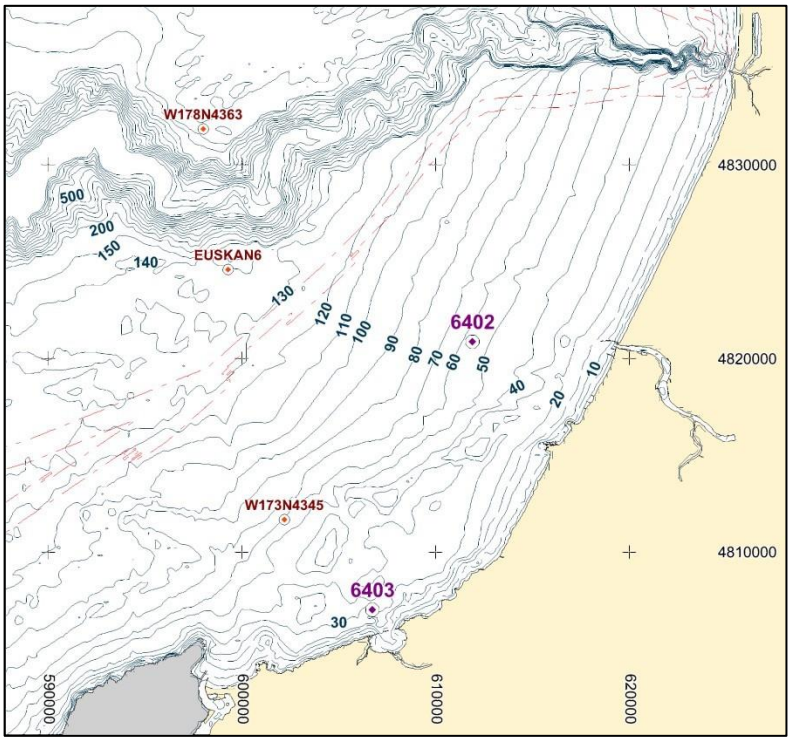

Figure 9. Location of the wave buoys CANDHIS 6402 and 6403

The buoy “6403” started to record data only from April 2013. The measurement cannot be used for the calibration because the forcing data from HOMERE stop at the end of 2012.

The buoy “6402” located at about 50 m depth is used for the calibration step. The measurements are available from 24 November 2009.

3.3.1.2. Comparison SWAN model / Wave buoy

The wave offshore model has been calibrated by comparison with the buoy within a period of 2 months (December 2011 – January 2012) . This period has been chosen as it includes both calm periods and important storm events. Then, the model has been validated from December 2009 to December 2012 (the common period between the model and the measurements).

The results of the model are compared with the buoy data in terms of H_{m0}, T_p and Mean Direction fof the calibration period. The comparisons are presented on the next Figure 10, Figure 11 and Figure 12.

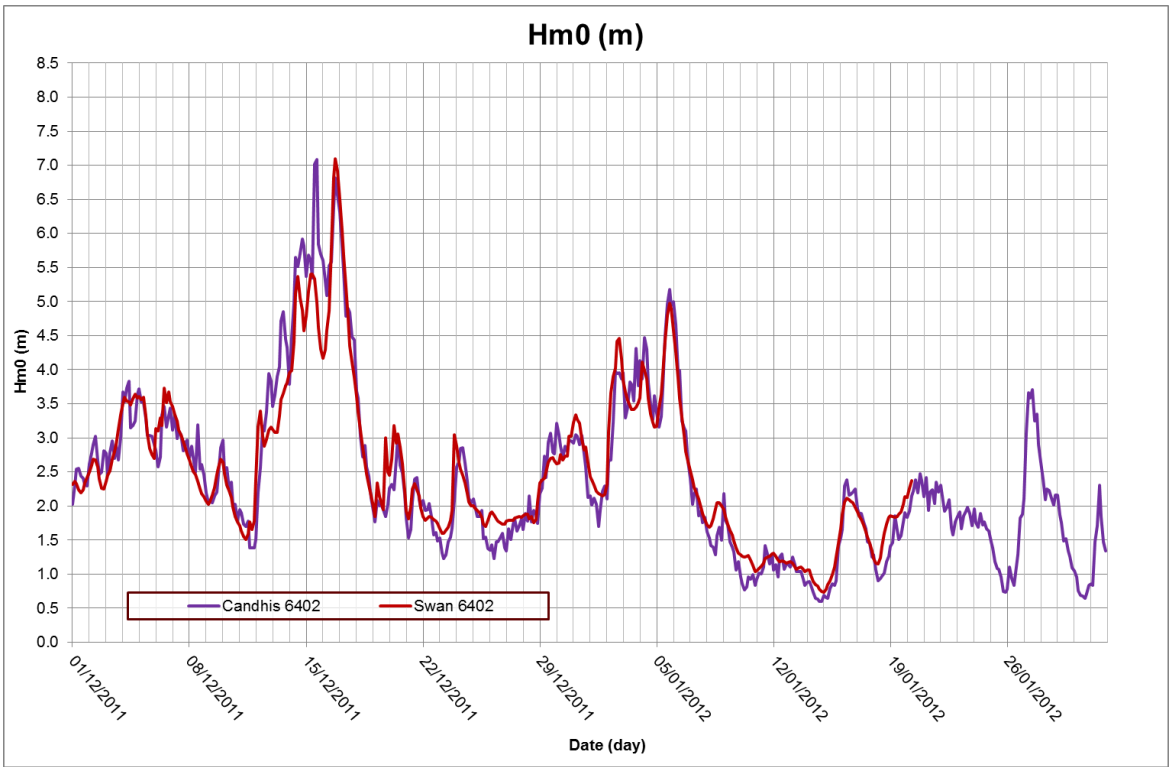

Figure 10. Comparison wave model / Buoy – H_{m0}

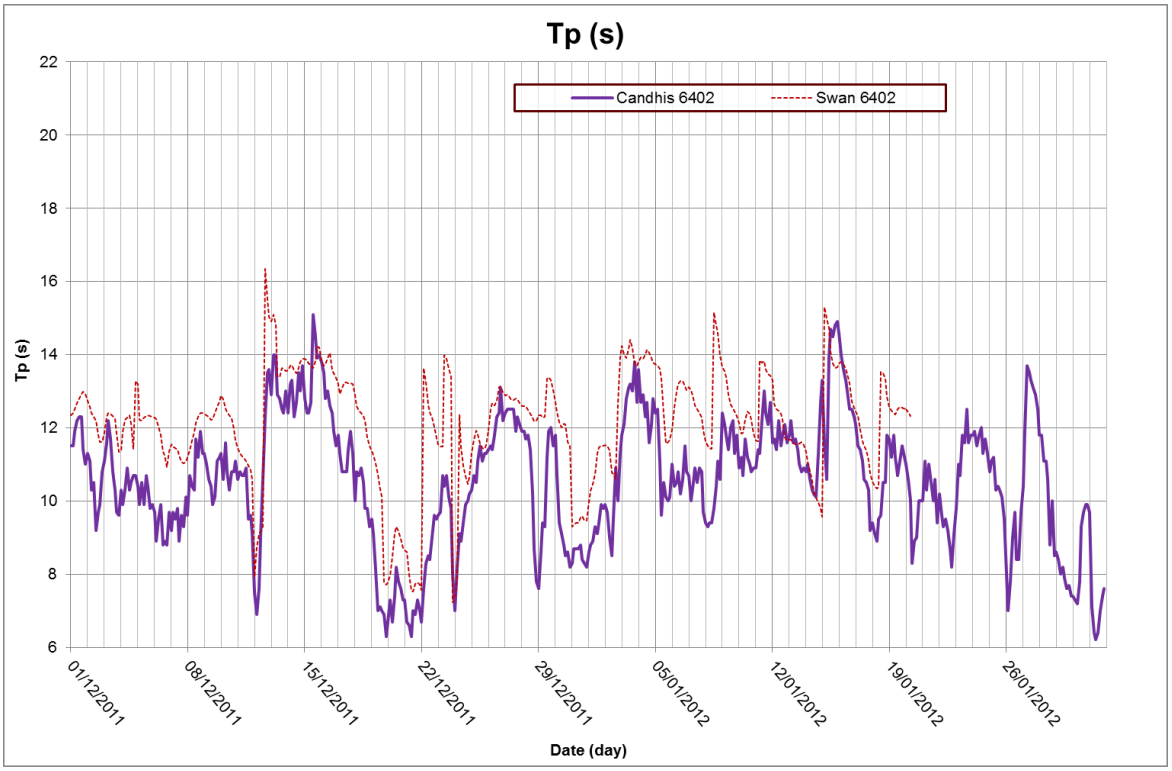

Figure 11. Comparison wave model / Buoy – T_p

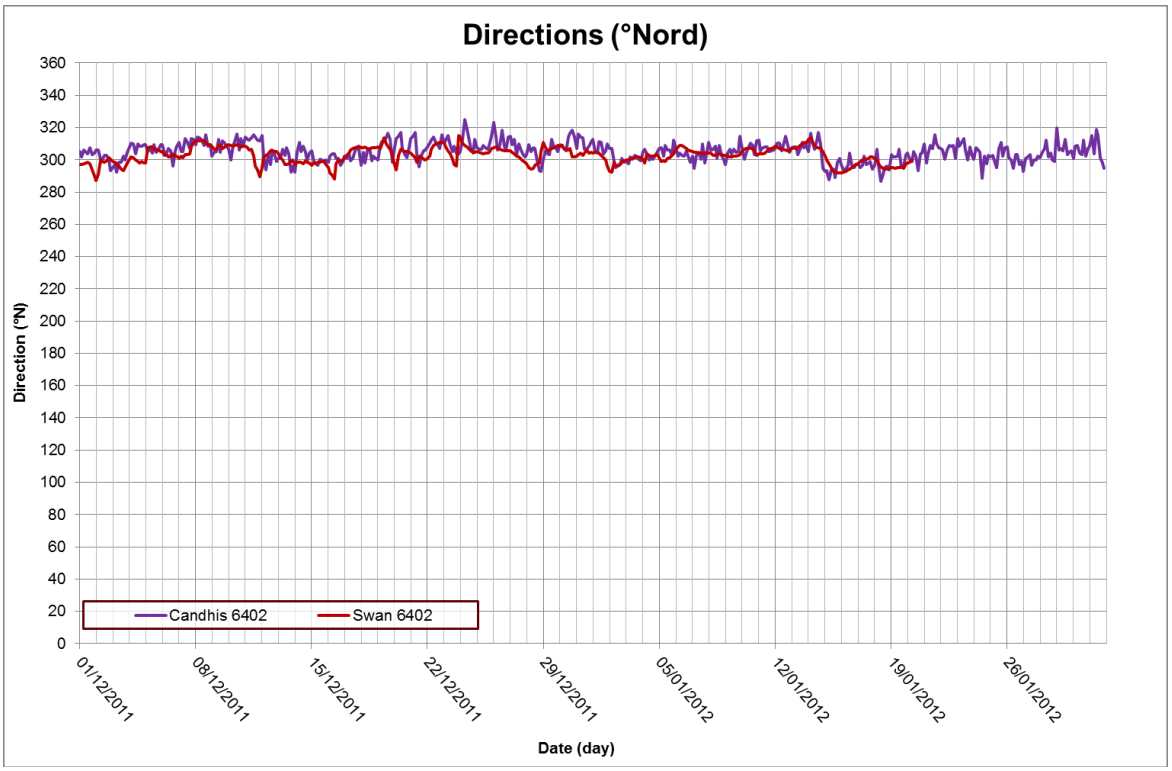

Figure 12. Comparison wave model / Buoy – Direction

The model results are consistent with the buoy measurements for all parameters.

An under-estimation of the first storm peak of December 15th, 2011 is observed but all other events are well represented. After checking the boundary conditions of the wave model, it appears that HOMERE database does not reproduce the storm peak of December 15th as strong as the one of December 16th. Thus, the wave model which is consistent with the offshore boundary conditions (HOMERE) cannot reproduce this event.

As shown in Figure 13, the wave directions modeled are consistent with data. All the directions measured (North-West and West-North-West) are reproduced by the model.

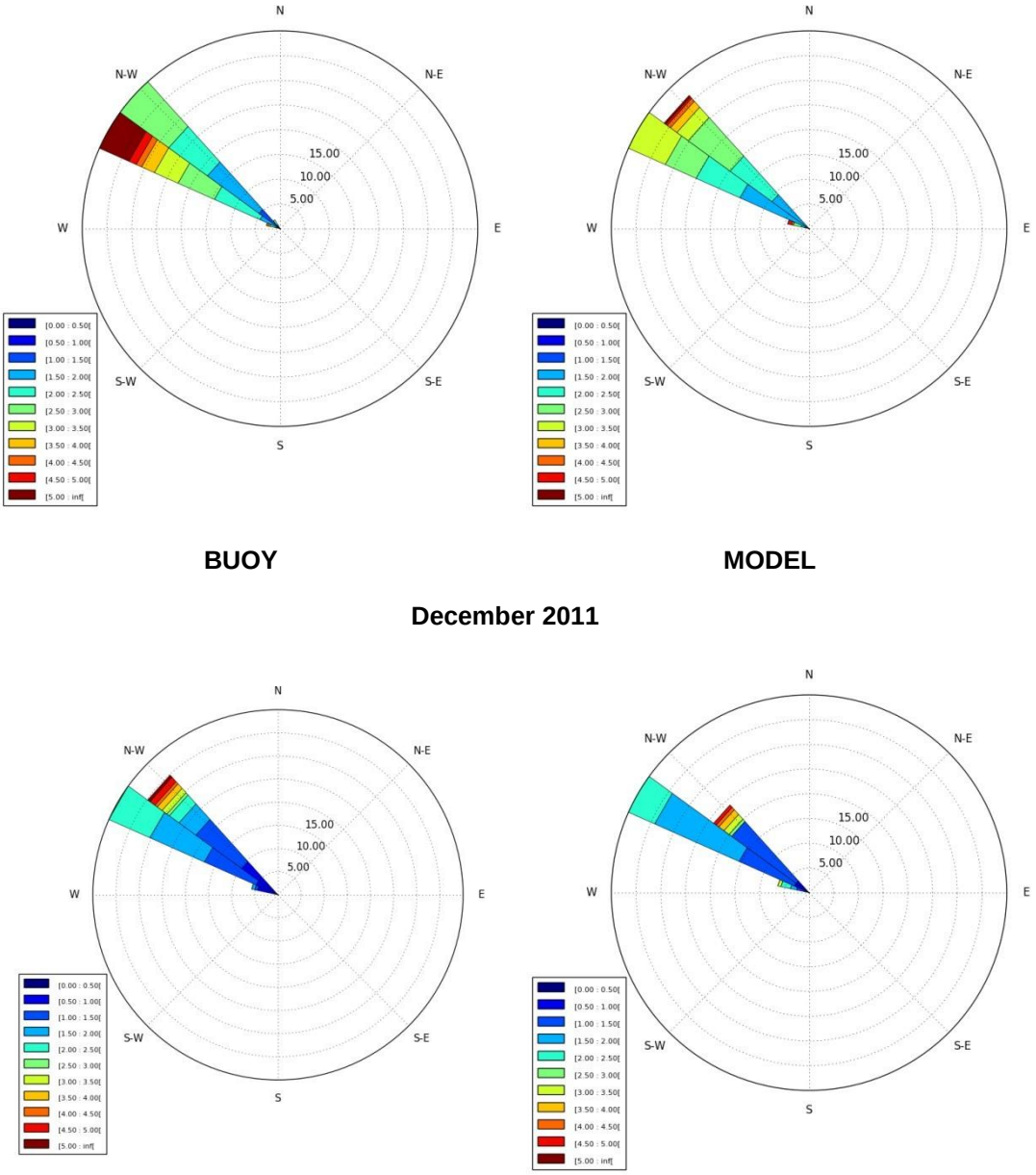

Figure 13. Wave rose: Model vs Buoy

The calibration is completed by a statistic analysis on the H_{m0} value. The definitions related to statiscal variables studied are given in the next Table 1.

The results described in Table 2 confirm the good behaviour of the model by comparison with the buoy. The standard deviation and RMSE values are 10 cm. Error remains lower than 20 cm during more than 90% of time and lower than 10 cm during around 80% of time which is acceptable.

Table 1 - Definition of statistical variables

Variables	Definition
Standard deviation	$SD = \sqrt{\frac{1}{N-1}\sum_{i=1}^{N}(e_i - \bar{e})^2}$
RMSE	Root-mean-square error $= \sqrt{\frac{1}{N}\sum_{i=1}^{N} e_i^2}$
CF(X)	Part (percentage) of error included in the interval $[-X; X]$

In our case, the variables are calculated for X is equal to 0.10 m and 0.20 m.

Table 2 - Statistical analysis – H_{m0}

X (m)	0.10	0.20
Standard deviation	0.10	0.10
RMSE (m)	0.10	0.10
CF(X) (%)	79	92

The next Figure 14 presents the validation of the model by comparison of the buoy from December 2009 to December 2012. The upper graph shows the Quantile-Quantile Plot (Q-Q plot) taking into account the entire time serie modelled. As noted previously, the highest wave heights (> 7 m) are underestimated by the model because of the underestimation of the HOMERE database (see APPENDIX 2). An accurate analyse lays in stress the fact that 2 storms are badly represented: the storms of the 9th of November 2010 and the 15th of December 2011. The lower graph shows the Q-Q Plot obtained once these 2 storms removed from the time series. The wave model is consistent with the buoy over the entire period available (December 2009 – December 2012).

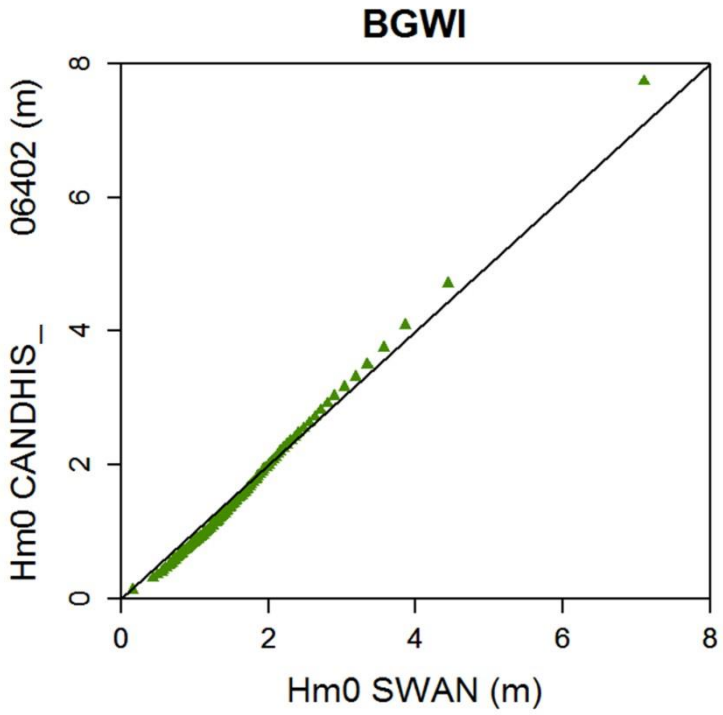

Complete Time serie

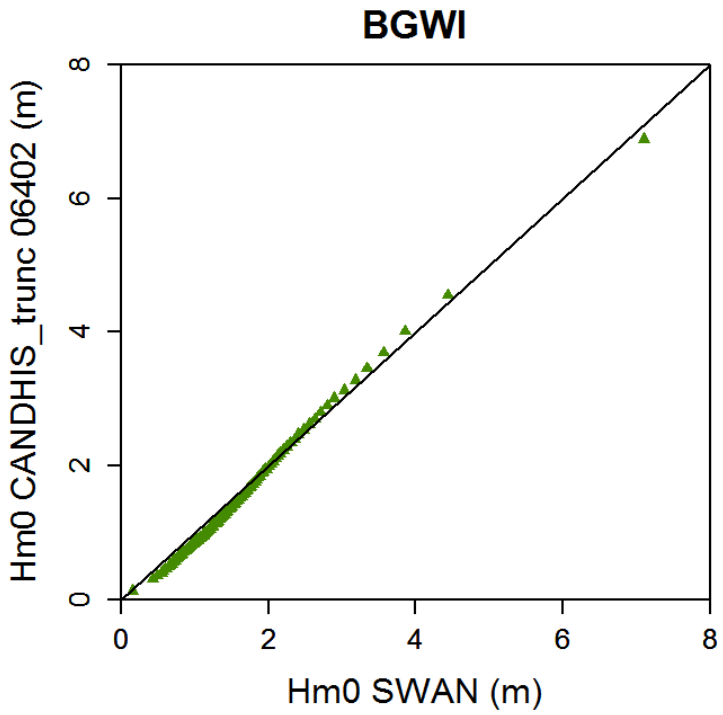

Truncated time serie (2 storms have been removed)

Figure 14. Q-Q PLOT : Model vs Buoy (December 2009 – December 2012)

In conclusion, the model is able to reproduce the wave propagation and is used to reproduce the wave propagation during 19 years in the next step of the study.

3.3.2. Spanish coast

3.3.2.1. Available data for wave calibration

The data available for the calibration of the models consist of the time series of the wave parameters (H_{m0}, T_p, Direction) at two buoys located in the west part of the offshore model (Figure 9). These buoys have been purchased from Puertos Del Estados.

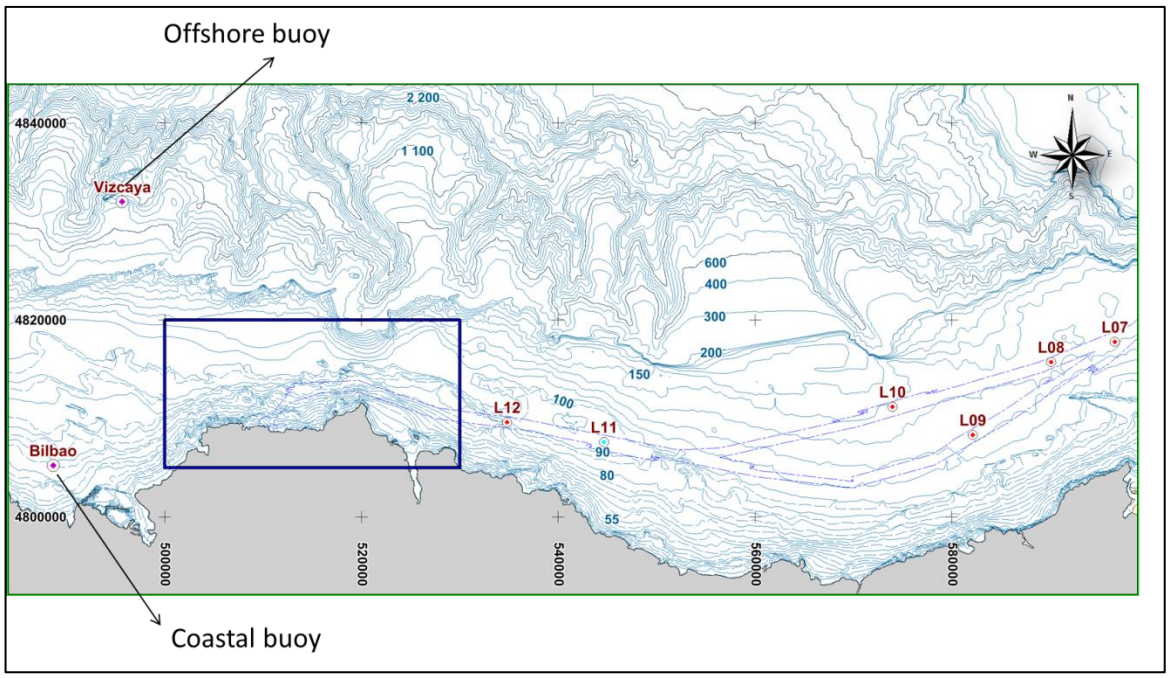

Figure 15. Location of the wave buoys Vizcaya and Bilbao

The buoy "Vizcaya" is located around 30 km offshore Bilbao by 600m water depth. The records available started from 1990 but some data are missing especially for the wave direction.

The buoy "Bilbao" is a coastal buoy (around 5 km from the coastline). The records available started from 1987 until November 2013. This buoy doesn't provide wave direction values.

3.3.2.2. Comparison SWAN model / Wave buoy

The wave offshore model has been calibrated by comparison with the buoy within a period of 2 months (February – March 2008) . This period has been chosen as it includes both calm periods and important storm events. Then, the model has been validated over the 19 years of analyse.

The results of the model are compared with the buoy data in terms of H_{m0}, T_p (and Mean Direction) for the calibration period. The comparisons are presented on the next Figure 16, Figure 17 and Figure 18 for the Vizcaya Buoy and on the Figure 19 and Figure 20 for the Bilbao Buoy.

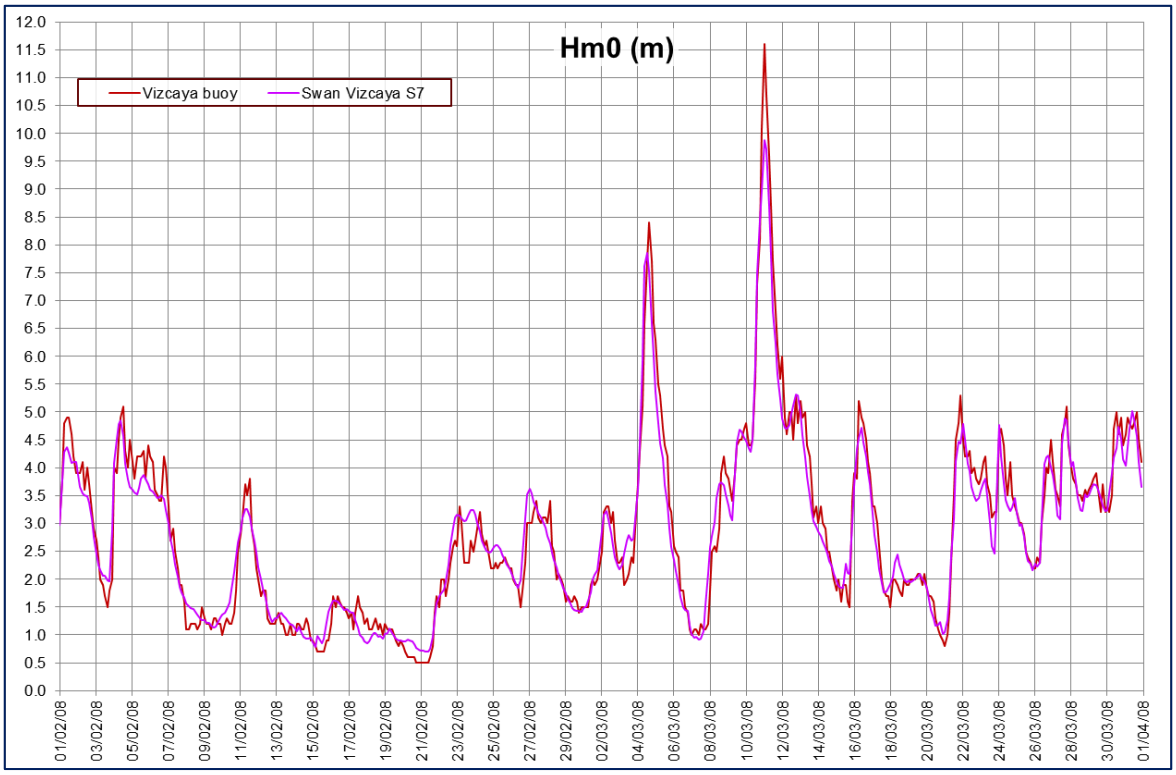

Figure 16. Comparison wave model / Vizcaya Buoy – H_{m0}

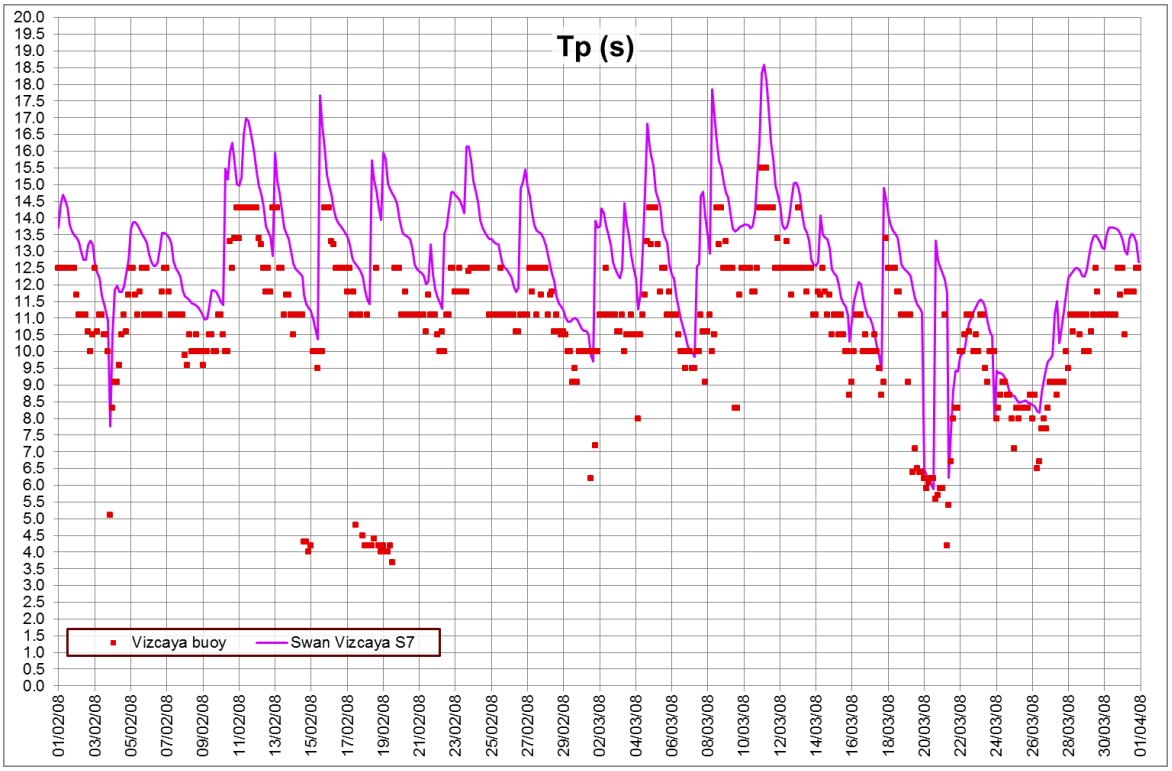

Figure 17. Comparison wave model / Vizcaya Buoy – T_p

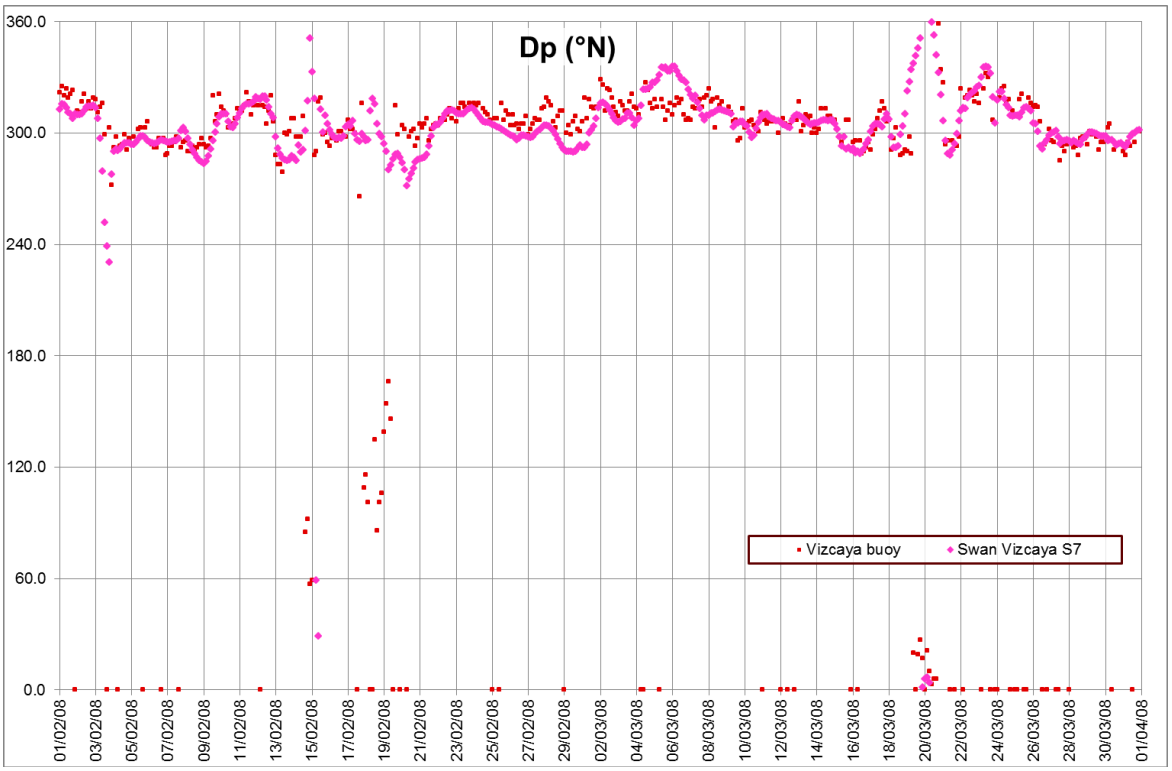

Figure 18. Comparison wave model / Vizcaya Buoy – Direction

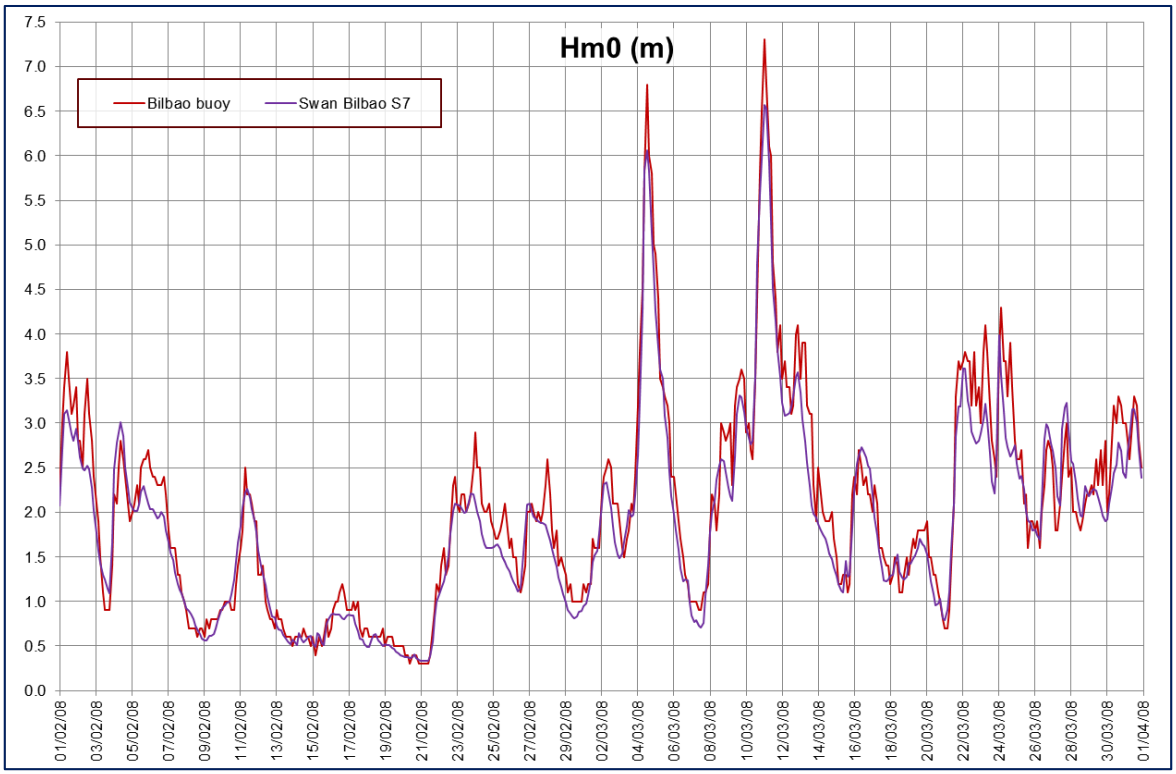

Figure 19. Comparison wave model / Bilbao Buoy – H_{m0}

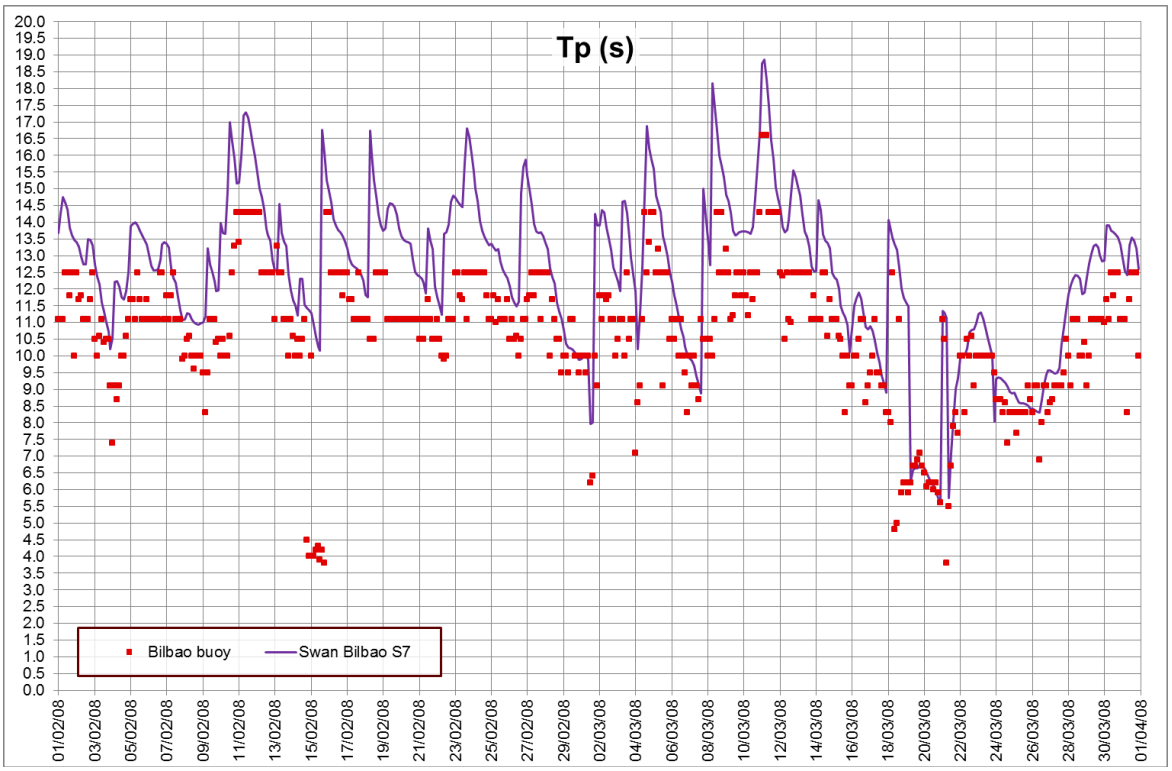

Figure 20. Comparison wave model / Bilbao Buoy – T_p

The model results are consistent with the 2 buoy measurements for all parameters.

An under-estimation of the storm peak of December 11th (and in a lesser extend of December 4th) is observed but all other events are well represented. As for the French model, it appears that HOMERE database does not reproduce some storm peak.

As shown in Figure 18, the wave directions modeled are consistent with data. The main direction (North-West) is reproduced by the model.

The calibration is completed by a statistic analysis on the H_{m0} value (February-March 2008). The definitions related to statiscal variables studied are given in the next Table 3.

The results described in Table 4 confirm the good behaviour of the model by comparison with the buoy. The standard deviation and RMSE values are 10 cm (Bilbao) and 14 cm (Vizcaya). Error remains lower than 20 cm during more than 93% of time and lower than 10 cm during around 83% of time which is acceptable.

Table 3 – Definition of statistical variables

Variables	Definition
Standard deviation	$SD = \sqrt{\frac{1}{N-1}\sum_{i=1}^{N}(e_i - \bar{e})^2}$
RMSE	Root-mean-square error $= \sqrt{\frac{1}{N}\sum_{i=1}^{N} e_i^2}$
CF(X)	Part (percentage) of error included in the interval $[-X; X]$

In our case, the variables are calculated for X is equal to 0.10 m and 0.20 m.

Table 4 – Statistical analysis – H_{m0}

Site	Bilbao		Vizcaya	
X (m)	**0.10**	**0.20**	**0.10**	**0.20**
Standard deviation	0.10	0.10	0.14	0.14
RMSE (m)	0.10	0.10	0.14	0.14
CF(X) (%)	86	95	83	93

The Q-Q plots realised over the period 1993-2012 and presented in Figure 21 confirm the good behavior of the model

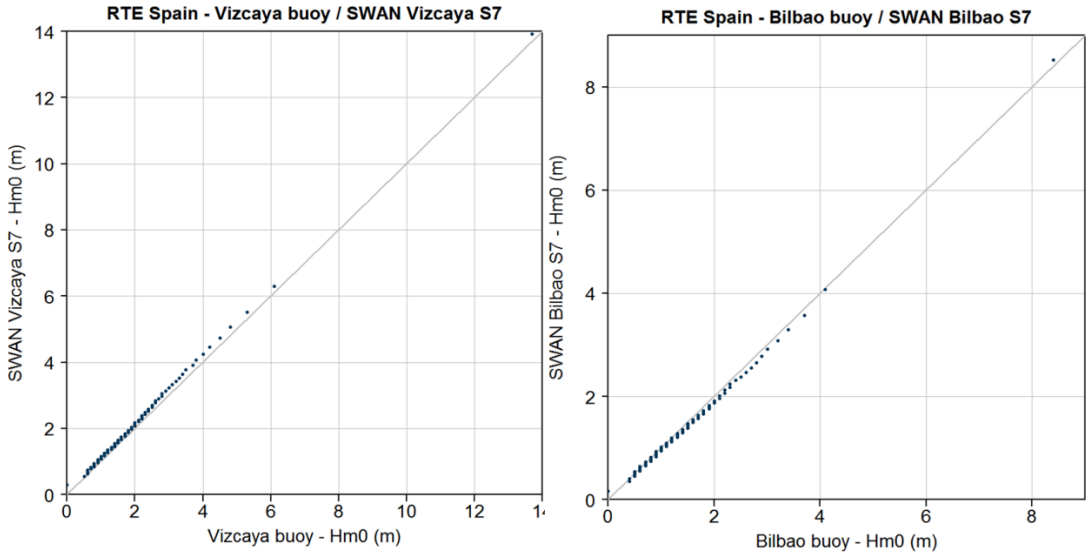

Figure 21. Q-Q PLOT : Model vs Buoy (1993-2012)

In conclusion, the model is able to reproduce the wave propagation and is used to reproduce the wave propagation during 19 years in the next step of the study.

3.4. MODEL OUTPUT

Each wave model has run during 19 years from 1 January 1994 to 31 December 2012. According to the model (Spain or France, large or nearshore), the computation time to be achieved is more or less 1 day per year modelled.

3.4.1. Output points

Figure 22 and APPENDIX 3 present the output points along the **French coast**. These points are located:

- every 20 km along the probable cable route (point L01 to L06);
- around the canyon (points S01 to S14);
- at the landfall (points N01 to N07).

The blue points are those which are analyzed whereas the brown ones are only archived (the untreated results at these points are kept for potential later processing if required). Areas of

relevance of each of the points with respect to metocean analyses are shown on Figures 2 and 4 of APPENDIX 3 and corresponding polygon corrdinates are provided in GIS format (file *Zones_Validation_Swan.TAB*).

The coordinates and the depth at the analysis points are specified in the next Table 5.

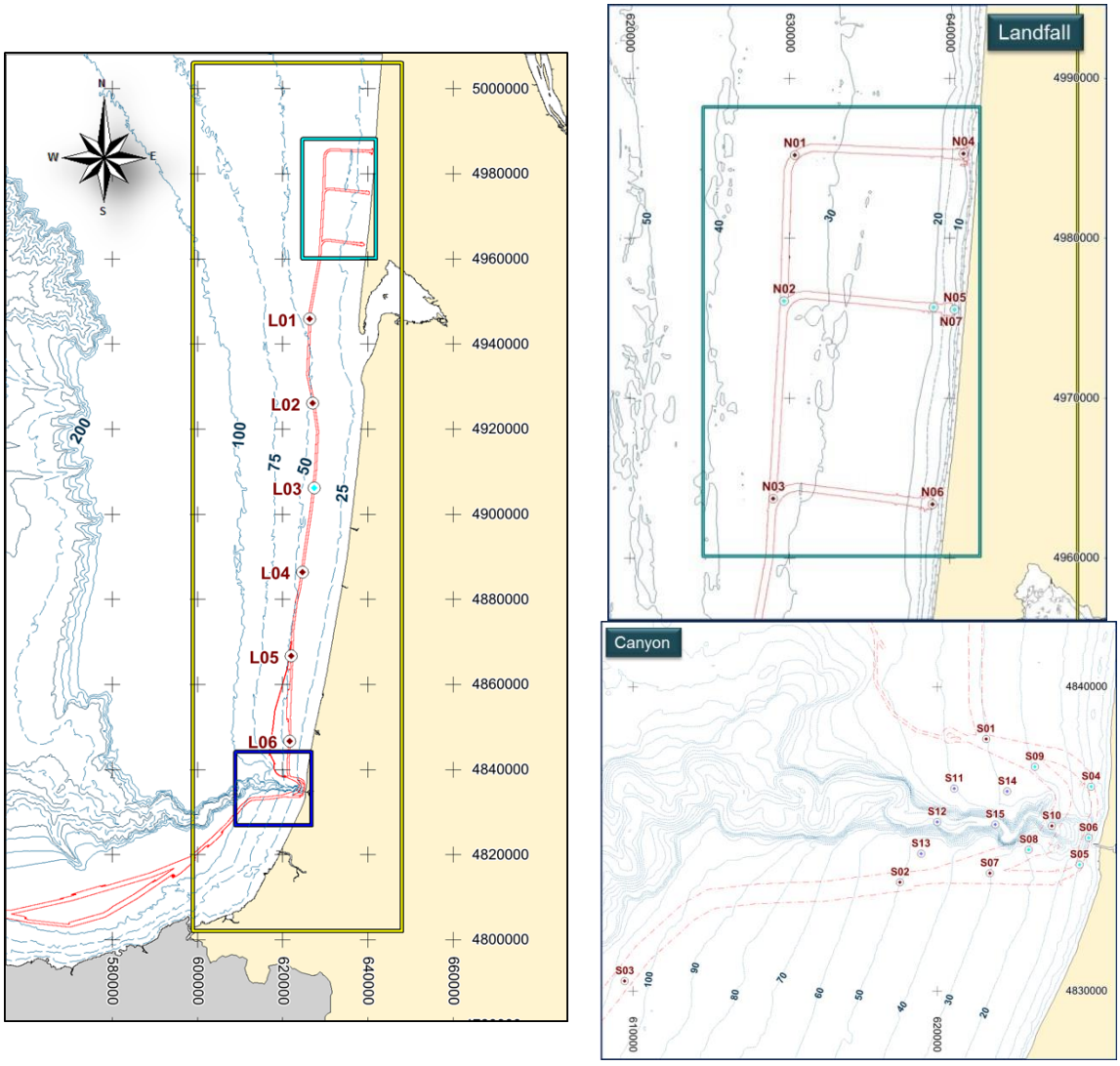

Figure 22. Output location (analysis points in blue, archive points in brown – see APPENDIX 3 for more details)

Table 5 – Coordinates (WGS84 - UTM30N) and depth at the analysis points - France

Point	X	Y	Z (m MSL)	Area of relevance
L03	627 357.5	4 906 238.4	- 43.3	French offshore route
N02	629 646.1	4 976 085.7	- 32.5	Offshore Landfall (from -35 to -20 m MSL)
N05	640 305.8	4 975 541.5	- 10.25	Landfall (from -10 MSL to the coast)
N07	639 004.6	4 975 686.9	- 19.8	Landfall (from -20 to -10 MSL)
S04	625 059.5	4 836 728.0	- 9.7	Canyon (north)
S05	624 677.9	4 834 159.7	- 10.1	Canyon (south)
S06	624 975.0	4 835 042.5	- 10.5	Canyon (head)
S08	623 008.5	4 834 652.9	- 19.1	Canyon (south)
S09	623 210.4	4 837 380.2	- 29.5	Canyon (north)

Figure 23 and APPENDIX 6 present the output points along the **Spanish coast**. These points are located:

- between 5 to 35 km of distance, along the probable cable route (point L07 to L12);
- at the landfall (points Sp01 to Sp06).

The blue points are those which are analyzed whereas the brown ones are only archived (the untreated results at these points are kept for potential later processing if required).

The coordinates and the depth at the analysis points are specified in the next Table 6. Areas of relevance of each of the points with respect to metocean analyses are shown on Figures 3 and 5 of APPENDIX 6 and corresponding polygon corrdinates are provided in GIS format (file *Zones_Validation_Swan.TAB*).

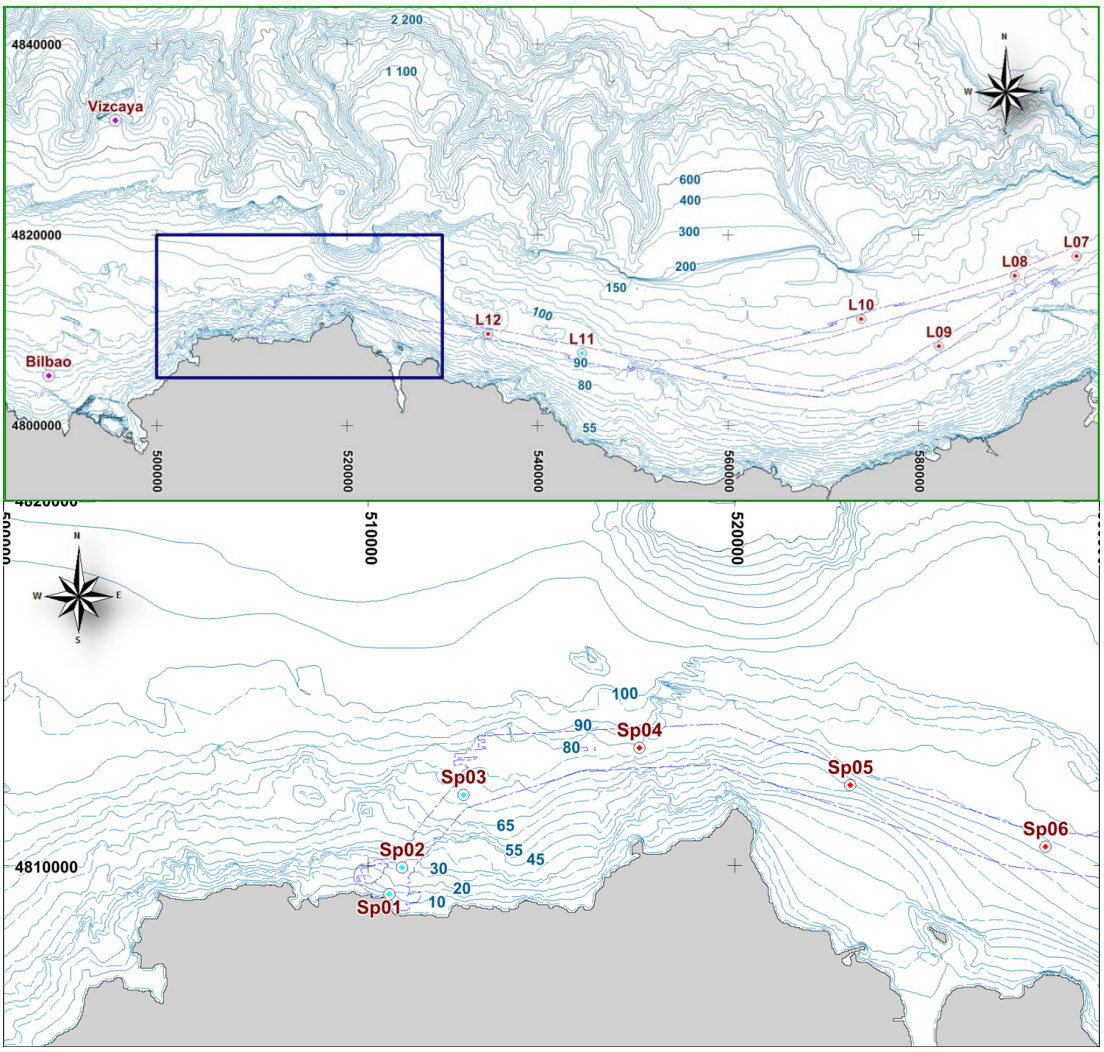

Figure 23. Output location (analysis points in blue, archive points in red – see APPENDIX 6 for more details)

Table 6 – Coordinates (WGS84 - UTM30N) and depth at the analysis points - Spain

Point	X	Y	Z (m MSL)	Areas of relevance
L11	544 631.0	4 807 595.4	- 91.1	Offshore Spanish routes (until -70 m MSL)
SP01	510 574.3	4 809 220.6	- 9.8	Landfall (from -10 MSL to the coast)
SP02	510 926.2	4 809 946.9	- 25.1	Landfall (from -25 m to -10 MSL)
SP03	512 600.0	4 811 940.1	- 67.0	Offshore Landfall (from -70 to -25 m MSL)

3.4.2. Type of output

For each analysis point, operational statistics have been produced for key wave parameters (H_s, T_p, Dir_p):

- The **annual and monthly wave climate** files are directly provided in the Excel format. These files contain for each point various analysis (see Table 7 hereafter). For each point, the names of the files are under the form: "`Fr_ Point Name_Clim_h050d10p0.xlsx`" for the annual climate and "`Fr_ Point Name _Month_Clim_h050d10p0.xlsx`" for the monthly climates (*Month = 1 for January, 2 for February…; Point Name = L03, N02, N05; N07…). "h050d10p0" means resolution of 0.5 m for H_{m0} (h050) and 10° for the direction (d10) for the analyses.*

Table 7 – Description of the analysis available in the Excel files

Sheet name	Description of content
climat_Hs	Correlogram H_{m0}/θ_p (resolution 0.5 m/10°) in number of events, in occurrence frequency and in exceedance frequency
climat_Tp	Correlogram T_p/θ_p (resolution 1 s/10°) in number of events, in occurrence frequency and in exceedance frequency
Rep_HsTp	Correlogram H_{m0}/T_p (resolution 0.5 m/1s) in number of events per directional sector (resolution 10°), over all directions and in occurrence frequency over all directions.
G_Rose	Occurrence frequency wave rose
Maxis	Tables of maximum observed T_p per wave height and direction classes and maximum observed H_{m0} per wave period and direction classes
G_App_Hs	Occurrence frequency of H_{m0} plot
G_Dep_Hs	Exceedance frequency of H_{m0} plot
G_Dep_HsLog	Exceedance frequency of H_{m0} logarithmic plot
G_App_Tp	Occurrence frequency of T_p plot
G_Dep_Tp	Exceedance frequency of T_p plot
G_Dep_TpLog	Exceedance frequency of T_p logarithmic plot

- The figures in the APPENDIX 3 (France) and APPENDIX 6 (Spain) show the followings analysis:
  - annual and monthly **wave roses**,
- some **colour maps** of the wave propagation are also proposed for specific dates (APPENDIX 4 and APPENDIX 7);
- the **extreme wave analysis** is described in the APPENDIX 5 for the French coast and in APPENDIX 8 for the Spanish coast.

3.5. WAVE ANALYSIS

3.5.1. French coast

3.5.1.1. Operational conditions

All the analyses lead to the followings remarks:

- as regards the climate **offshore** (points L03, N02), the wave direction is mainly West/North-West for every month (Figure 24 and APPENDIX 3). The highest waves occur during the winter season (December to February) with H_s higher than 3 m more than 10 % of the time. It corresponds to long period waves (T_p > 12 s). During the summer season (May to September), the waves remain lower than 3 m most of the time and the periods are shorter.

Figure 25 and Figure 26 representing the exceedance frequency of H_s and T_p confirm this. During the winter, the wave height H_s is mainly between 1.5 and 3 m (about 60% of the time for example in January) and is higher than 3 m (more than 25% of the time in January); the wave period exceeds 12 s. When the summer season approaches, the H_s and the T_p tends to decrease to reach the most frequent values between 0.5 and 1.5 m and 8 to 10 s (see example in July on Figure 26 – the other figures are in the Excel files provided).

- It is worth noting that the wave direction at the offshore point N02 in front of the landfall is oriented slightly more often from the West than at the point L03 located at the south of the landfall.

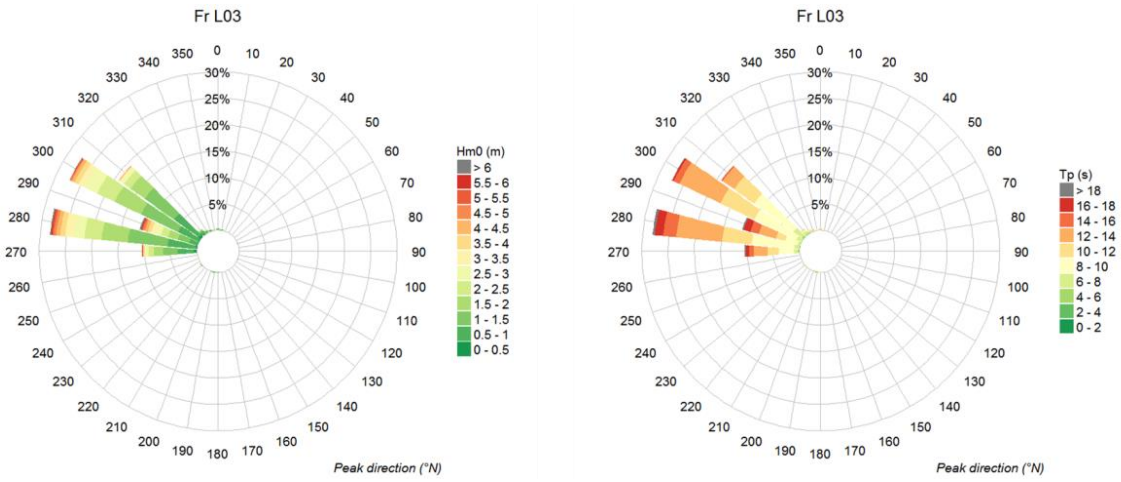

Figure 24. Annual wave rose – Point L03 - Offshore

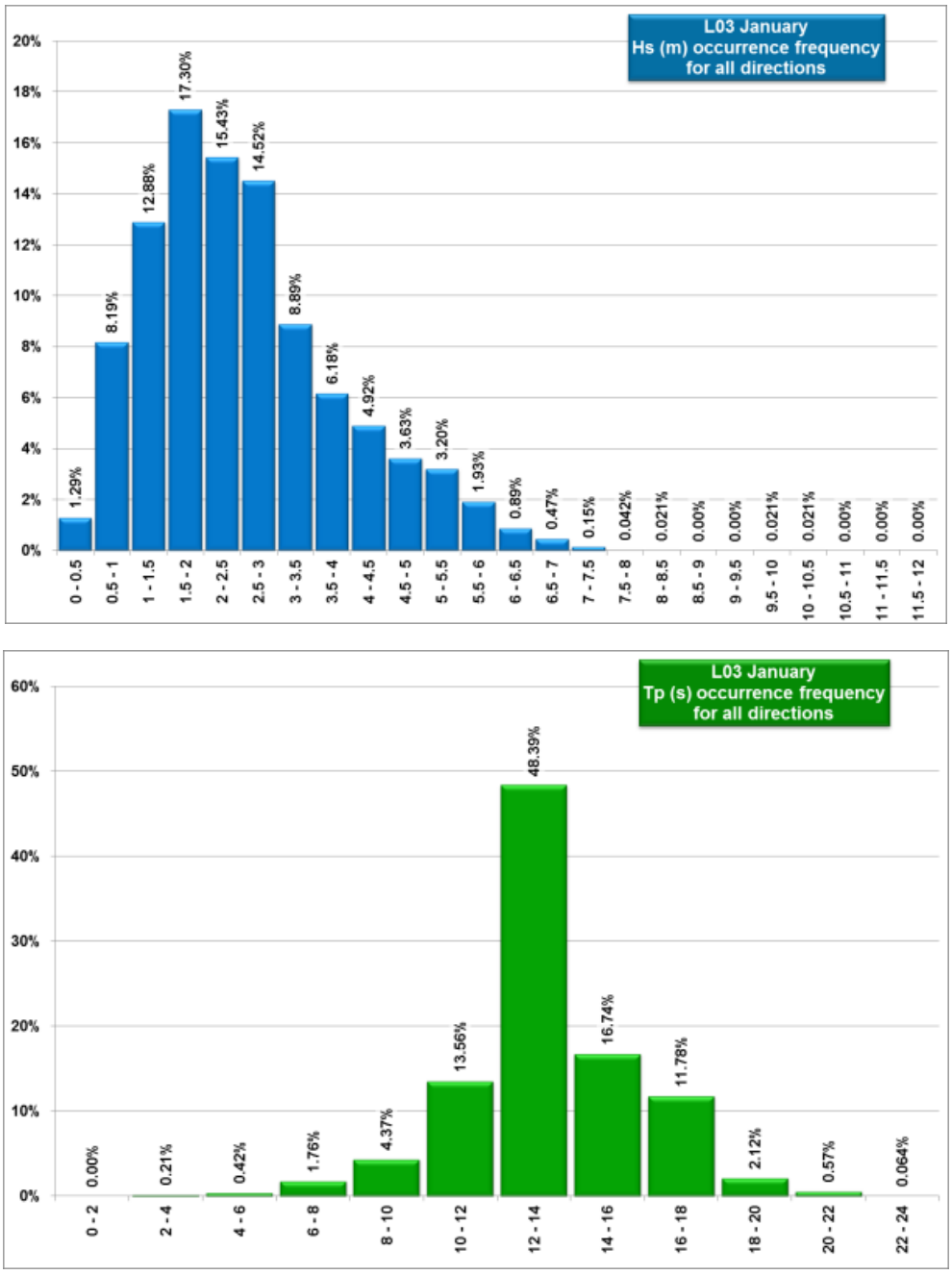

Figure 25. ***Exceedance frequency (Hs on the left side – Tp on the right side) – January - Point L03 – Offshore***

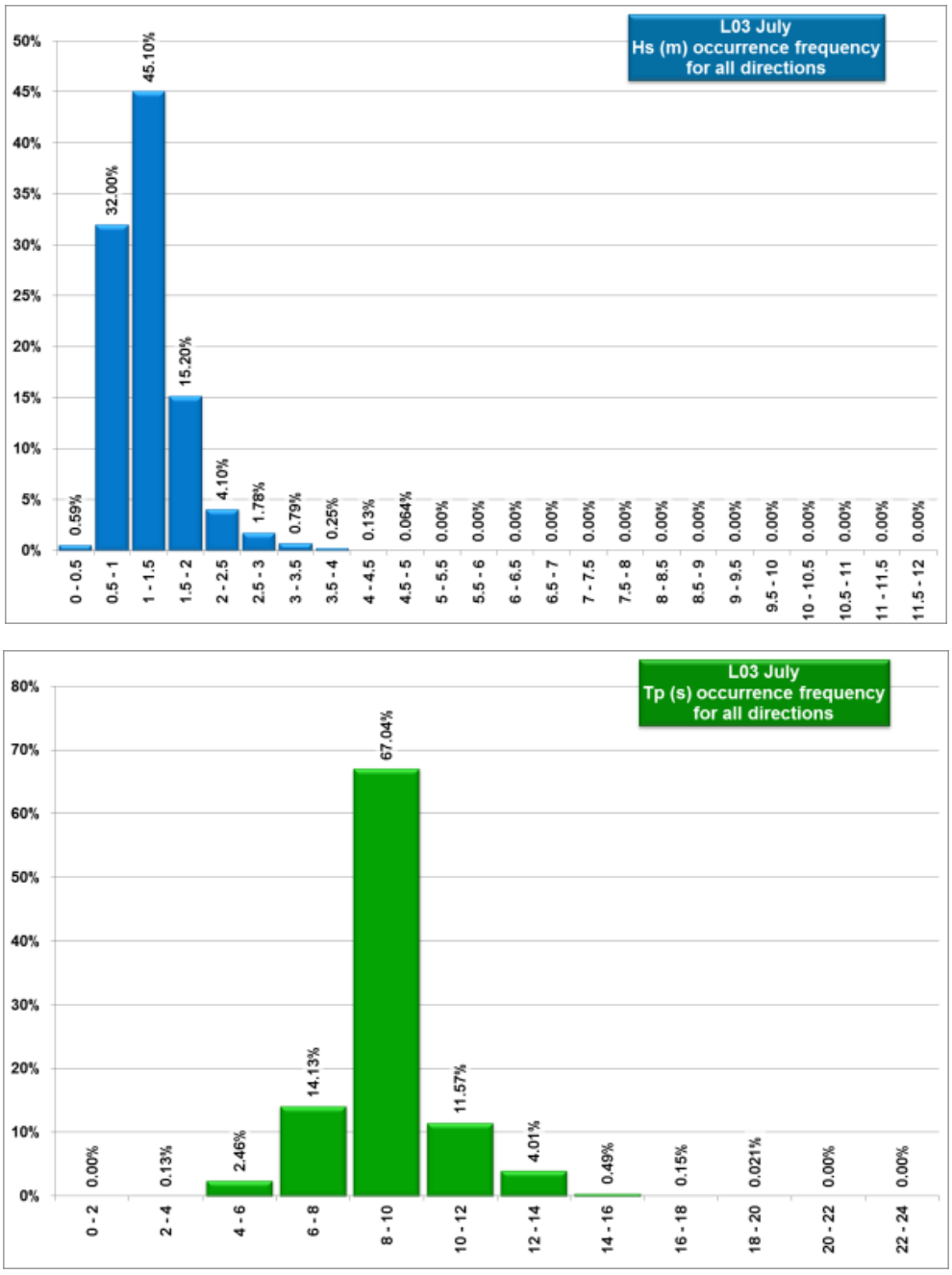

Figure 26. Exceedance frequency (Hs on the left side – Tp on the right side) – July - Point L03 – Offshore

- In front of the **landfall** (points N02, N05, N07), the wave climates are consistent with the offshore climate. The main directions are West/West-North-West with a narrower spread around the main direction near the coastline (point N05 - Figure 27) due to refraction. The highest H_s and the longest periods (12-14 s) appear frequently during winter months whereas the summer season sees waves with lower H_s (0.5 to 1.5 m) and shorter period (Figure 28, Figure 29).

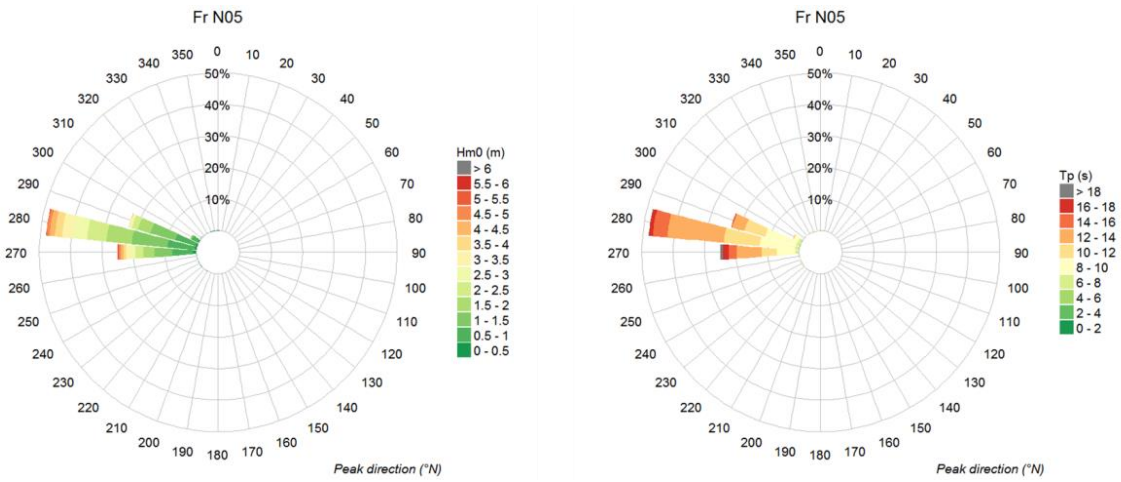

Figure 27. Annual wave rose – Point N05 – Coast - Landfall

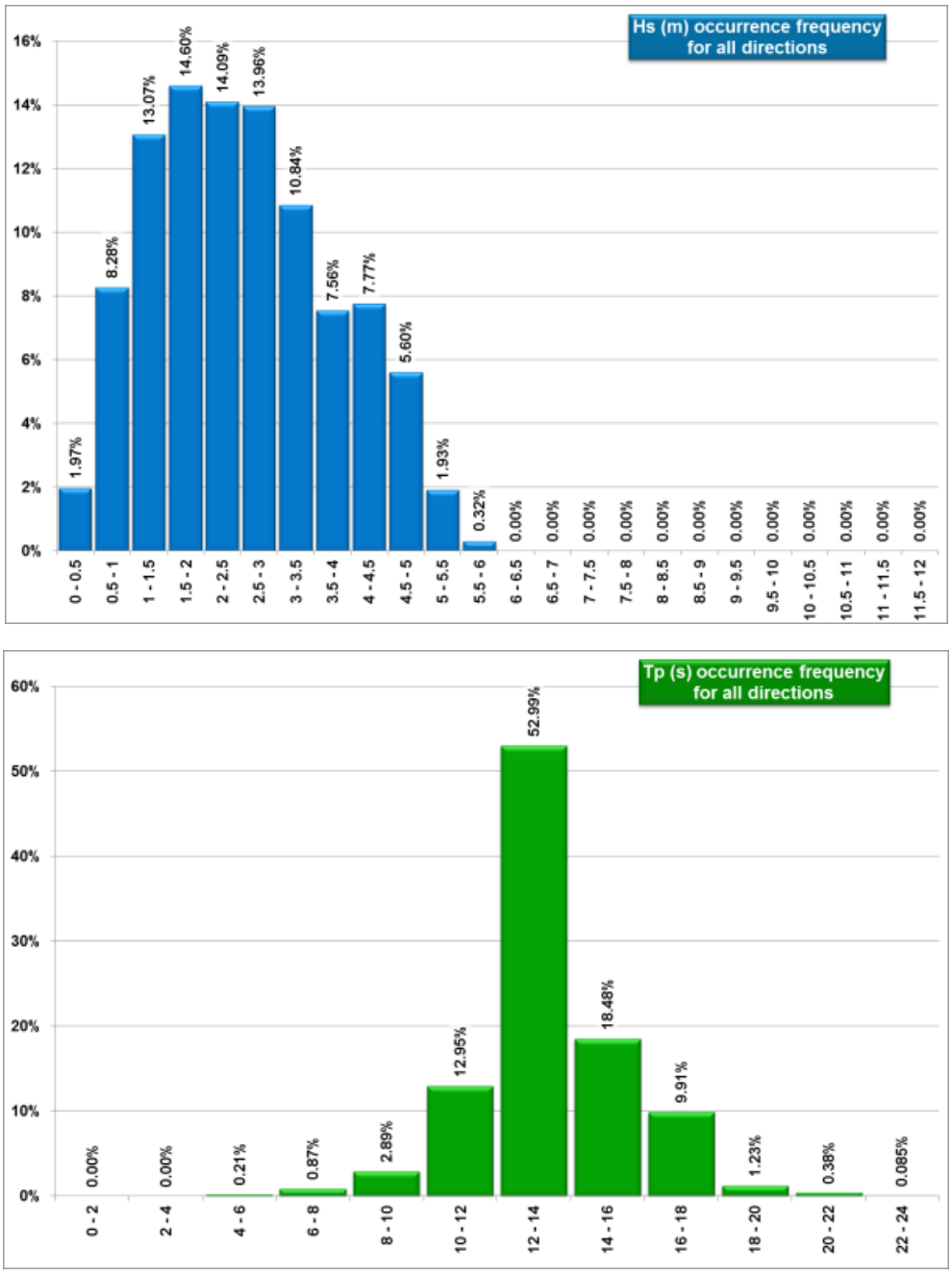

Figure 28. ***Exceedance frequency (Hs on the left side – Tp on the right side) – January - Point N05 – Coast – Landfall***

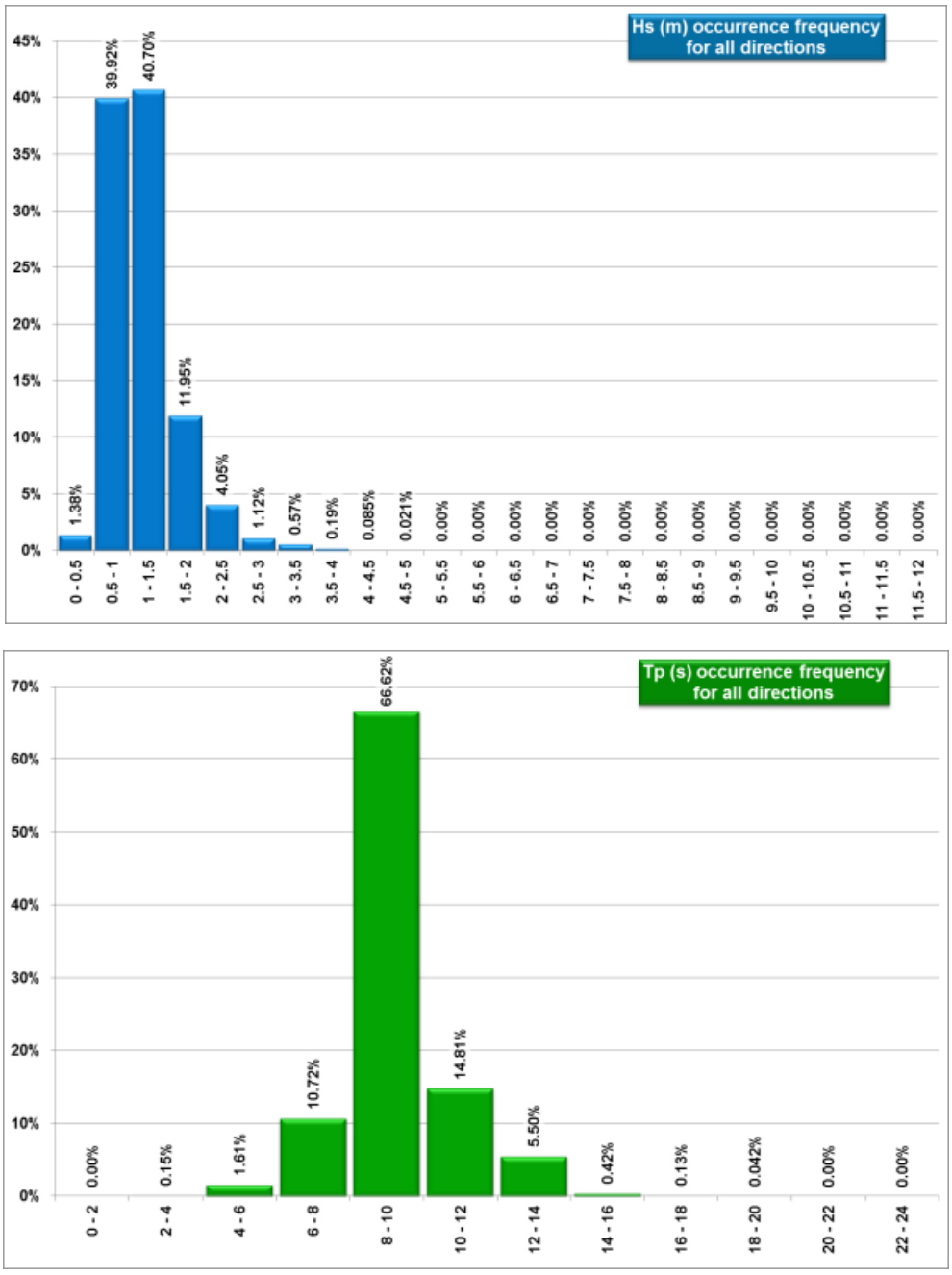

Figure 29. Exceedance frequency (Hs on the left side – Tp on the right side) – July - Point N05 – Coast - Landfall

- The **canyon** has an important effect on wave propagation through the phenomena of **reflection** and **refraction**. Waves approaching the canyon obliquely (mainly from the north-west) will tend to be reflected on the northern side of the canyon because the depth stops decreasing and suddenly increases again. The longer the period is, the more important the effect on wave propagation is. This creates **areas of over-agitation north of the canyon** and **areas of under-agitation south of the canyon**.

  North of the canyon (point S09, Figure 30), the waves come from the West-North-West sector. During winter and spring, the main direction is N280° whereas the second direction N300° appears during summer and autumn.

Closer to the coastline (point S04 - Figure 31), the wave climate is mainly westerly from November to April. Then, the direction turns slightly and the waves come from the West-North-West sector. The values of H_s and T_p evolve depending on the season; they are consistent with those offshore (Figure 32, Figure 33).

What is interesting to note is that the reflection of wave conditions with wave periods larger than ~10 - 12 s against the canyon leads to :

- The more westerly incidence direction at point S04 compared to S09
- overagitation at point S04 with respect to point S09 “until it breaks” as S04 is in shallower water than S09.

This appears on the wave roses, in the annual occurrence frequency graphs (Figure 34) and is shown in Table 8, where more agitation in the range]2;6] m at S04 than at S09.

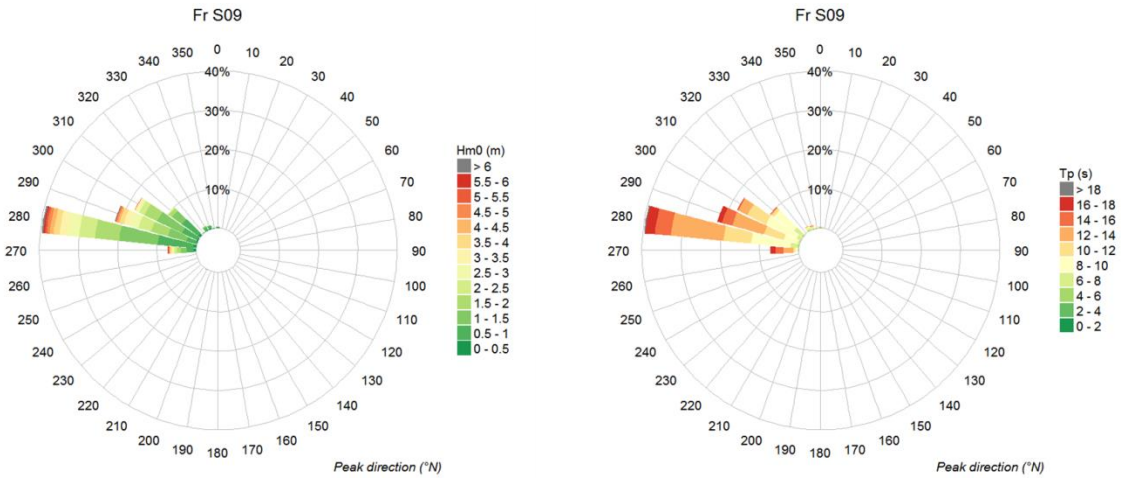

Figure 30. Annual wave rose – Point S09 – North of the canyon

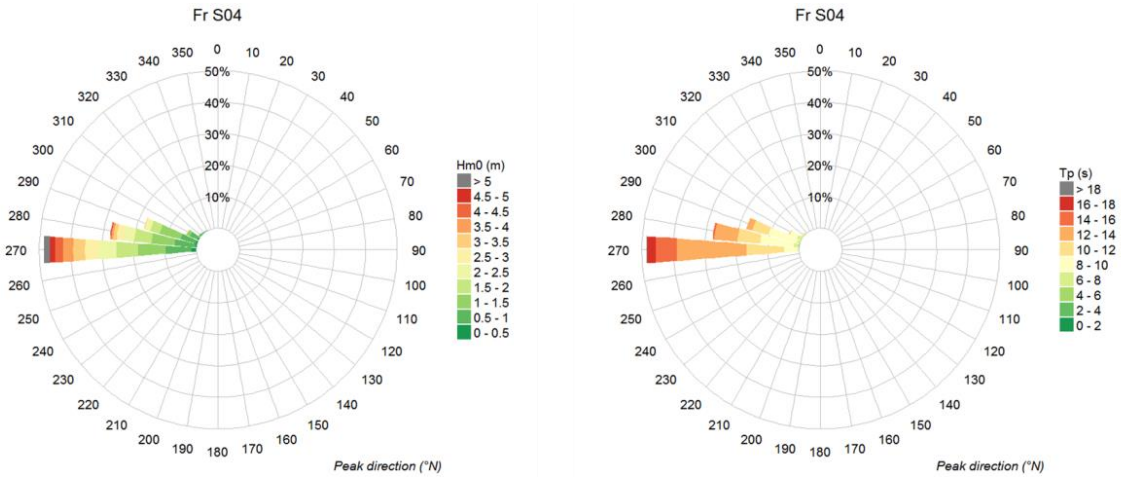

Figure 31. Annual wave rose – Point S04 – North of the canyon

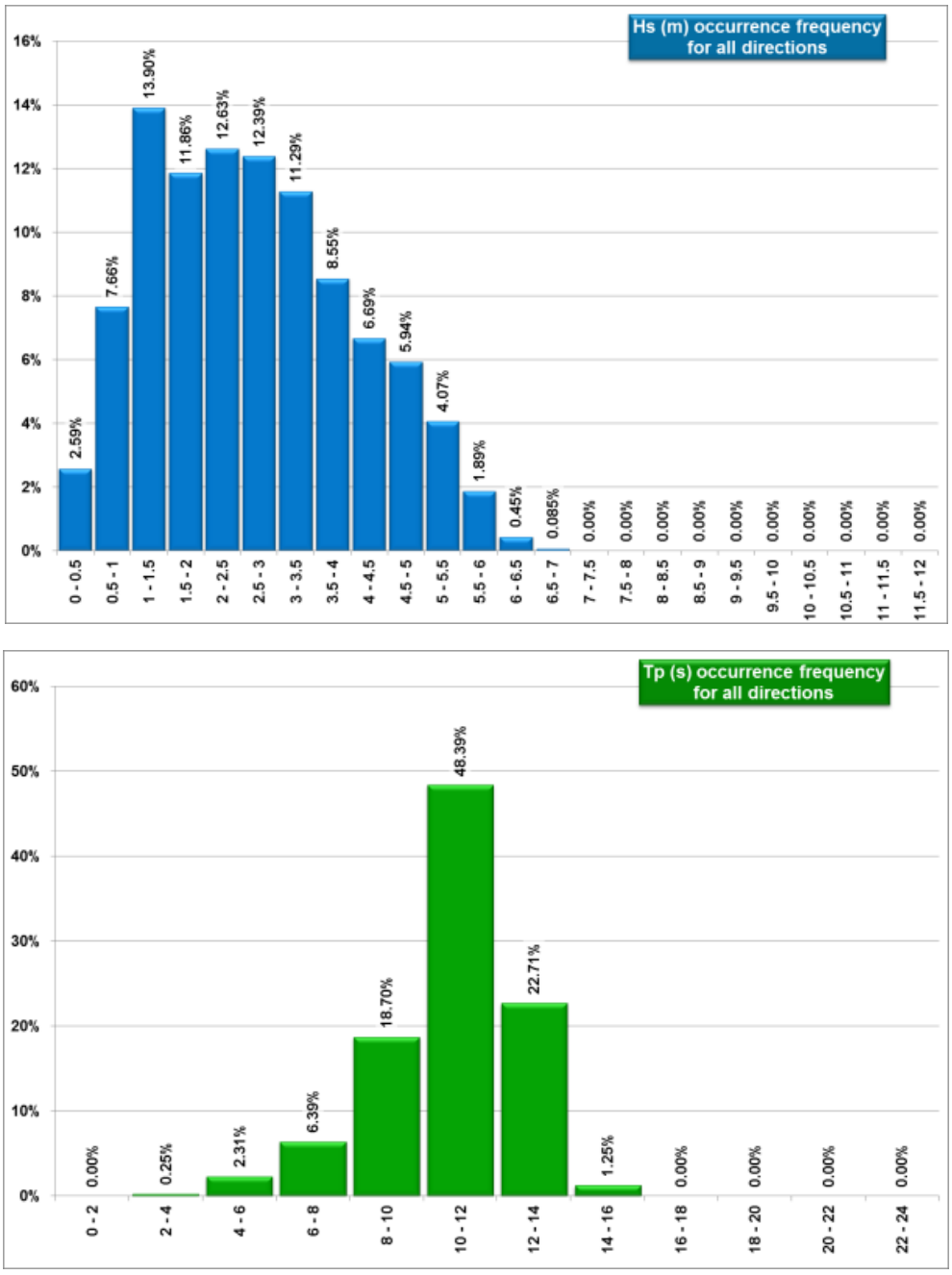

Figure 32. ***Exceedance frequency (Hs on the left side – Tp on the right side) – January - Point S04 – North of the canyon***

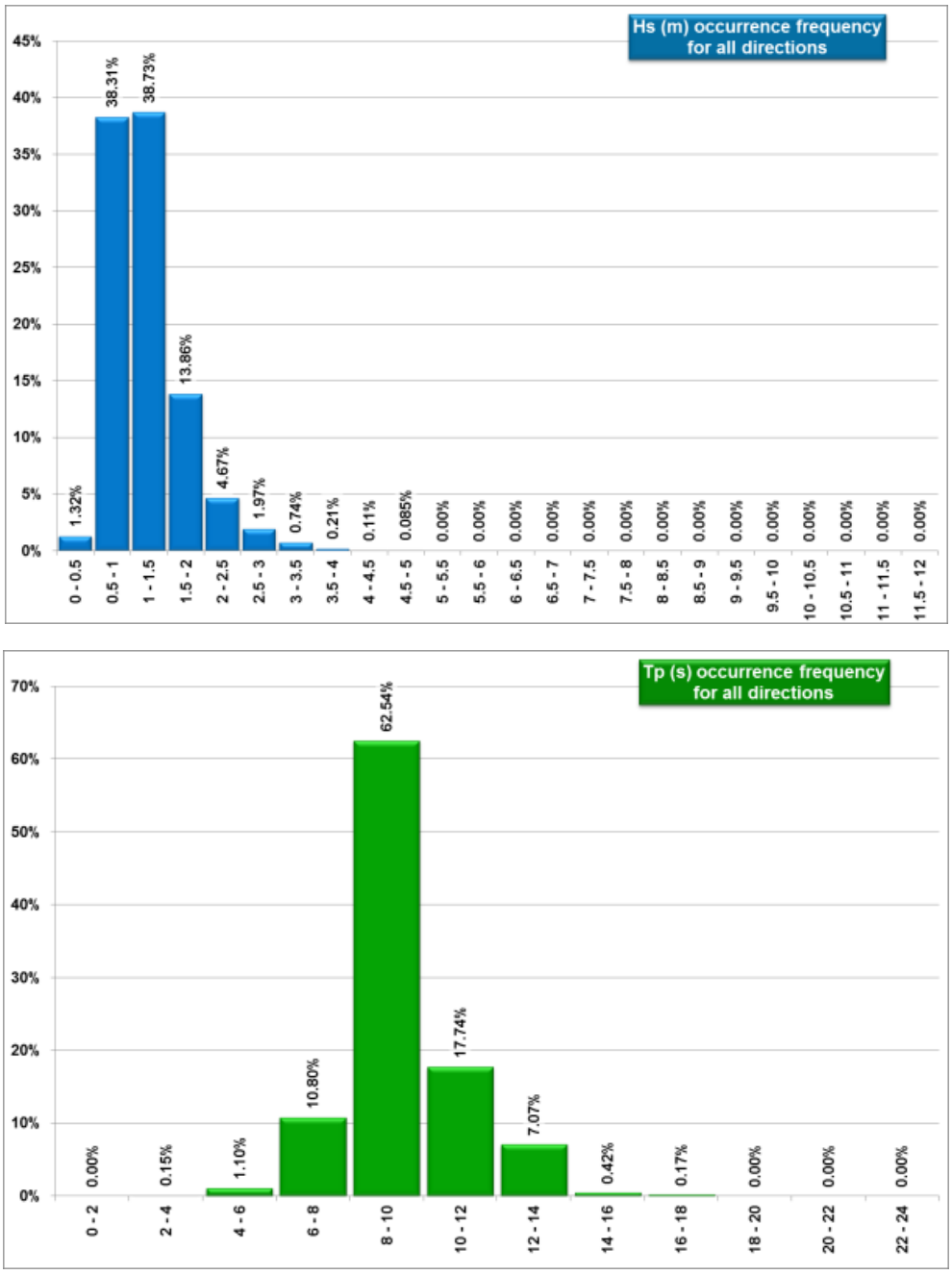

Figure 33. ***Exceedance frequency (Hs on the left side – Tp on the right side) – July - Point S04 – North of the canyon***

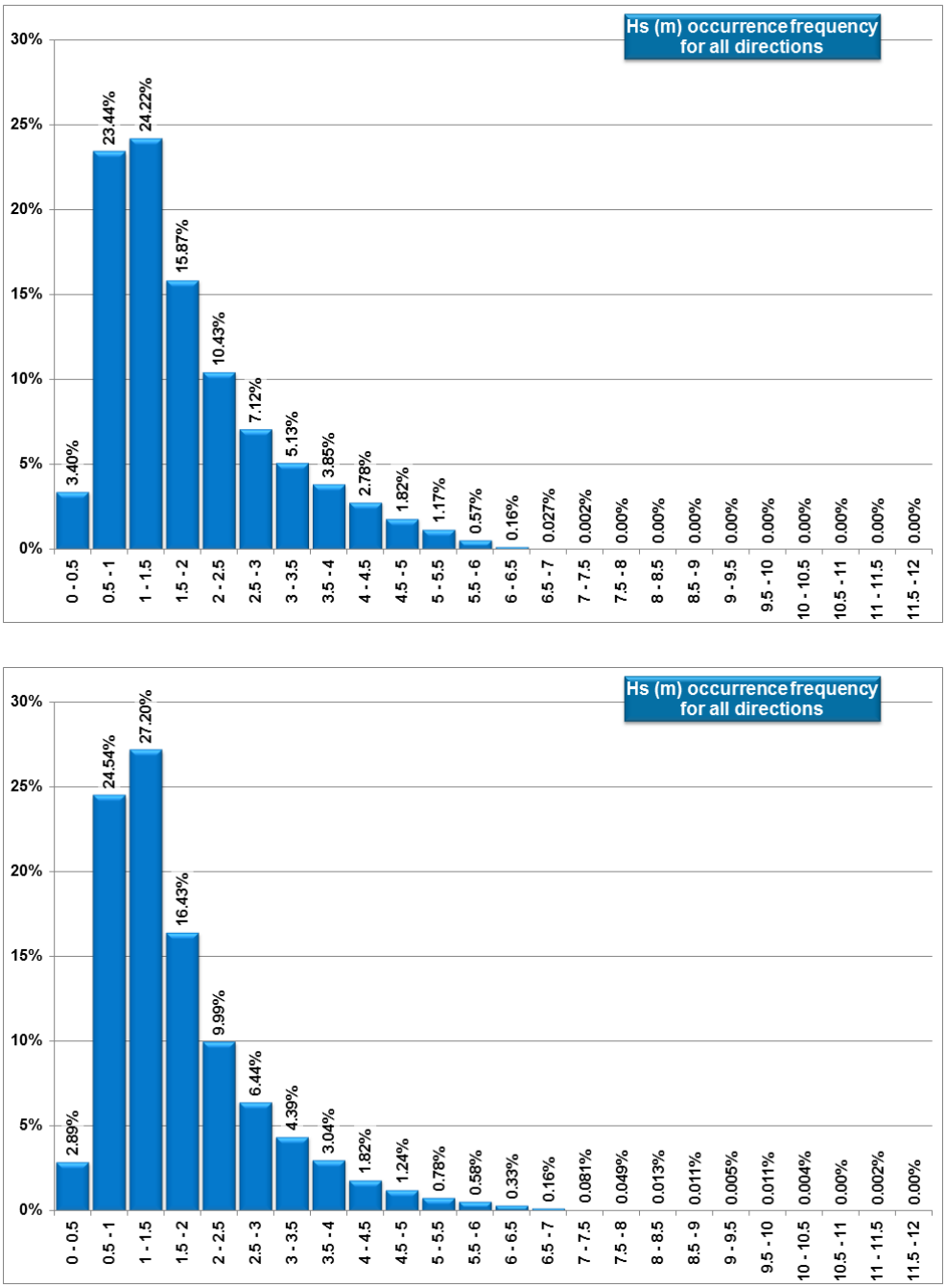

Figure 34. Annual occuring frequency at points S04 located at ~-10 MSL (top) and S09 located at ~-30 m MSL (bottom)

Table 8 – Annual occurring frequency at locations 04 and S09

Point	Depth (m MSL)	0 < Hm0 ≤ 2	2 < Hm0 ≤ 6	6 < Hm0
S04	-10	66.43 %	32.88 %	0.19 %
S09	-30	71.05 %	28.28 %	0.67 %

At the head of the canyon (point S06 - Figure 35), the waves are clearly directed by the canyon shape with a narrow rose around the direction N280°/N290° and the wave propagation phenomena at the canyon's border deflects part of the wave energy away from the canyon's head especially in winter (wave with longer periods are more sensitive to the reflection/refraction processes) with H_s lower than 3.5 m all the time (Figure 36, Figure 37).

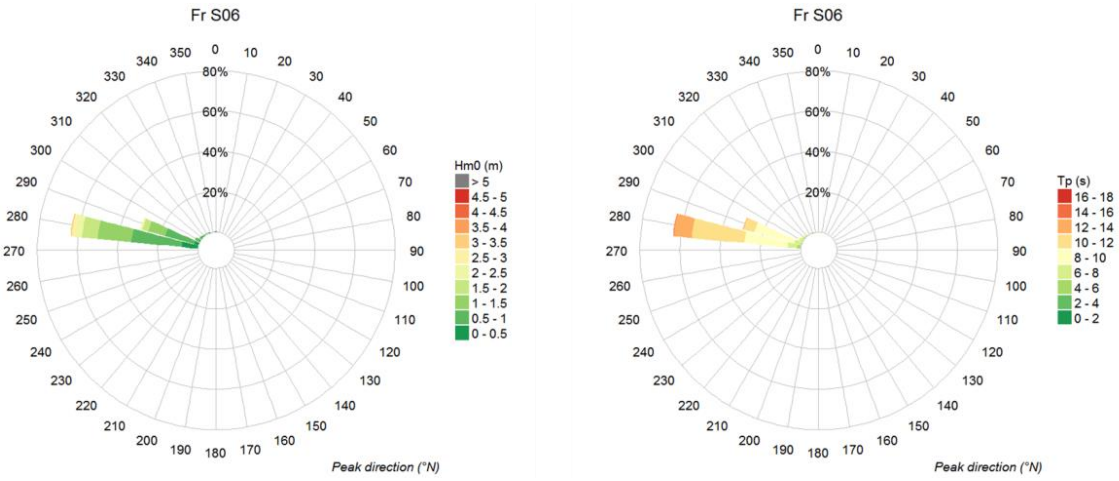

Figure 35. Annual wave rose – Point S06 – Head of the canyon

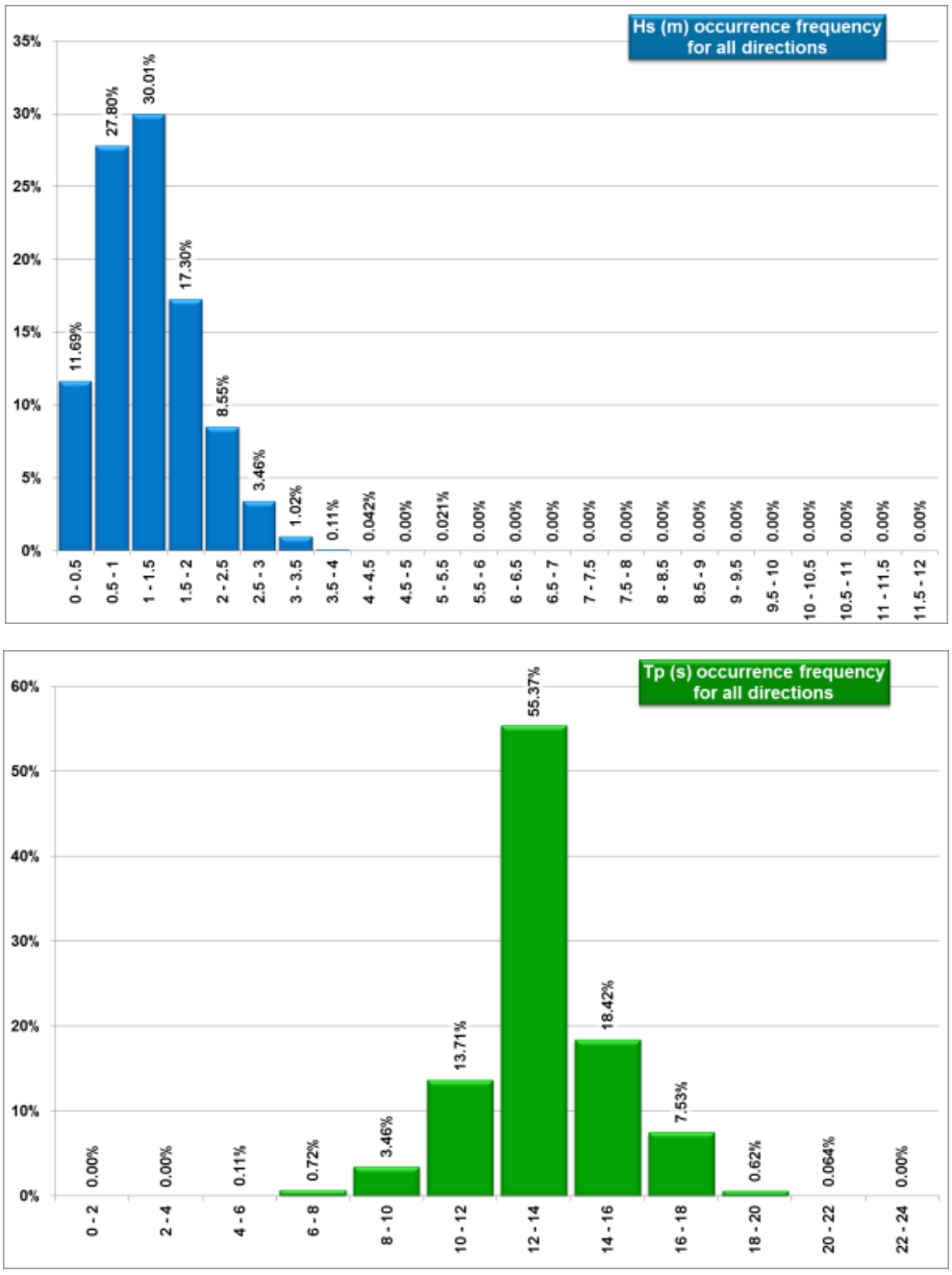

Figure 36. ***Exceedance frequency (Hs on the left side – Tp on the right side) – January - Point S06 – Head of the canyon***

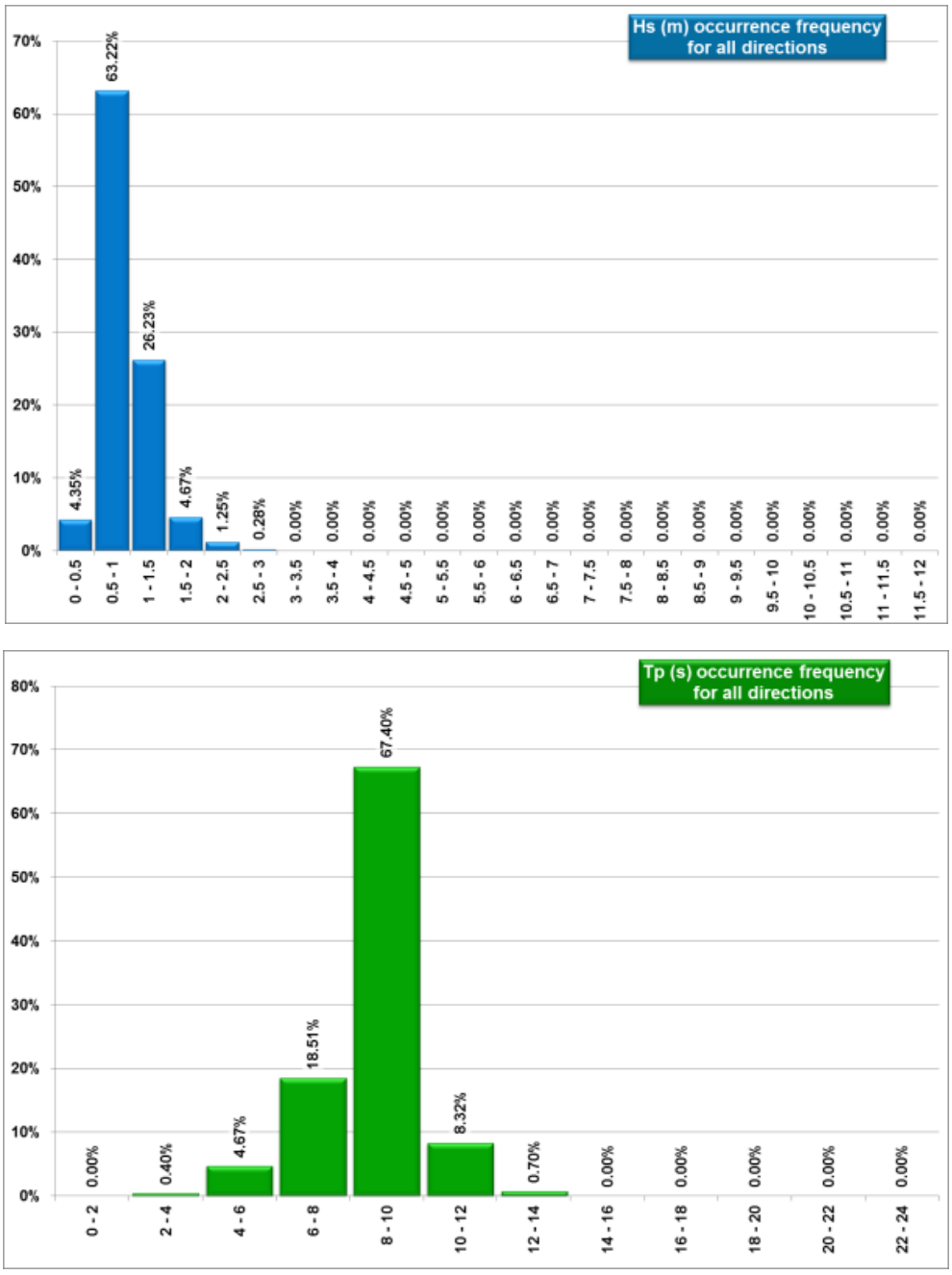

Figure 37. Exceedance frequency (Hs on the left side – Tp on the right side) – July - Point S06 – Head of the canyon

South of the canyon (point S08, by -20 m MSL , Figure 38), the waves are still centered around the direction N300°/N310°.

Closer to the coastline (point S05 - Figure 39, Figure 40, Figure 41), the influence of the canyon on the wave propagation appears(reflection and refraction phenomena) with no waves coming from [280-300] . Hence, on the contrary of the previous points, the waves come clearly from 2 different directions: the West and the North-West (especially in summer).

We can note that due to reflection/refraction phenomena, wave periods at S05 are shifted to longer periods with respect to S08 (see Figure 42).

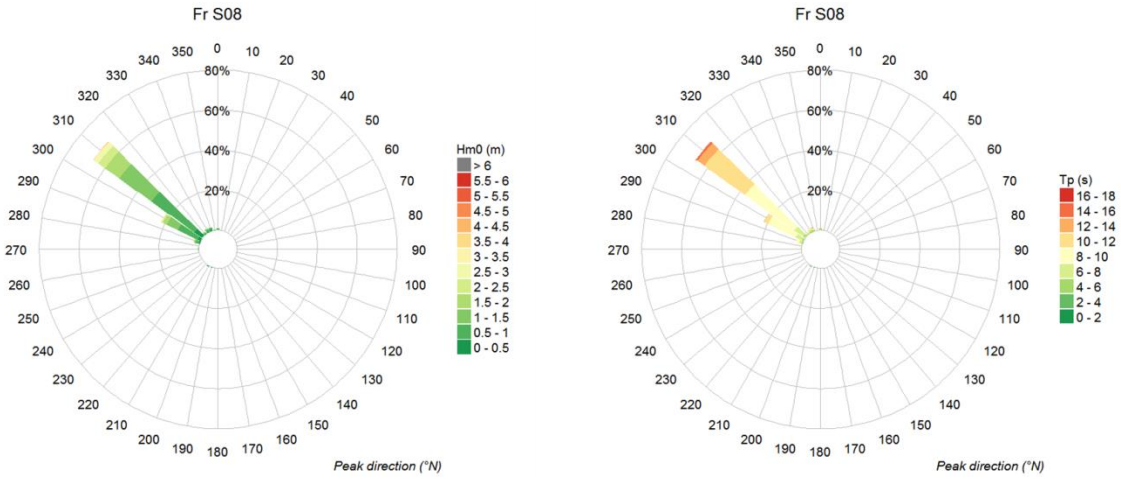

Figure 38. Annual wave rose – Point S08 – South of the canyon

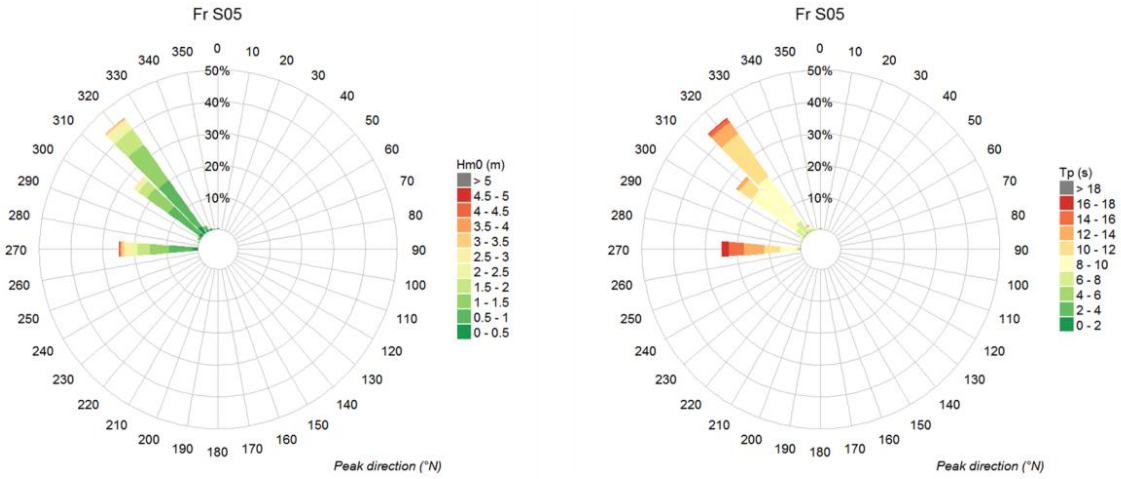

Figure 39. Annual wave rose – Point S05 – South of the canyon

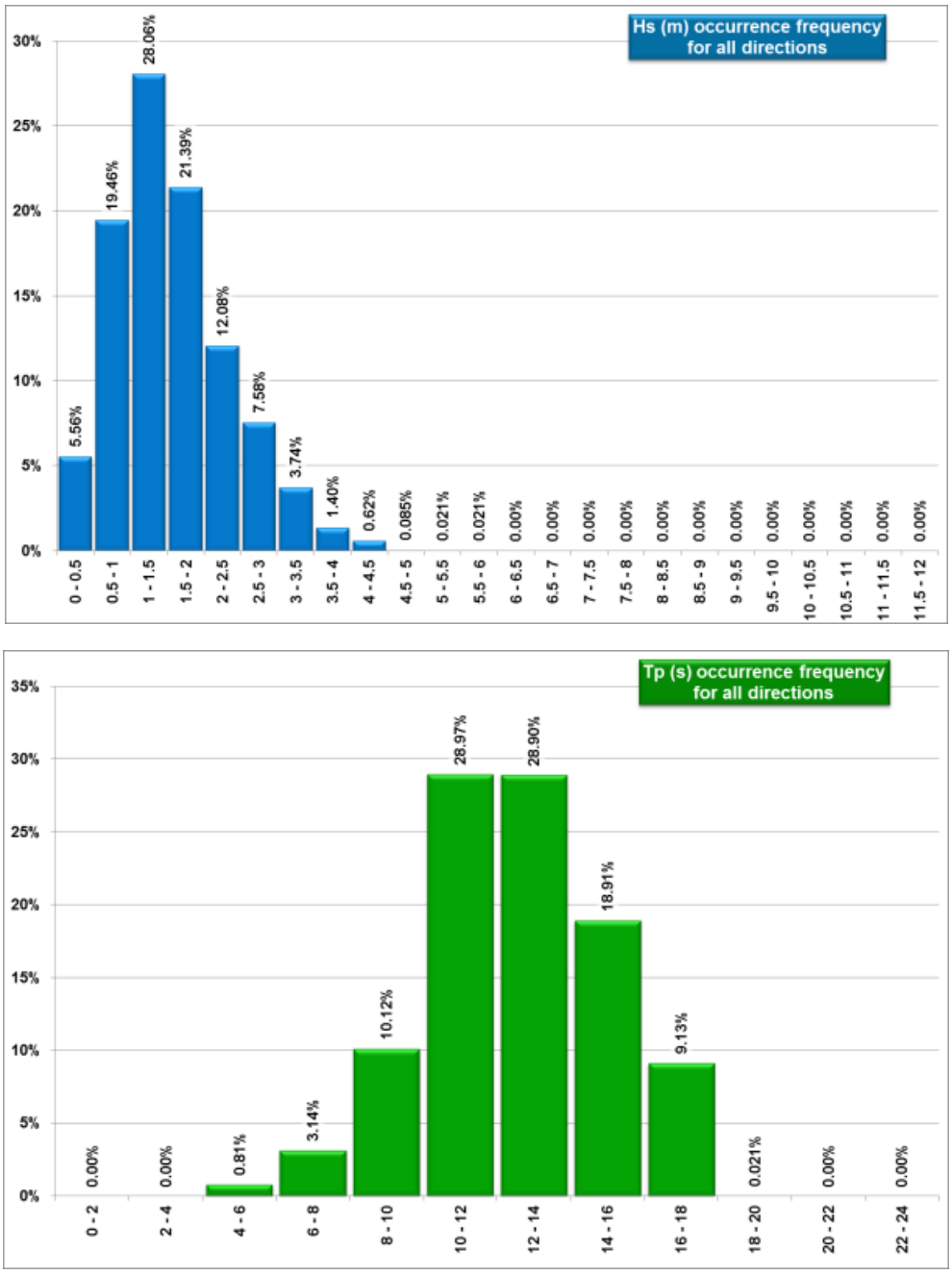

Figure 40. Exceedance frequency (Hs on the left side – Tp on the right side) – January - Point S05 – South of the canyon

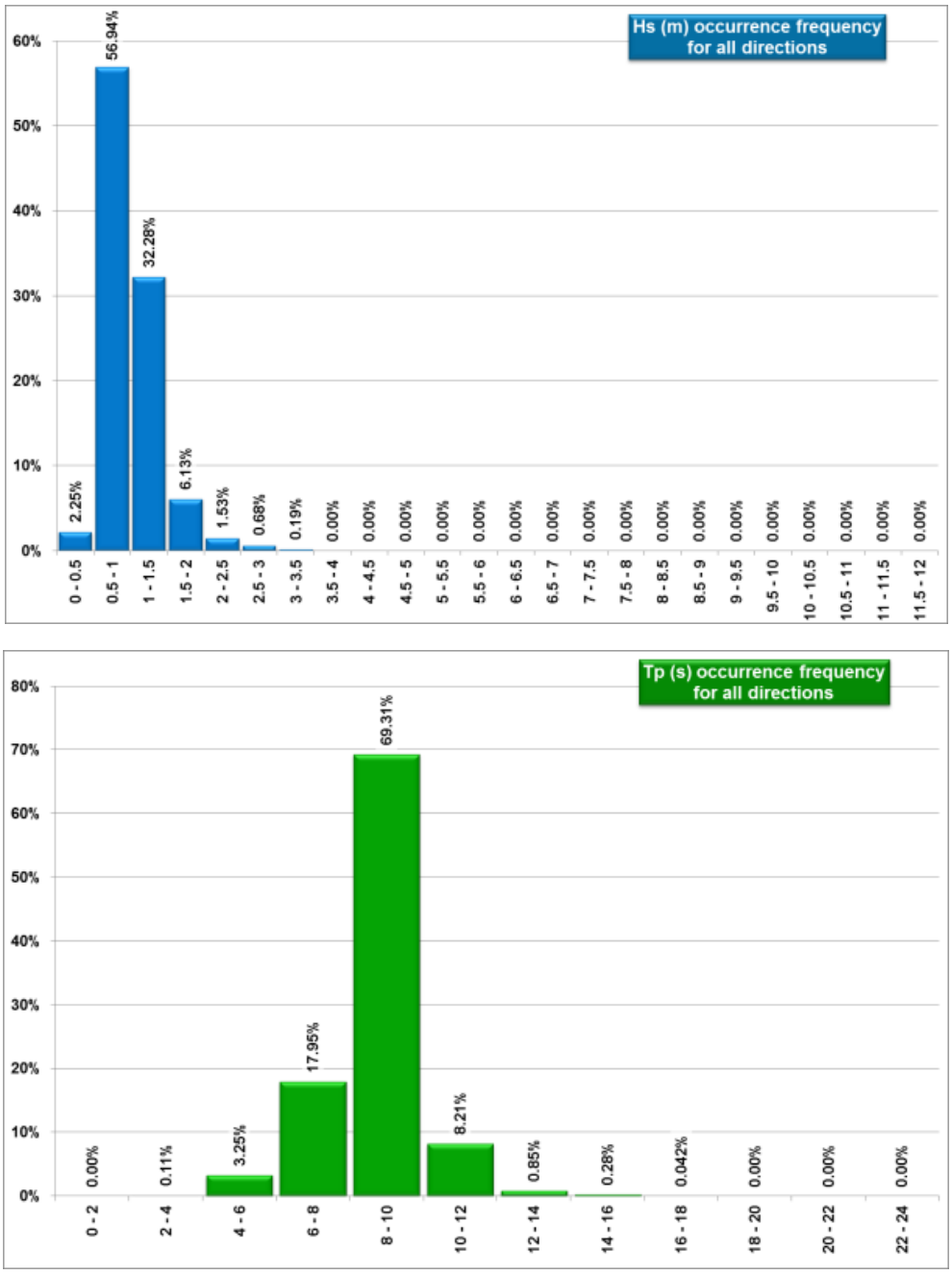

Figure 41. ***Exceedance frequency (Hs on the left side – Tp on the right side) – July - Point S05 – South of the canyon***

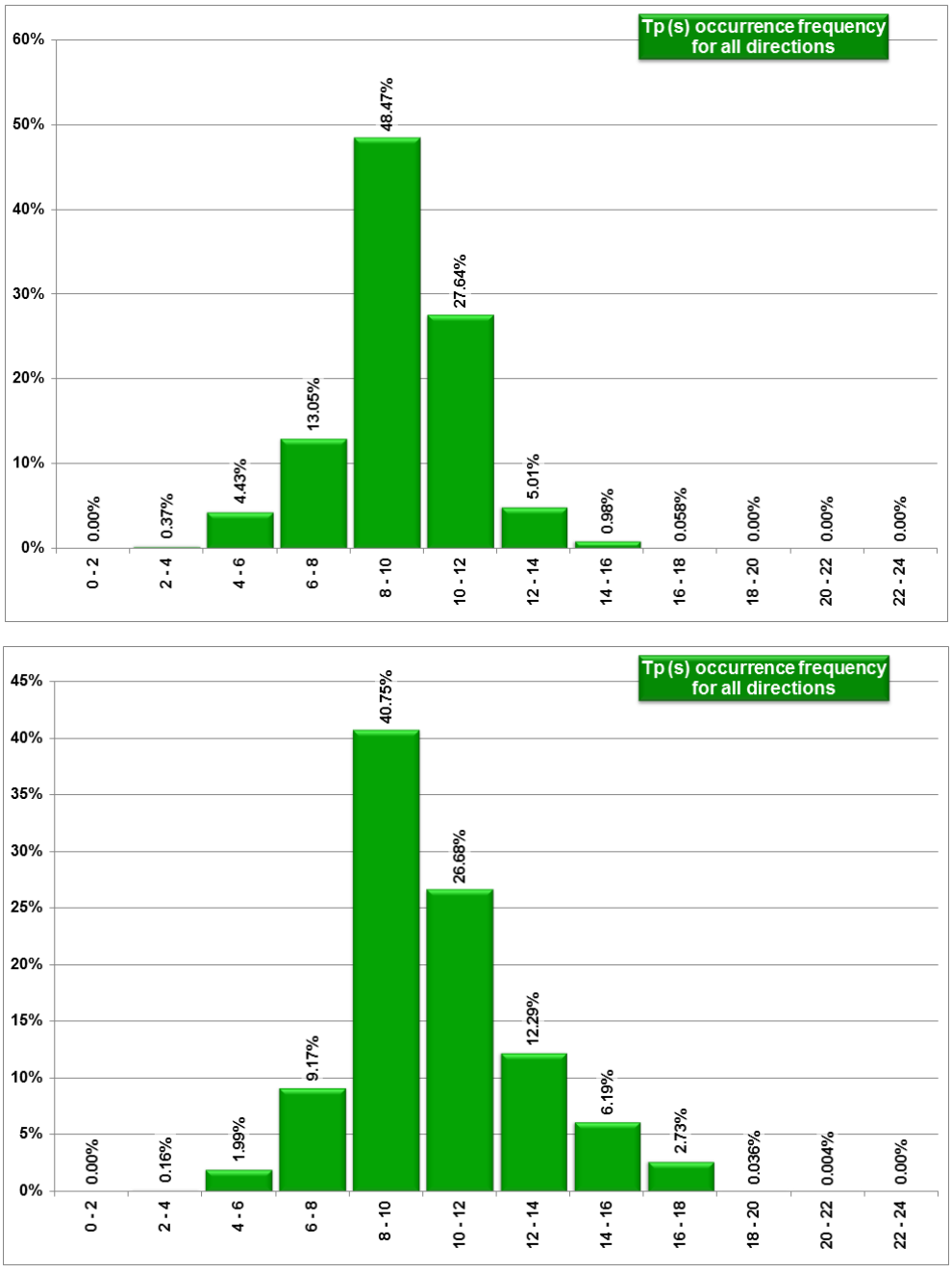

Figure 42. Annual occuring frequency for Tp at S08 by ~-20 m MSL (top) and at S05 by ~-10 m MSL (bottom)

The next Table 9 provides the H_{m0} and T_p values corresponding to the frequencies of exceedance of 10%, 5% and 1%.

Table 9 – Annual exceedance probability (all directions) for wave height (H_{m0}) and period (T_p) – France

Exceedance frequency	Point L03 *Offshore*		Point N02 *Landfall (offshore)*	
	H_{m0} (m)	T_p (s)	H_{m0} (m)	T_p (s)
10%	3.2	14.3	3.1	14.0
5%	4.0	16.0	3.8	15.3
1%	5.5	18.0	5.0	17.5
Exceedance frequency	**Point N07 *Landfall***		**Point N05 *Landfall (coast)***	
	H_{m0} (m)	T_p (s)	H_{m0} (m)	T_s (s)
10%	3.1	14.1	3.3	14.2
5%	3.8	15.4	3.9	15.6
1%	5.1	17.6	4.8	17.7
Exceedance frequency	**Point S08 *Canyon (south)***		**Point S09 *Canyon (north)***	
	H_{m0} (m)	T_p (s)	H_{m0} (m)	T_p (s)
10%	1.9	11.7	3.3	14.9
5%	2.3	12.7	4.0	16.1
1%	3.1	14.9	5.7	17.4

Exceedance frequency	Point S04 *Canyon (north)*		Point S06 *Canyon (head)*		Point S05 *Canyon (south)*	
	H_{m0} (m)	T_p (s)	H_{m0} (m)	T_p (s)	H_{m0} (m)	T_p (s)
10%	3.6	14.0	1.8	11.9	2.1	13.7
5%	4.3	15.2	2.2	12.4	2.6	15.0
1%	5.4	16.9	2.9	13.4	3.5	16.5

It is reminded that all the figures are presented in the APPENDIX 3 and the Excel files.

- The colour maps presented in the APPENDIX 4 show the wave propagation from the offshore to the coast during specific storm events. The wave height decreases as the waves propagate towards the coast. The wave direction changes slightly to be perpendicular near the coastline due to refraction. As the wave comes from the W-NW sector most of the time, the north part of the canyon is the most exposed. With the passage of the canyon, the wave direction changes and the H_s decreases. Along the possible cable route and in the French landfalls, the wave conditions appear quite homogenous.

3.5.1.2. Extreme waves

3.5.1.2.1. Methodology

A statistical extrapolation of extreme waves was carried out, according to the following methodology:

- determination of homogeneous (identically distributed) wave populations, based on directional criteria (see above);
- declustering of the time series (over a K-year duration, here $K = 19$ years) using the Peaks-Over-Threshold (POT) approach (example in Figure 43):
  - identification and extraction from the time series of storm events exceeding a "physical threshold" u_p set so as to get $\lambda_p = 5 - 10$ storm events per year in average;
  - selection of the wave height peaks of the storm events for setting up a sample of N_p independent and identically distributed (i.i.d.) data ($\lambda_p = N_p/K$);
- statistical extreme value analysis applied to the i.i.d. sample:
  - determination of a "statistical threshold" u_s: the N peaks exceeding this threshold are considered as extreme values ($\lambda = N/K$ peaks per year in average);
  - fitting of statistical distributions (GPD, Weibull, Gamma, Exponential) to these extreme peaks;
  - determination of the best-fitting distribution using a statistical test (such as χ^2 or Kolmogorov-Smirnov);
  - computation of quantiles (return values) for a set of return periods (e.g. 1, 5, 10, 50, 100 years);
  - computation of 90% confidence intervals using the parametric bootstrap method.

ARTELIA presented this state-of-the-art methodology in several presentations in international congresses (both coastal engineering- and statistics-oriented) and in several papers published in international peer-reviewed journals – Ref. [3], Ref. [4], Ref. [5]).

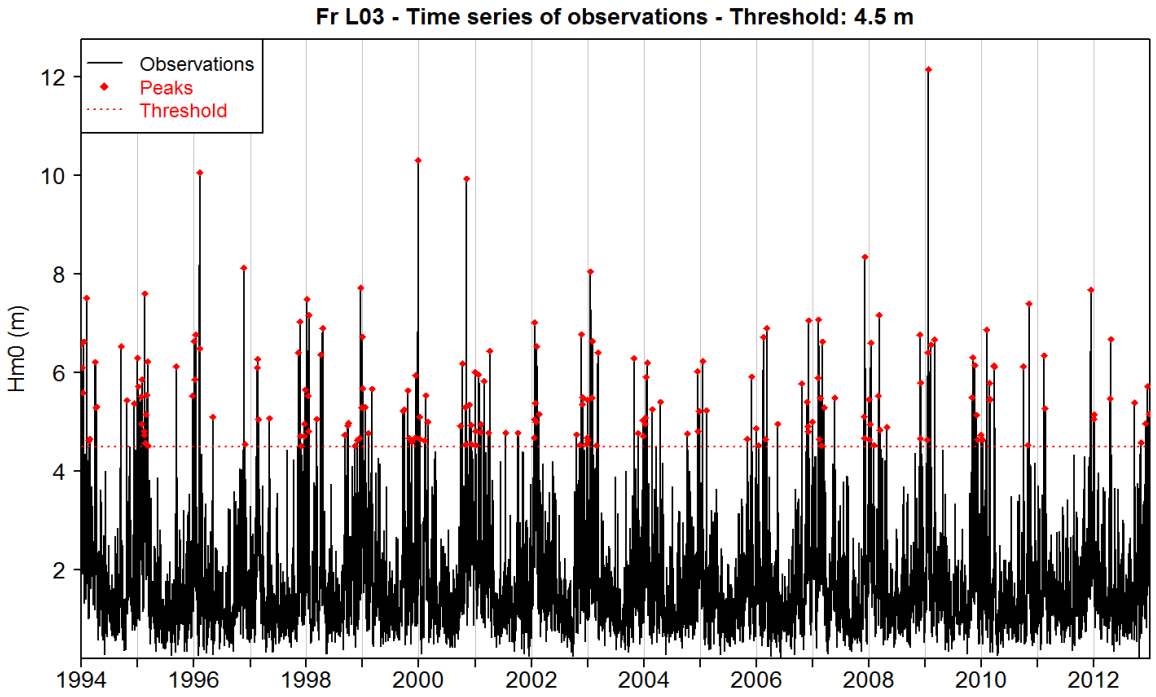

Figure 43. Point L03 - POT declustering of the H_{m0} time series

3.5.1.2.2. Results

First, the extreme sea states have been extrapolated at the point L03, considered as the reference point (Figure 44).

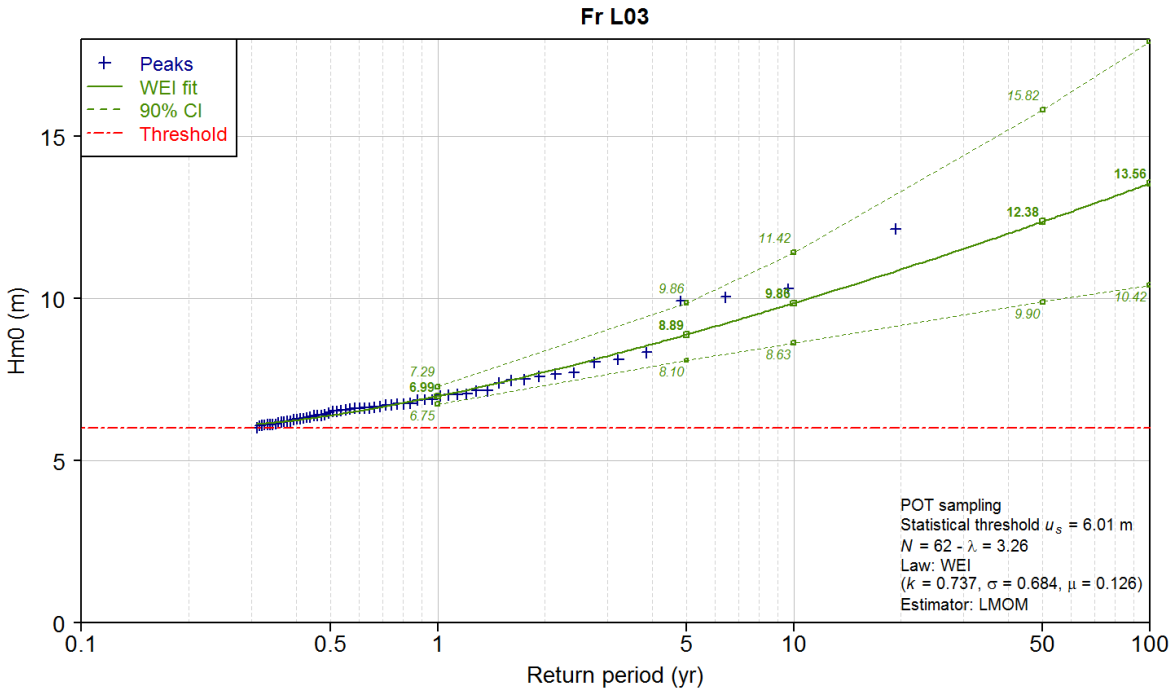

Figure 44. Point L03 – Extrapolation of storm peaks by a Weibull distribution

Then the extreme sea states are extrapolated at the other analysed points that are consistent with the choices made for the reference point (in particular choice of the statistical threshold u_s and of the statistical distribution). This approach provides consistent results over the whole set of output points.

Table 10 sums up the results presented in detail in APPENDIX 5. At the offshore (point L03), the 1-year significant wave height H_{m0} reaches 7 m and the 100-year significant wave height H_{m0} reaches 13.5 m with a large confidence interval (between 10.42 m at the lower bound of the interval and 17.9 m at the upper bound of the interval). Obviously, the extreme sea states are lower near the coastline (point N05 – landfall area) where the values of the 1-year significant wave height (5.58 m) and the 100-year significant wave height (6.37 m) are closer because of depth-induced breaking and to a lesser extent because of wave refraction.

Around the canyon, the extreme sea states are consistent with the previous conclusions (statistics and spatial pattern of wave propagation). South of the canyon (points S05 and S08), the extreme sea states evolve between 4.03 m and 6.98 m depending on the return period (1 to 100 years); it is lower than the values at the north of the canyon (point S04 and especially point S09 where the values are the highest of the canyon, between 7.21 and 13.08 m). At the head of the canyon (point S06), the extreme values are the lowest with 3.61 m for the 1-year significant wave height H_{m0} and 5.43 m for the 100-year significant wave height.

Table 10 - Results of statistical extrapolation of extreme waves - France

Return period (year)	H_{m0} (m)				T_p (s)
	90% confidence interval				
	L03	**N02**	**N05**	**N07**	**All points**
1	6.99	6.38	5.58	6.40	11.5 – 15.0
	6.75-7.29	*6.15-6.63*	*5.51-5.64*	*6.20-6.59*	
10	9.86	8.96	6.03	8.08	14.0 - 17.5
	8.63-11.42	*7.86-10.35*	*5.87-6.19*	*7.45-8.78*	
100	13.56	12.32	6.37	9.75	16.5 - 20.0
	10.42-17.9	*9.44-16.31*	*6.1-6.68*	*8.42-11.47*	

Return period (year)	H_{m0} (m)					T_p (s)
	90% confidence interval					
	S04	**S05**	**S06**	**S08**	**S09**	**All points**
1	6.27	4.46	3.61	4.03	7.21	11.5 – 15.0
	6.18-6.37	*4.34-4.59*	*3.51-3.72*	*3.89-4.17*	*6.93-7.51*	
10	6.97	5.50	4.54	5.40	10.00	14.0 - 17.5
	6.73-7.25	*5.14-5.93*	*4.16-4.92*	*4.85-6.06*	*8.91-11.30*	
100	7.57	6.46	5.43	6.98	13.08	16.5 - 20.0
	7.09-8.16	*5.69-7.44*	*4.68-6.36*	*5.67-8.73*	*10.57-16.38*	

3.5.2. Spanish coast

3.5.2.1. Operational conditions

All the analyses lead to the followings remarks:

- as regards the climate **offshore** (points L11), the wave direction is mainly North-West for every month (Figure 45 and APPENDIX 6). The highest waves occur during the winter season (November to March) with H_s higher than 3 m more than 12 % of the time. It corresponds to long period waves (T_p > 10 s). During the summer season (May to September), the waves remain lower than 3 m most of the time and the periods are shorter.

  Figure 46 and Figure 47 representing the exceedance frequency of H_s and T_p confirm this. During the winter, the wave height H_s is mainly between 1.5 and 3 m (about 63% of the time for example in January) and is higher than 3 m (more than 25% of the time in January); the wave period exceeds 12 s. When the summer season approaches, the H_s and the T_p tends to decrease to reach the most frequent values between 0.5 and 1.5 m and 8 to 10 s (see example in July – the other figures are in the Excel files provided).

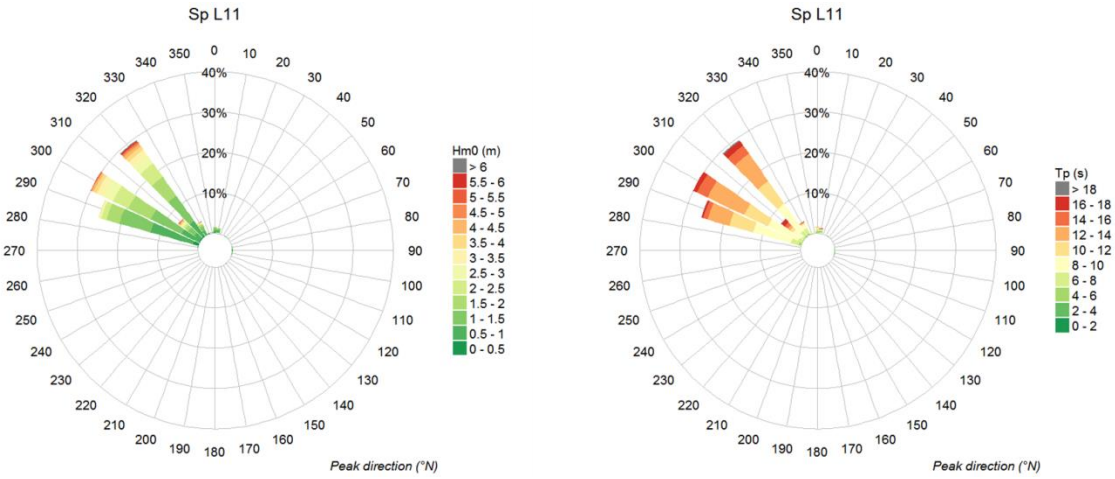

Figure 45. Annual wave rose – Point L11 - Offshore

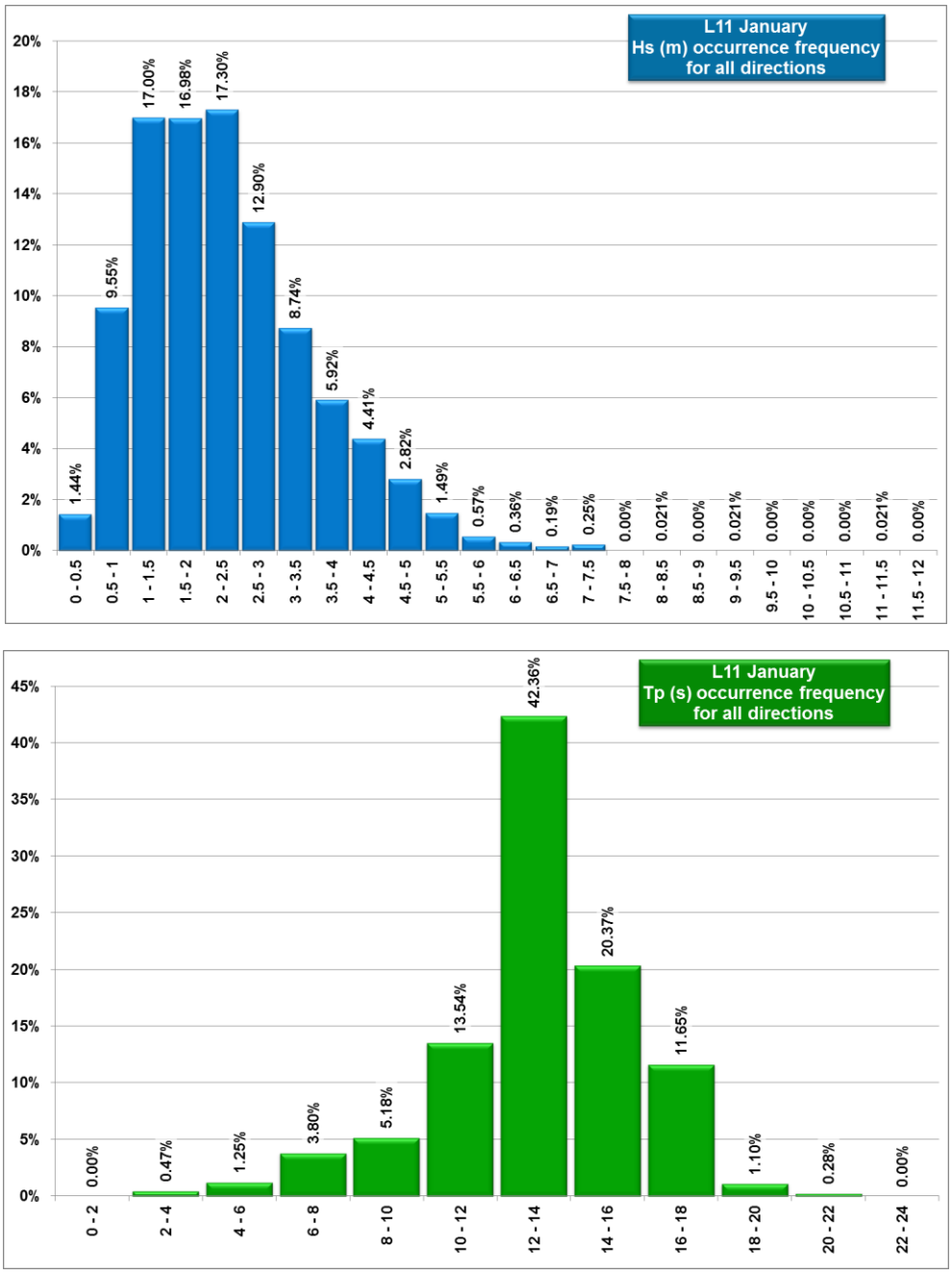

Figure 46. ***Exceedance frequency (Hs on the left side – Tp on the right side) – January - Point L11 – Offshore***

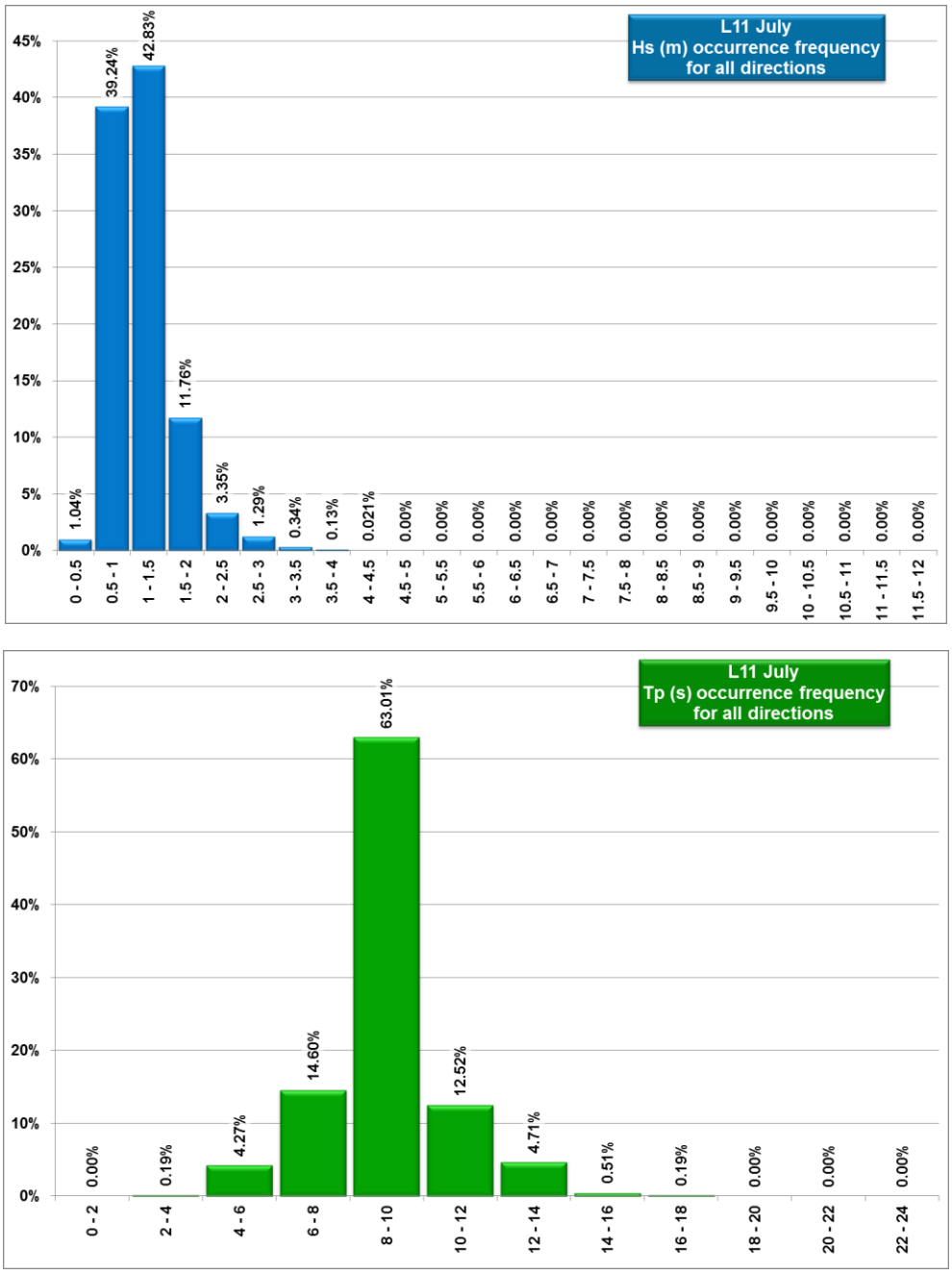

Figure 47. Exceedance frequency (Hs on the left side – Tp on the right side) – July - Point L11 – Offshore

- In front of the **landfall** (points Sp02, Sp03), the wave climates are consistent with the offshore climate. The main directions are North-West (Figure 49) with a narrower spread around the main direction near the coastline. Near the coastline (point Sp01 - Figure 48), the direction change due to refraction, the wave come mainly from the North. The highest H_s (> 3 m) and the longest periods (12-18 s) appear frequently during winter months whereas the summer season sees waves with lower H_s (0.5 to 1.5 m) and shorter period (Figure 50, Figure 51).

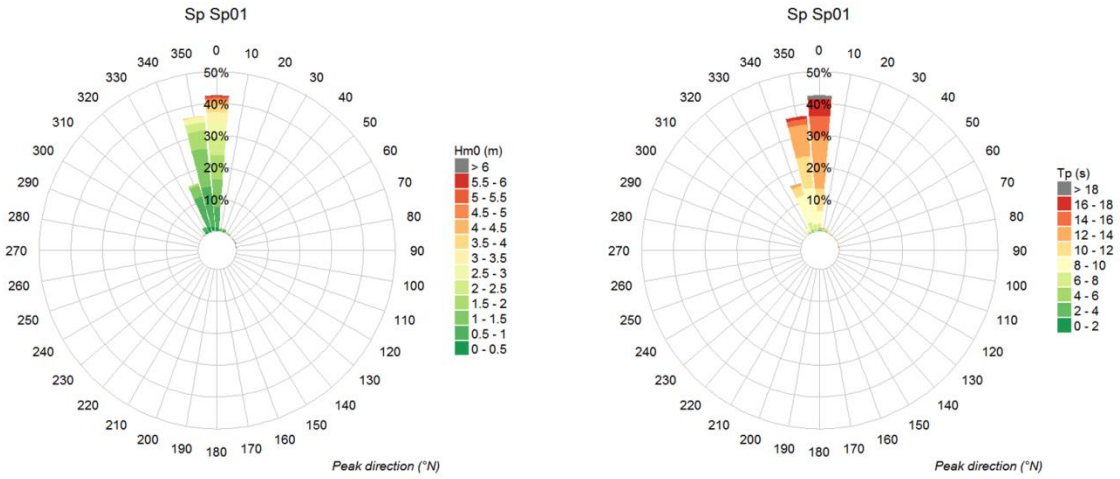

Figure 48. Annual wave rose – Point Sp01 – Coast - Landfall

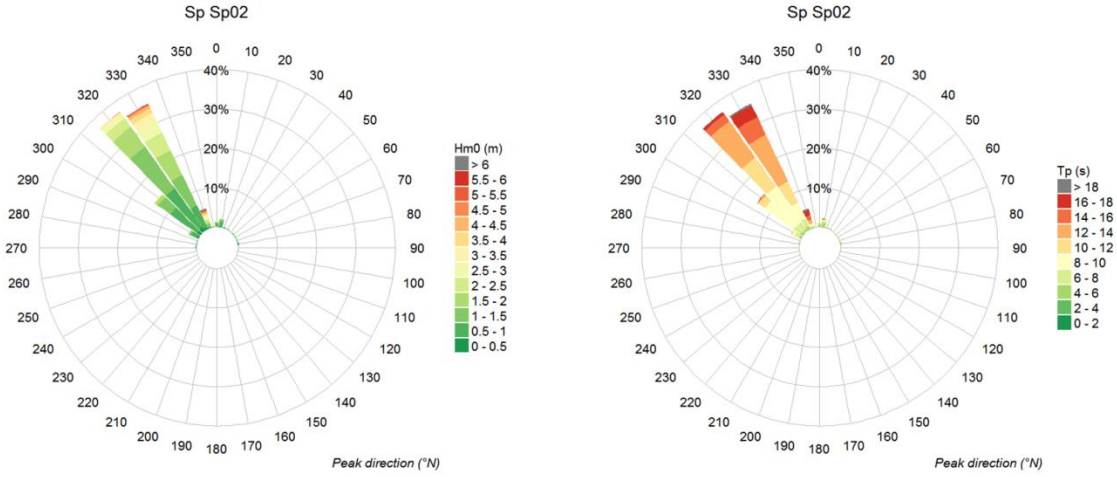

Figure 49. Annual wave rose – Point Sp02 – Coast - Landfall

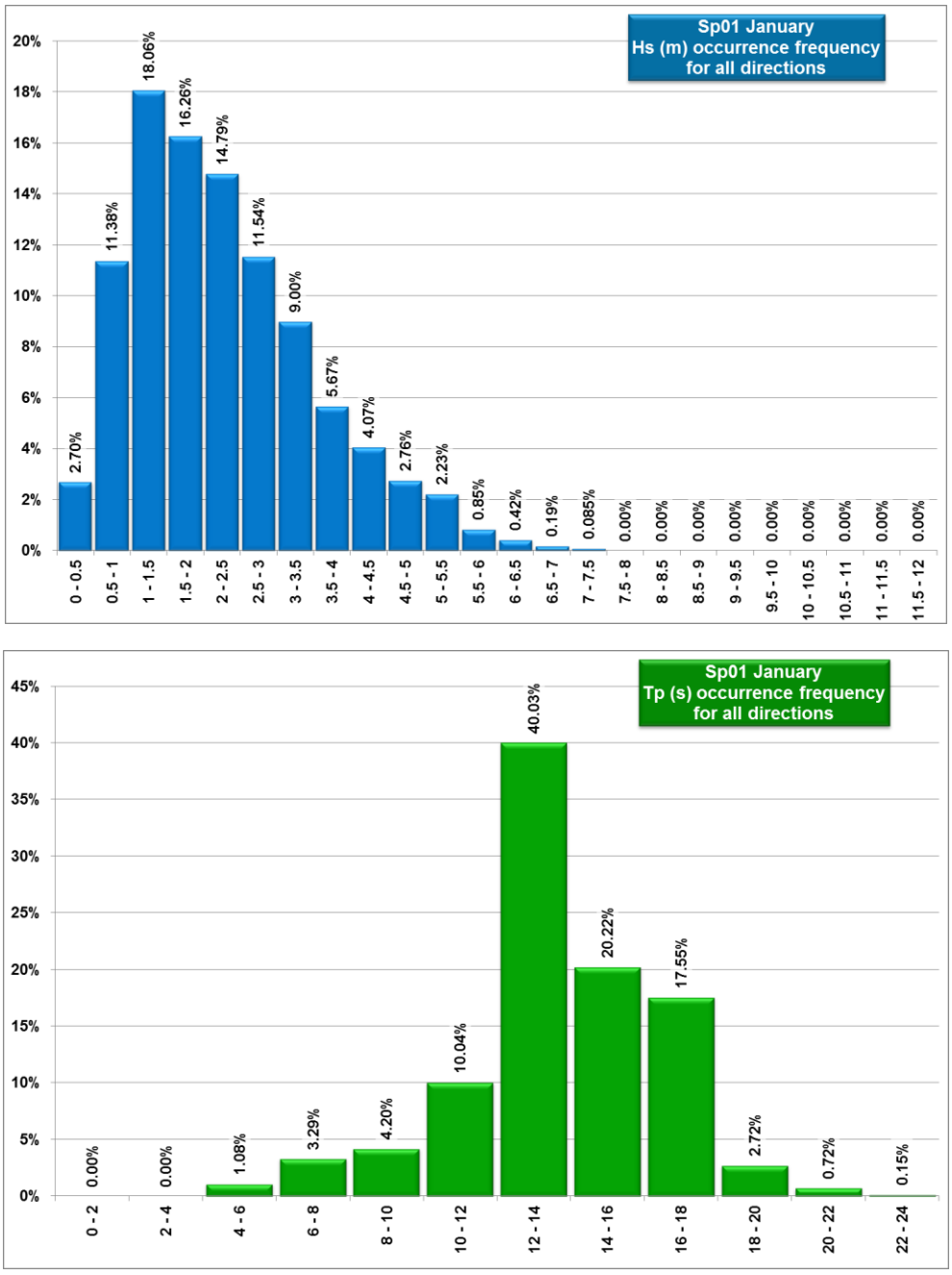

***Figure 50.** Exceedance frequency (Hs on the left side – Tp on the right side) – January - Point Sp01 – Coast – Landfall*

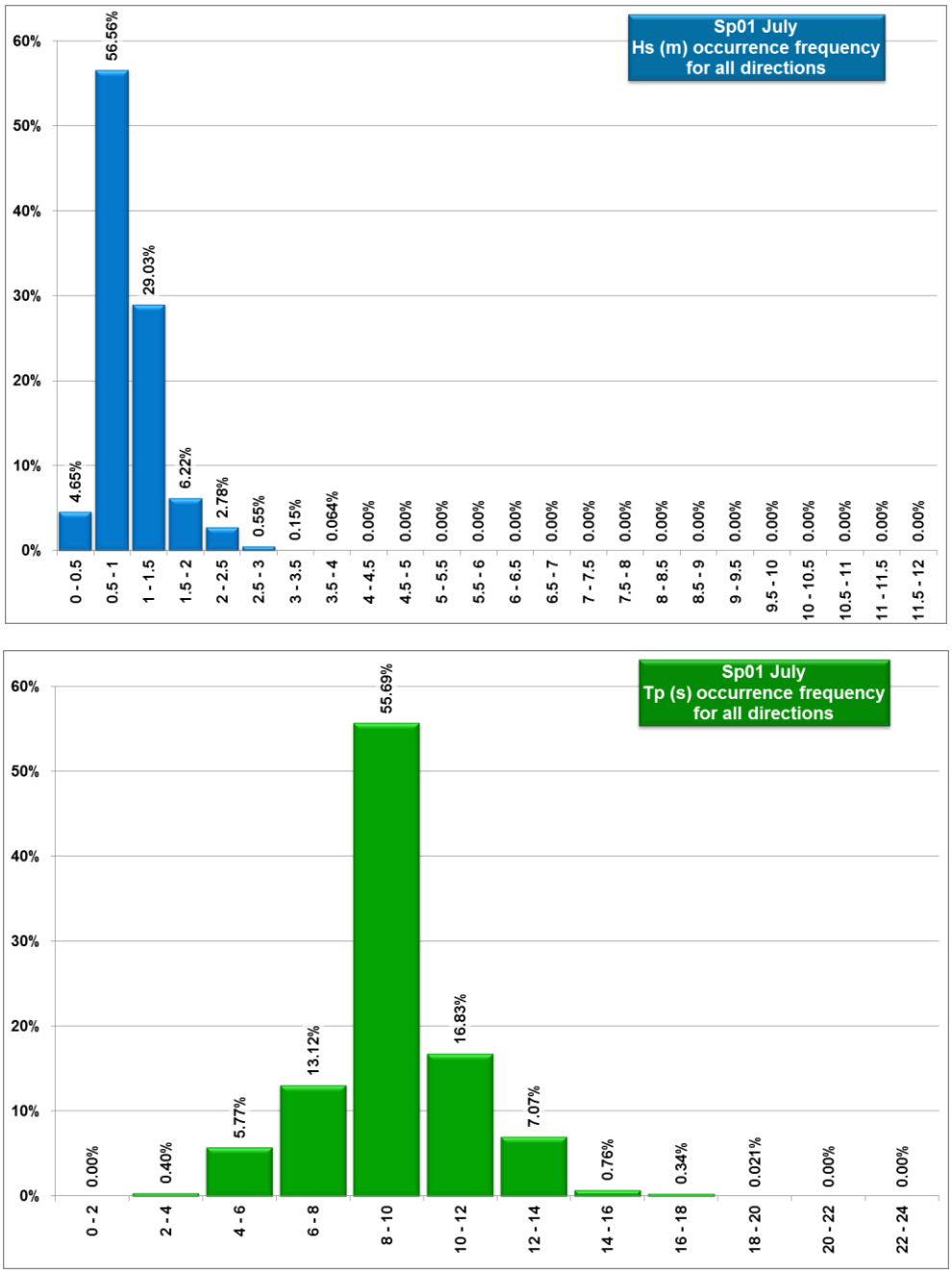

Figure 51. Exceedance frequency (Hs on the left side – Tp on the right side) – July - Point Sp01 – Coast - Landfall

The next Table 11 provides the H_{m0} and T_p values corresponding to the frequencies of exceedance of 10%, 5% and 1%.

Table 11 – Annual exceedance probability (all directions) for wave height (H_{m0}) and period (T_p) – Spain

Exceedance frequency	Point L11 *Offshore*	
	H_{m0} (m)	T_p (s)
10%	3	14.4
5%	3.6	15.8
1%	5	17.5

Exceedance frequency	Point SP01 *Landfall (south)*		Point SP02 *Landfall*		Point SP03 *Landfall - offshore*	
	H_{m0} (m)	T_p (s)	H_{m0} (m)	T_p (s)	H_{m0} (m)	T_p (s)
10%	2.9	15.2	2.7	14.9	2.95	14.1
5%	3.8	16.4	3.4	16.2	3.6	15.5
1%	5.1	18.4	4.9	18.1	4.9	17.5

It is reminded that all the figures are presented in the APPENDIX 6 and the Excel files.

- The colour maps presented in the APPENDIX 7 show the wave propagation from the offshore to the coast during specific storm events. The wave height decreases as the waves propagate towards the coast. The wave direction changes slightly to be perpendicular near the coastline due to refraction. Along the possible cable route and in the Spanish landfall, the wave conditions appear quite homogenous.

3.5.2.2. Extreme waves

The methodology used for the extreme waves analyse is presented in the chapter 3.5.1.2.1.

First, the extreme sea states have been extrapolated at the point L11, considered as the reference point (Figure 52 and Figure 53).

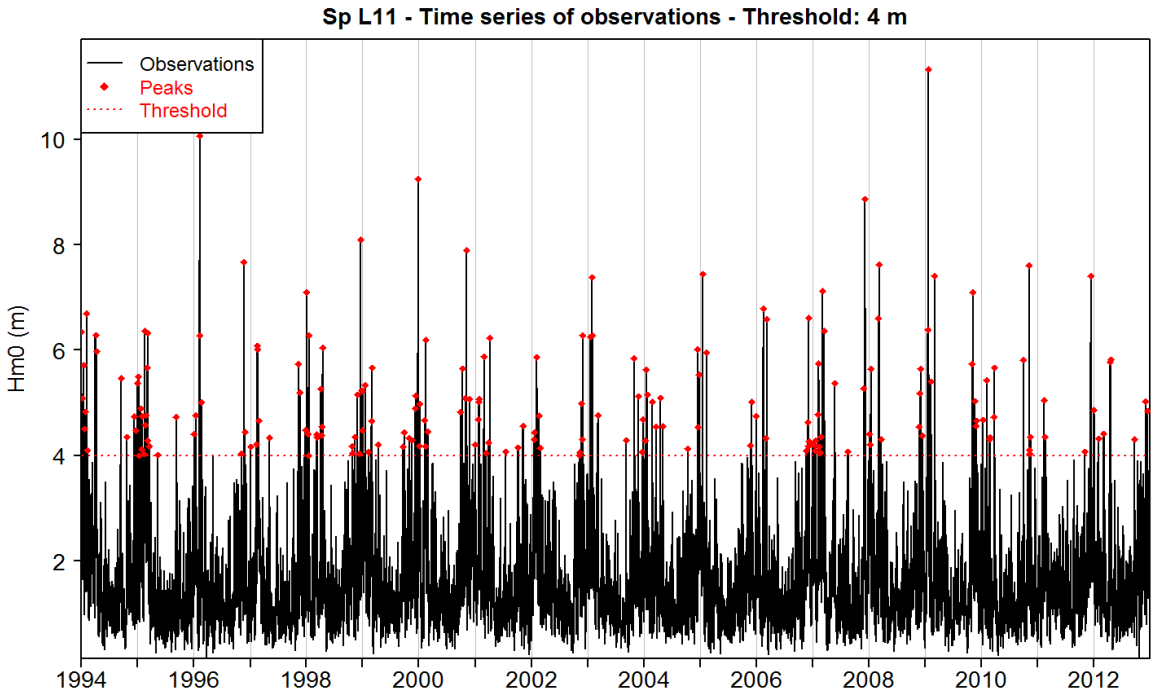

Figure 52. Point L11 - POT declustering of the H_{m0} time series

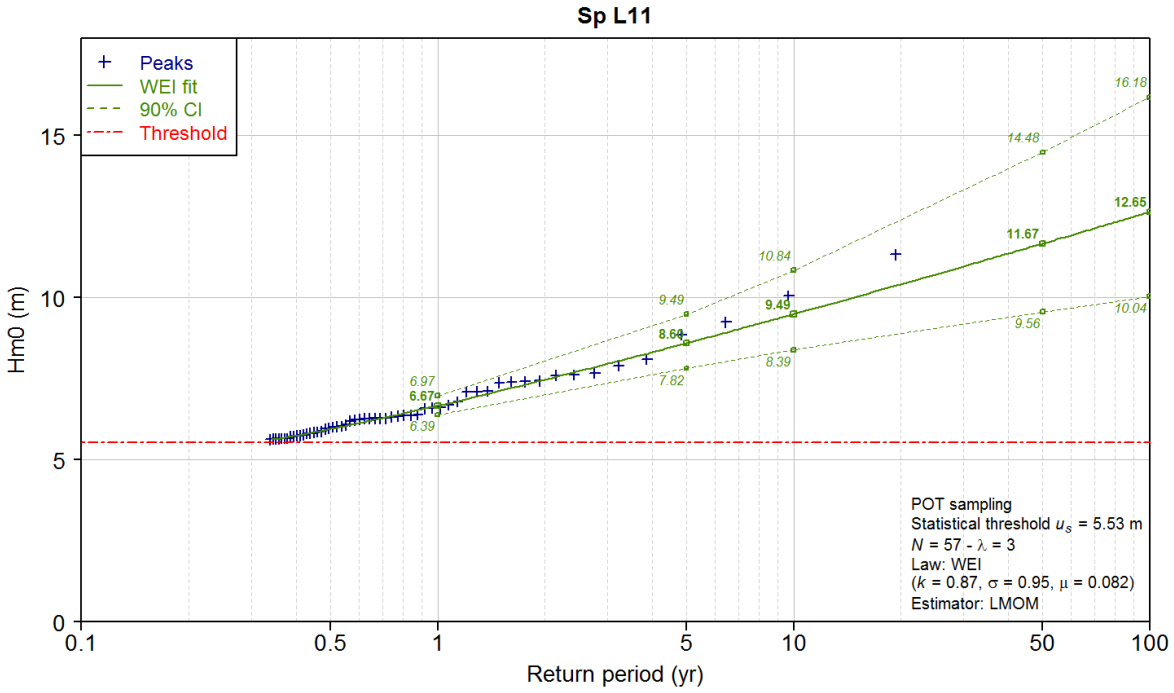

Figure 53. Point L11 – Extrapolation of storm peaks by a Weibull distribution

Then the extreme sea states are extrapolated at the other analysed points that are consistent with the choices made for the reference point (in particular choice of the statistical threshold u_s and of the statistical distribution). This approach provides consistent results over the whole set of output points.

Table 12 sums up the results presented in detail in APPENDIX 8. At the offshore (point L11), the 1-year significant wave height H_{m0} reaches 6.67 m and the 100-year significant wave height H_{m0} reaches 12.65 m with a large confidence interval (between 10.04 m at the lower bound of the interval and 16.18 m at the upper bound of the interval). The extreme values are less important than on the French side (point L03 offshore).

Near the coastline, the 1-year significant wave heights are in the same order of magnitude (6.24 m at point Sp01 to 6.66 m at point Sp02). The 100-year significant wave heights are also consistent for the points Sp02 and Sp03 (12.59 m and 12.14 m) whereas it is lower at the point Sp01 much closer to the coastline (8.69 m).

Table 12 - Results of statistical extrapolation of extreme waves - Spain

Return period (year)	H_{m0} (m) *90% confidence interval*				T_p (s)
	L11	**Sp01**	**Sp02**	**Sp03**	**All points**
1	6.67 *6.39-6.97*	6.24 *6.07-6.41*	6.66 *6.33-7.02*	6.63 *6.36-6.94*	11.5 - 17.0
10	9.49 *8.39-10.84*	7.56 *7.08-8.06*	9.61 *8.51-10.87*	9.34 *8.3-10.55*	14.5 - 20.0
100	12.65 *10.04-16.18*	8.69 *7.76-9.36*	12.59 *10.21-15.61*	12.14 *9.86-15.08*	17.0 - 22.5

oOo

4. WINDS

These statistics are based on the HOMERE database from which the hourly wind values have been extracted in 3 locations along the French coast and 2 locations along the Spanish coast, during 19 years (1994 – 2012).

For each analysis points, operational conditions have been assessed for key wind parameters (W_s,W_{dir}):

- annual wave roses;
- correlogramm wind speed/wind direction;
- exceedance frequency of w_S logarithmic plot.

4.1. FRENCH COAST

Annual wind statistics are presented in the present chapter and in the APPENDIX 9.

4.1.1. Output points

Considering the wind source resolution (CFSR wind fields with the resolution of about 0.5°) and the HOMERE mesh, the output points are located as shown in Figure 54:

- one point along the probable cable, about 10 km in front of the landfall area (point W1);
- one point along the probable cable between the landfall area and the canyon, 10 km offshore (point W2);
- one point in the canyon area (point W3).

The coordinates of the analyzed points are specified in the next Table 13.

Figure 54. Wind analysis – France - Output location

Table 13 – Coordinates (WGS84 - UTM30N) of the output points

Point	X	Y	Area
W01	629 669.99	4 976 209.45	Landfall
W02	627 583.23	4 907 433.08	Large / Landfall
W03	623 623.620	4 835 828.48	Canyon

4.1.2. Results

The wind roses are quite spread for the three points; all the wind directions appear between 2 and 4% of the time. More than 50% of the time, the wind speed evolves between 3 and 7 m/s at the points W01 and W02. At the point W03 which is closer to the coast, the wind speed is mainly between 1 and 5 m/s.

The next Table 14 presents the wind speed values for the annual exceedance frequency (1%, 5% and 10%).

Table 14 – Annual exceedance frequency (all directions) for wind speed (W_s) – French side

Exceedance frequency	Point W01 *Landfall*	Point W02 *Probable Cable*	Point W03 *Canyon*
	W_s (m/s)	W_s (m/s)	W_s (m/s)
10%	9.6	8.5	6.5
5%	10.8	10	7.8
1%	14.5	13	10.5

4.2. SPANISH COAST

Annual wind statistics are presented in the present chapter and in the APPENDIX 10.

4.2.1. Output points

Considering the wind source resolution (CFSR wind fields with the resolution of about 0.5°) and the HOMERE mesh, the output points are located as shown in Figure 55:

- one point along the probable cable, about 7 km offshore (point W4);
- one point along the probable cable about 2 km in front of the landfall area (point W5);

The coordinates of the analyzed points are specified in the next Table 15.

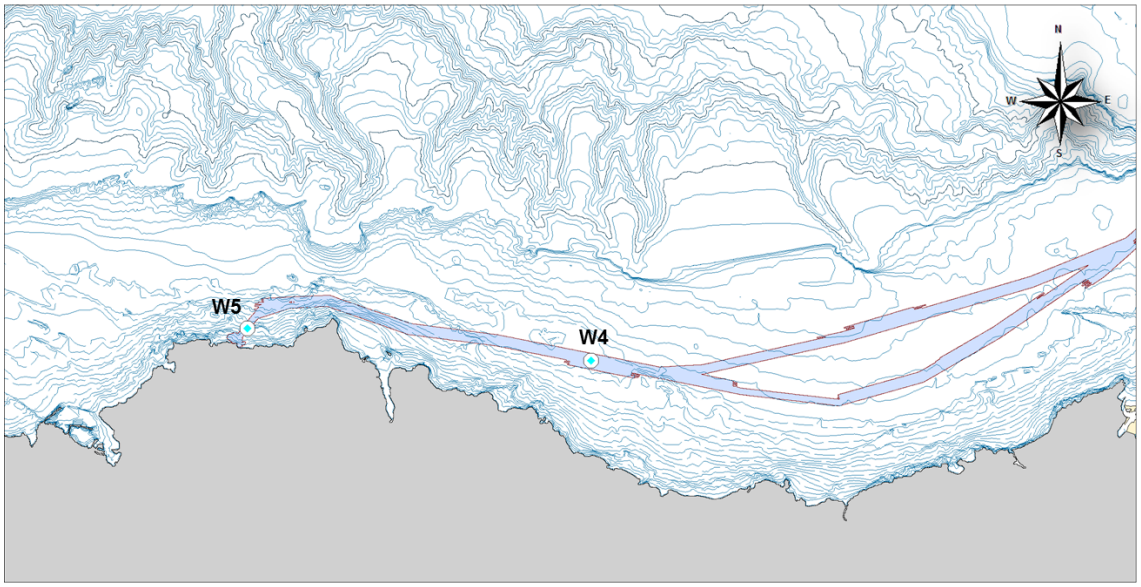

Figure 55. Wind analysis – Spain - Output location

Table 15 – Coordinates (WGS84 - UTM30N) of the output points

Point	X	Y	Area
W04	545 473.88	4 807 422.18	Large
W05	511 603.42	4 810 611.30	Landfall

4.2.2. Results

The wind roses are quite spread; all the wind directions appear at least 4 % of the time. However the direction North-West is slightly more present (around 5% at point W04 and almost 6% at point W05).

More than 55% of the time, the wind speed evolves between 3 and 7 m/s at the points W04 and W05.

The next Table 16 presents the wind speed values for the annual exceedance frequency (1%, 5% and 10%).

Table 16 – Annual exceedance frequency (all directions) for wind speed (W_s) – Spanish side

Exceedance frequency	Point W04 *Landfall*	Point W05 *Probable Cable*
	W_s (m/s)	W_s (m/s)
10%	8.5	8.9
5%	10.0	10.4
1%	13.3	13.6

oOo

5. HYDRODYNAMICS

5.1. MODELLING STRATEGY

A two-dimensional hydrodynamic model has been set up in order to provide on-site long-term time series of sea levels and depth-averaged currents. The results of the model inform the analysis of astronomical water levels, residual (due to meteorological conditions) water level, tidal currents.

The hydrodynamic model is forced at its maritime boundary by astronomical tide, extracted from a larger hydrodynamic model of ocean tides, and at its free surface by atmospheric conditions with wind and pressure fields. For a better representativeness, the general oceanic currents extracted from a global model are also added.

In-situ tidal measurements at the SHOM tide gauges within the modelling area are used for validation of water levels. Currents are compared with tidal stream data indicated on nautical SHOM charts for validation.

5.2. SOFTWARE

The hydrodynamic model developed for the present study is based on the software TELEMAC-2D, part of the TELEMAC-MASCARET system, owned by EDF R&D and developed by a consortium of core organizations including ARTELIA (www.opentelemac.org).

The TELEMAC-2D software solves the equations that govern the dynamics of so-called free-surface flows. It thus calculates time-dependent changes in water levels and currents at any point in the study area. With regard to currents, it calculates both the direction and intensity (i.e. flow speed) in two-dimensions (averaged over the water depth).

5.3. MODEL SETUP

5.3.1. Model area

The model area is presented on the Figure 56. The maritime boundaries were placed sufficiently far offshore to avoid edge effects on the currents along the cable route and at the landfalls . Its characteristic dimensions are more than 200 km northward and about 180 km westward.

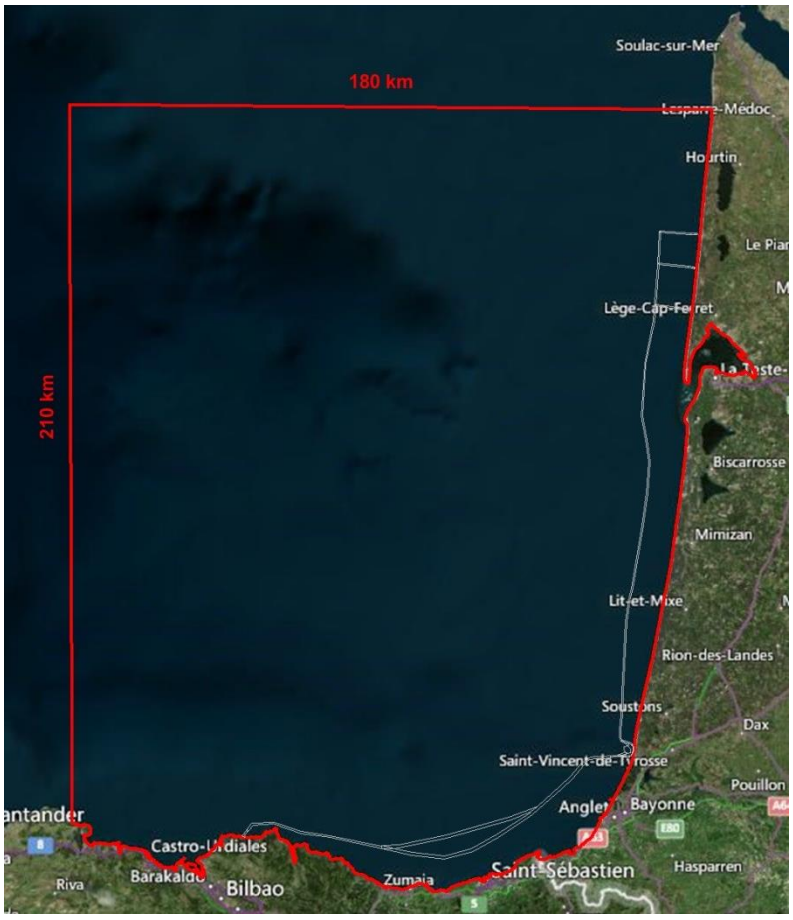

Figure 56. Hydrodynamic model area

5.3.2. Mesh

The unstructured computational grid, known as the mesh, is composed of triangles of different sizes according to interest zones. In the present study, the size of the mesh is about 5 km in the offshore areas and is reduced to 200 m along the cable route. Particular attention has been paid to the canyon and the slope of the continental shelf. In these areas, the mesh lfollows specific constraint lines to adequately represent the bathymetry gradients.

The model is composed of more than 67 000 nodes and 133 000 elements. Figure 57 shows the mesh grid of the model area.

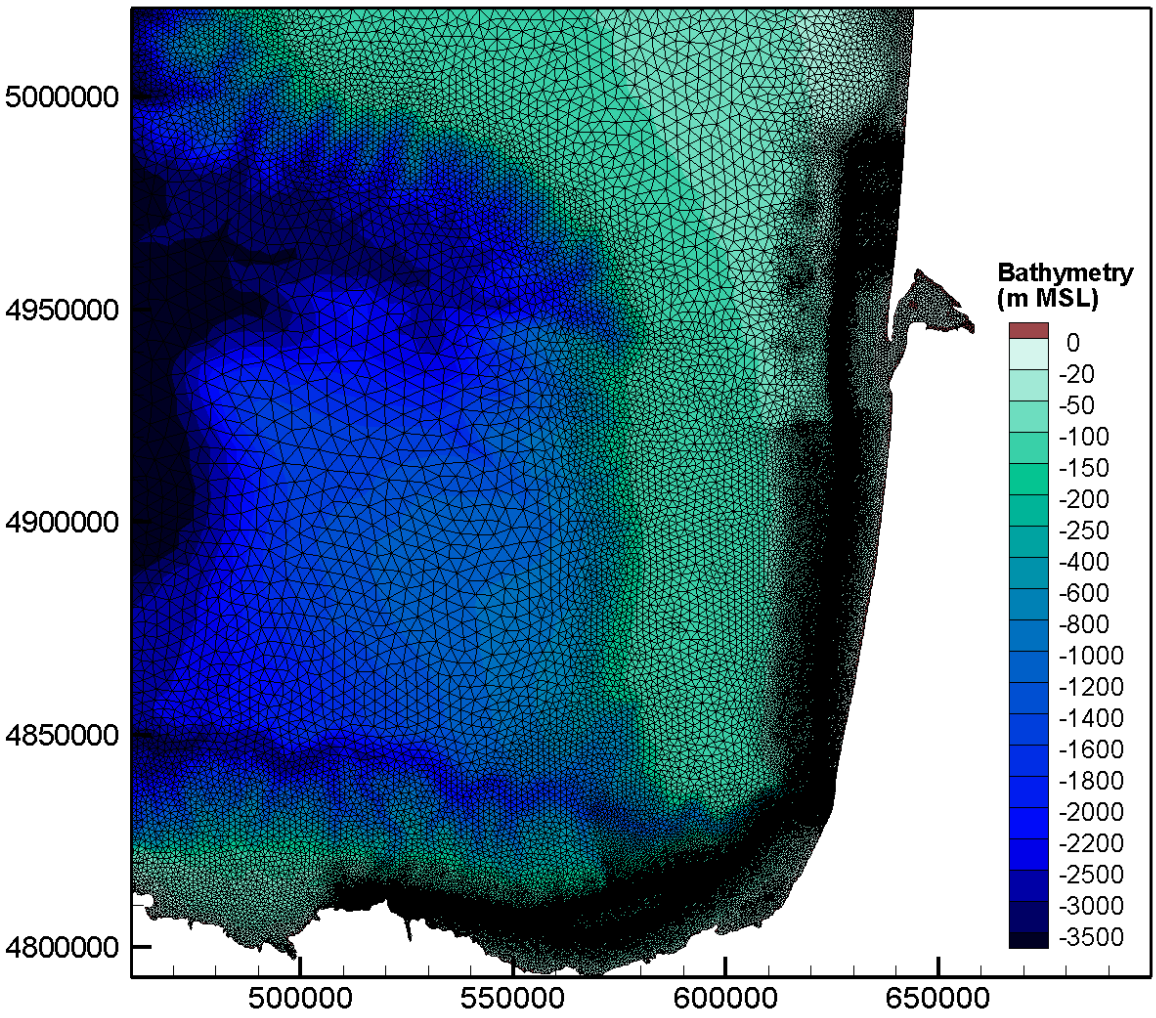

Figure 57. Mesh and bathymetry of the hydrodynamic model

The next Figure 58 shows zooms of the mesh grid on the landing zones.

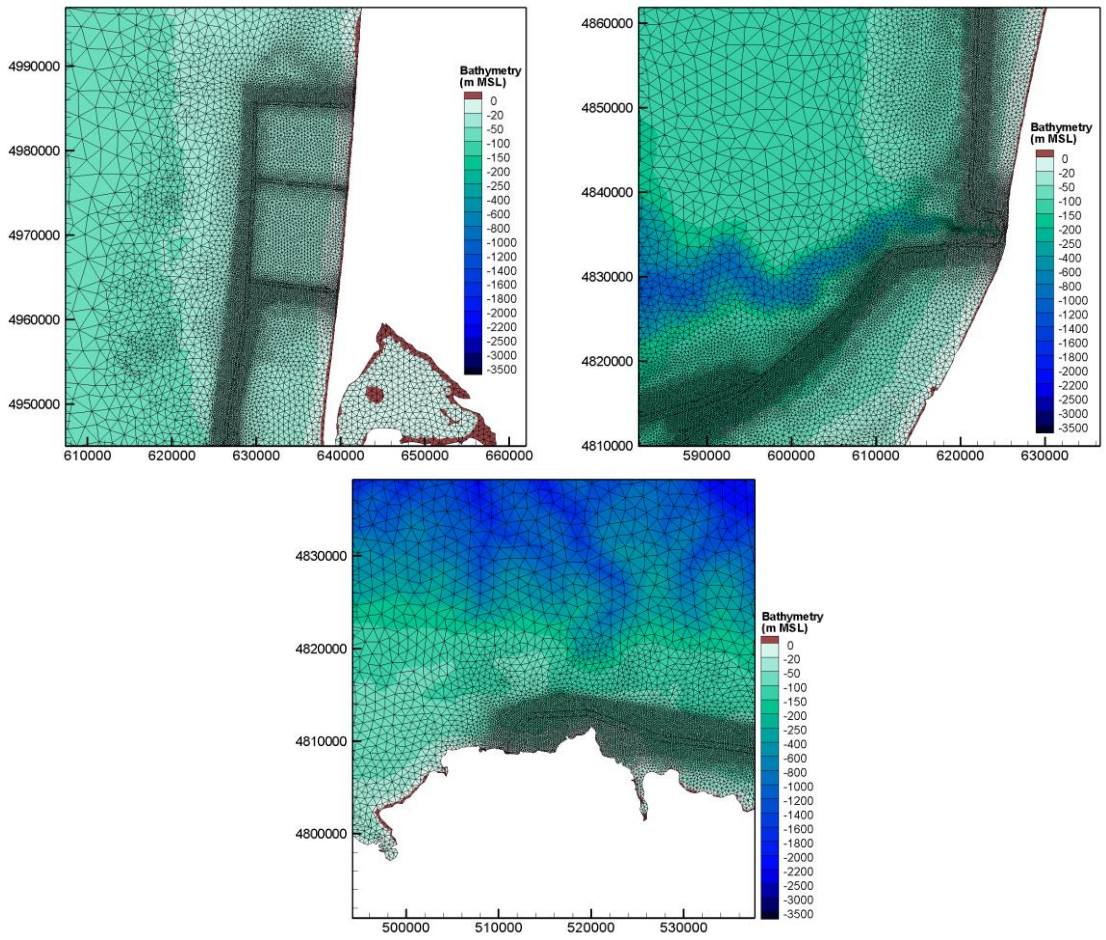

Figure 58. Mesh and bathymetry zooms on Lacanau landfall (top left), Capbreton canyon (top right) and Bilbao landfall (bottom)

5.3.3. Forcing data

The hydrodynamic model is forced at its maritime boundary by astronomical tide, extracted from a larger hydrodynamic model of ocean tides, and on its entire domain (source terms) by atmospheric conditions (wind and pressure fields) and general oceanic currents.

5.3.3.1. Tide

The astronomical tide data (sea level and currents) are extracted from the global model of ocean tides FES-2012 (Ref. [6]), built on the combination of hydrodynamic model and altimeter measurements. The data returned are the amplitude and phase of 32 tidal components distributed over a 1/16 degree grid.

5.3.3.2. Atmospheric forcing

The hydrodynamic model is forced on its surface by wind field coming from the HOMERE database developed by Ifremer and by atmospheric pressure field provided by the ECMWF (European Centre for Medium-Range Weather Forecasts) database. The initial temporal resolution is 1 hour for wind data and 6 hours for pressure data. They are re-interpolated spatially and temporally for the hydrodynamic modelling.

To check the consistency of atmospheric forcing data (wind and pressure) and choose the best data source, some comparisons have been realised. The Figure 59 present the comparison between wind measurement at the buoy Bilbao-Vizcaya and data provided by the HOMERE database at the same location over the 1994-2012 period.

Buoy measurement

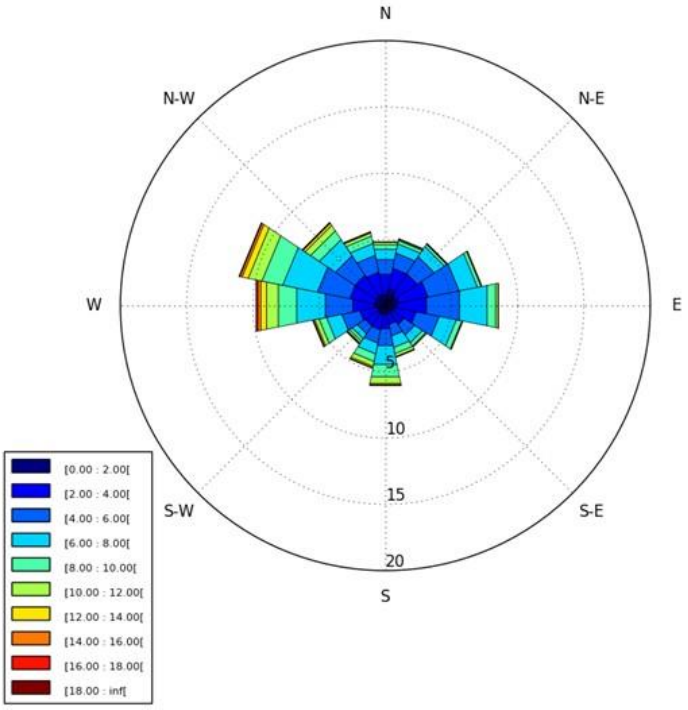

HOMERE database

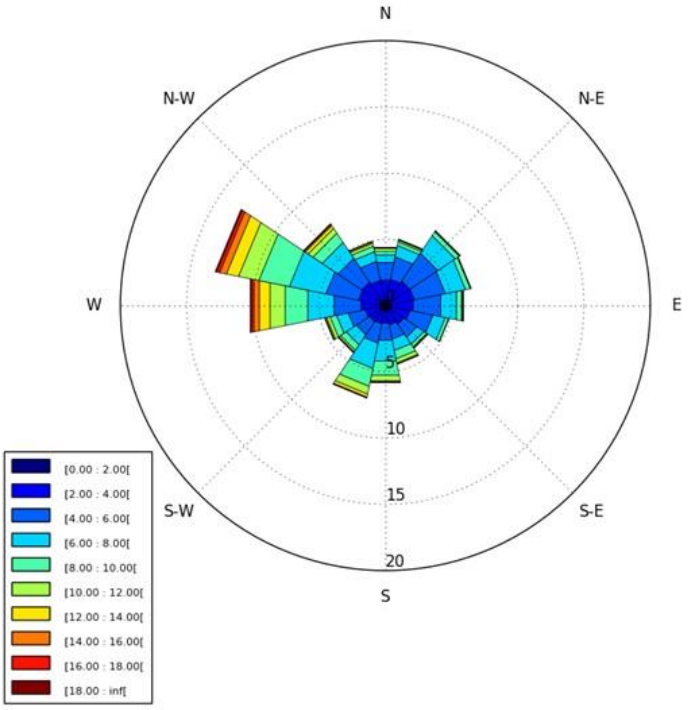

Figure 59. Wind roses comparison between measurement (left) and HOMERE database (right)

The wind distribution is similar between the measurements and the database. The main direction is west to northwest.

Figure 60 presents the comparison of atmospheric pressure between the measurement at the buoy and data from the ECMWF model.

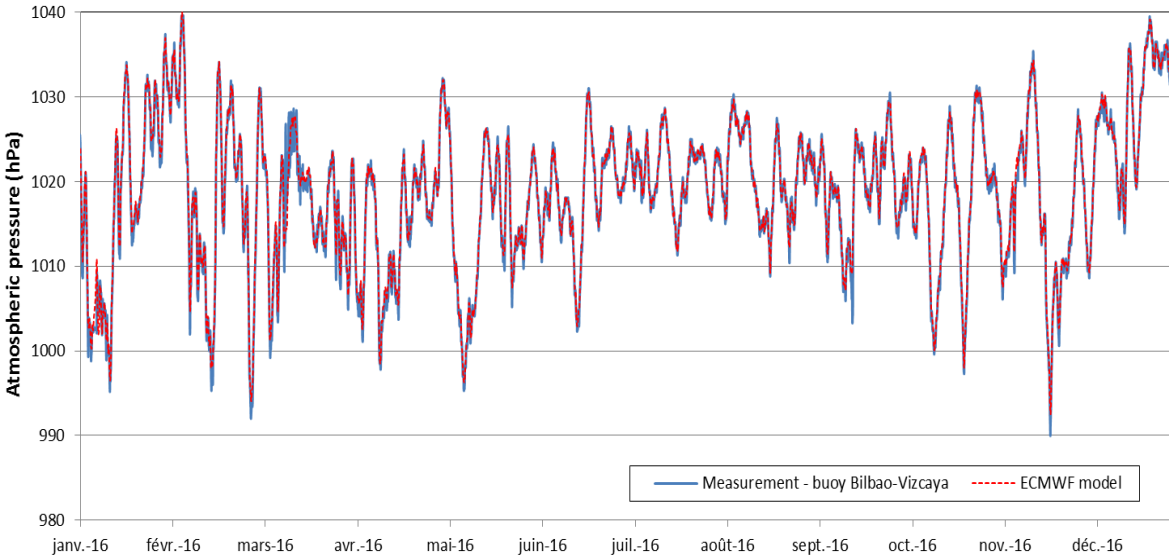

Figure 60. Validation of pressure data

At the buoy location, the agreement between the atmospheric pressure data of the ECMWF model and the measurements is very good.

5.3.3.3. Global oceanic currents

Global oceanic currents are extracted from the global re-analyze GLORYS2V3 or the high resolution global analysis and forecasting system PSY4V3R1. These models are based on a general circulation model of the oceans and on a method of data assimilation (Ref.[7]). They provide 3D daily mean fields of temperature, salinity and current throughout the whole water column on a regular grid at 1/4 or 1/12 degree. Data are then re-interpolated spatially and temporally and are imposed as a source flux (like assimilation) on the hydrodynamic model area.

5.4. VALIDATION

The validation of the model was carried out from 1st of October to 16th of November 2016. This period corresponds to the unique period long sufficient to support the calibration and for which all the data are available.

- the sea levels computed are compared with tide gauge measurements at Arcachon, Bilbao and Saint Jean de Luz and;
- currents (intensity and direction) are compared with the buoy of Bilbao-Vizcaya measurements and the nautical SHOM charts within the Biscay Gulf.

The positions of the tide gauges are indicated in red and the buoy (Bilbao-Vizcaya) is in yellow on next Figure 61.

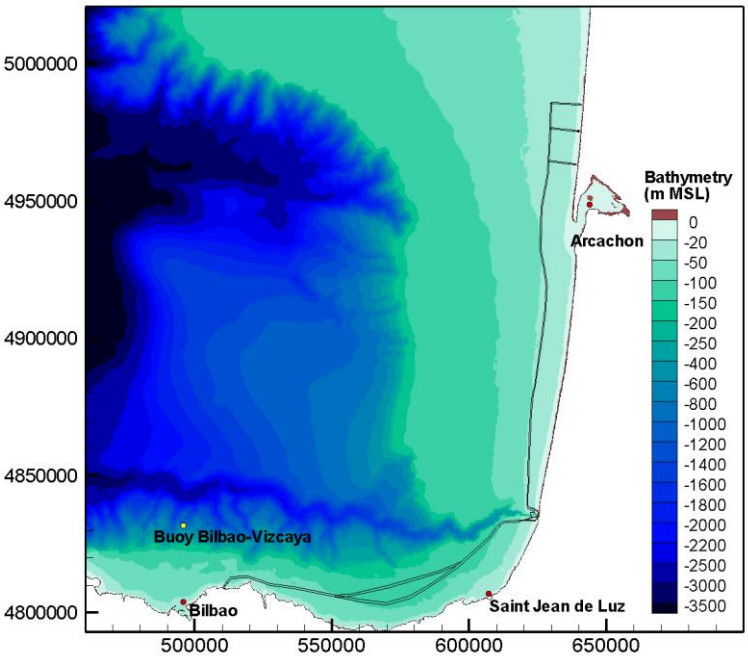

Figure 61. Tide gauges and buoy position

5.4.1. Sea levels validation

The sea levels computed by the hydrodynamic model were compared with the measurements at the SHOM and Puertos Del Estado tide gauges available: Saint-Jean-de-Luz and Arcachon for the French coast and Bilbao for the Spanish coast. Results for the period from 1st to 16th of November are presented in Figure 62.

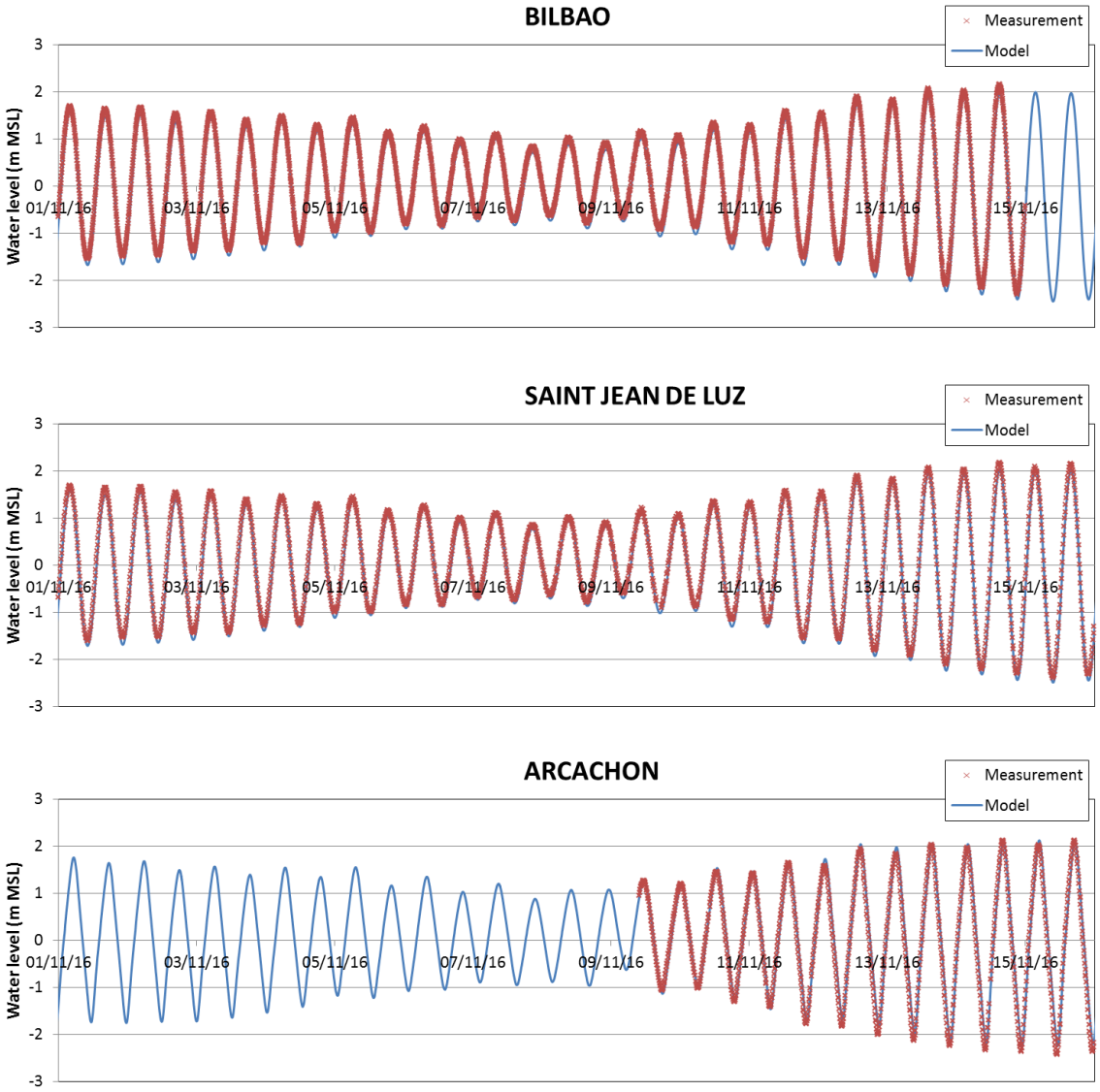

Figure 62. Comparison of modelled vs measured sea levels

The levels at low tide are slightly overestimated at Bilbao and Saint-Jean-de-Luz stations nevertheless, the representation of the model is good over the whole period.

Various statistics were computed to quantify the fit between model and measured values. They are described and computed hereafter (Table 17).

Table 17 – Definition of statistical variables

Variables	Definition
MAE	Mean Absolute Error $= \frac{1}{N}\sum_{i=1}^{N}\lvert e_i \rvert$
RMSE	Root-mean-square error $= \sqrt{\frac{1}{N}\sum_{i=1}^{N} e_i^2}$
CF(X)	Part (percentage) of error included in the interval $[-X; X]$
POF(X)	Part (percentage) of error upper to X
NOF(X)	Percentage of modelled sea levels which are at least X (strictly) greater than observed sea levels.

In our case, the variables are calculated for X is equal to 0.10 m.

The results of the model validation are presented below. These indicate good agreement between model and measured values. The quality of the results in the Bassin d' Arcachon is lower than for the other 2 gauges because the model does not represent the basin accurately.

Table 18 – Statistical analysis

Variables	Bilbao	Saint-Jean-de-Luz	Arcachon
MAE (cm)	2.7	3.3	9.9
RMSE (cm)	3.5	4.2	11.7
CF(X) (%)	99.5	97.7	54.4
POF(X) (%)	0.4	1.4	26.9
NOF(X) (%)	0.1	0.9	18.7

In addition, the residual water level for model and measured values (Averaged over 12 hours) at Bilbao and Saint-Jean-de-Luz stations are compared (data series at Arcachon is too short for analysis). The results are presented in Figure 63.

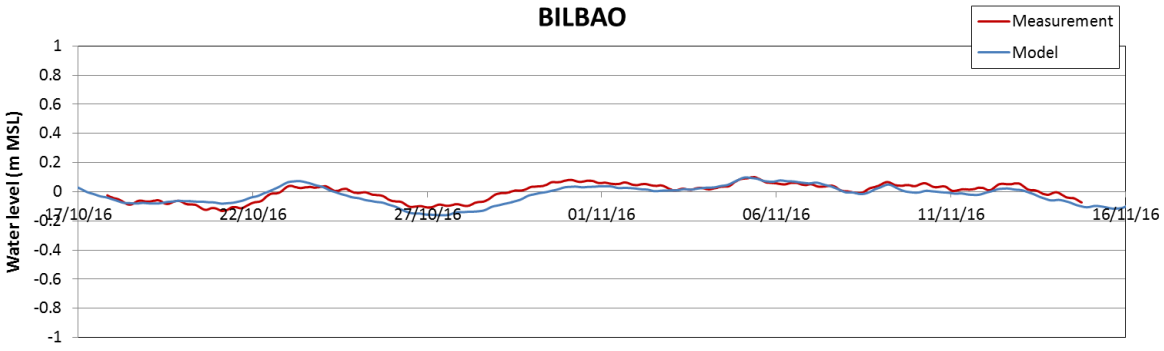

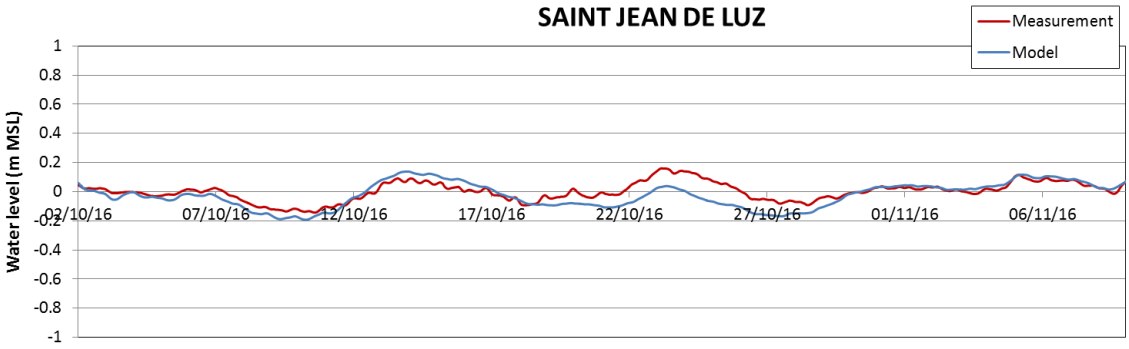

Figure 63. Comparison of modelled vs measured residual sea levels

The variation in time of residual sea level is mainly caused by meteorological phenomena. The good agreement between model and measured values shows that the atmospheric conditions (wind and pressure) are sufficiently represented by the model.

In conclusion, the representation of sea level is very good over the entire period. The model is able to reproduce the astronomical water levels and the meteorological water levels.

5.4.2. Tidal current validation

Model currents were compared with tidal stream data indicated on nautical SHOM charts. The comparison is presented on Figure 64 to Figure 67 for 4 tidal instants. In order to be in agreement with the nautical charts, the current velocity is exceptionally indicated in knot[2].

[2] 1 knot = 0.514 m/s

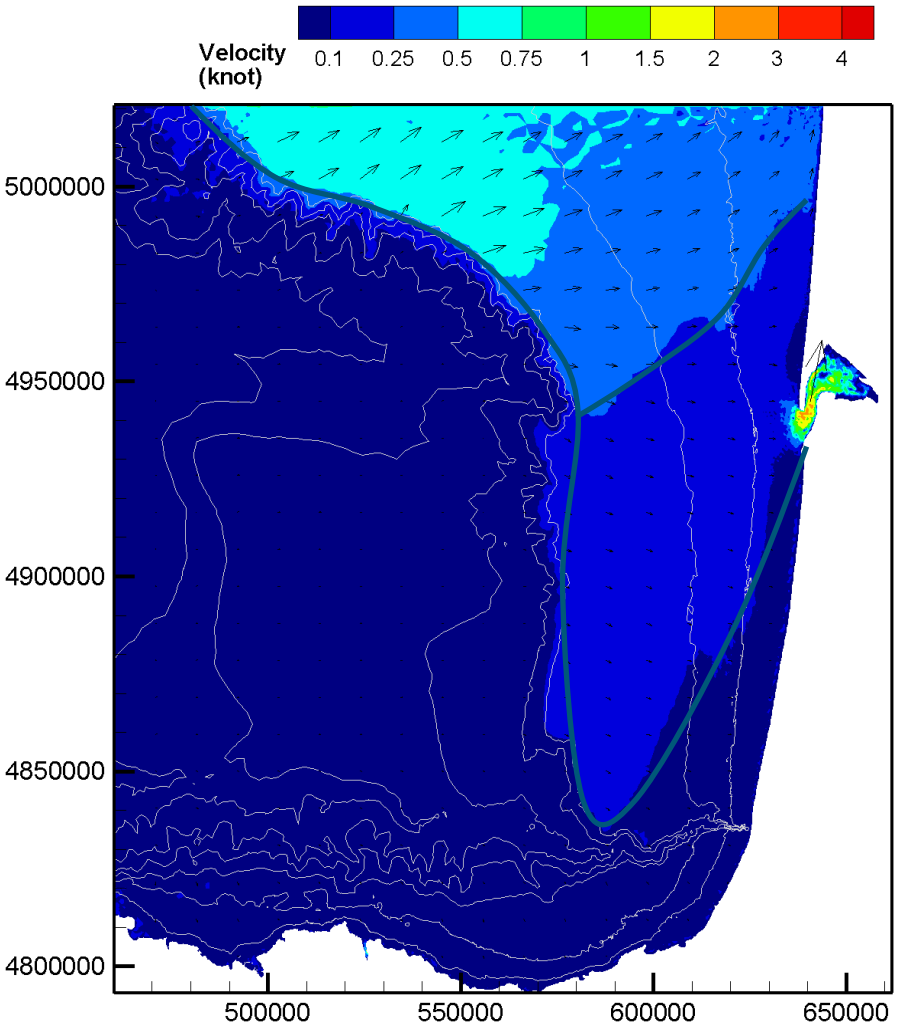
Velocity
(knot)
0.1
0.25
0.5
0.75
1
1.5
2
3
4
5000000
4950000
4900000
4850000
4800000
500000
550000
600000
650000

Model

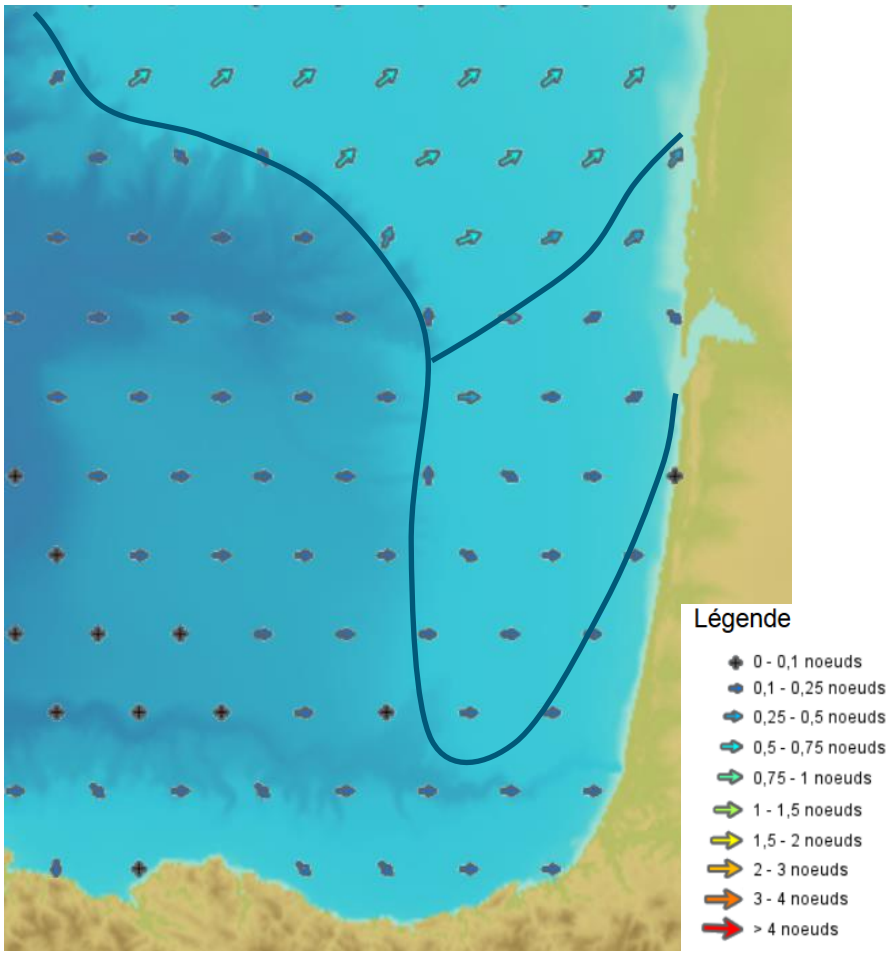

Nautical chart

Figure 64. Tidal currents 2h25' before high tide at Saint-Jean-de-Luz – Spring tide: model on the top, nautical SHOM chart on the bottom

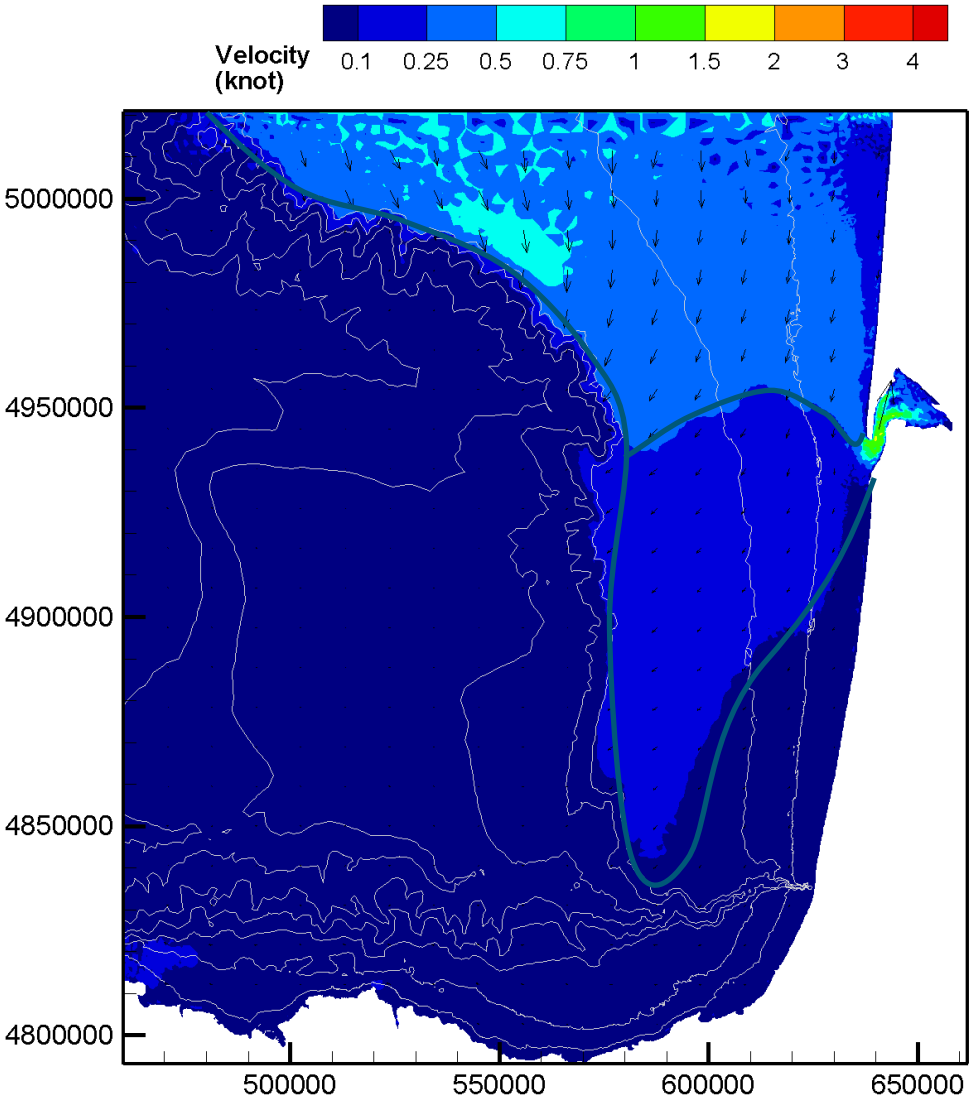
Velocity
(knot)
0.1
0.25
0.5
0.75
1
1.5
2
3
4
5000000
4950000
4900000
4850000
4800000
500000
550000
600000
650000
Model

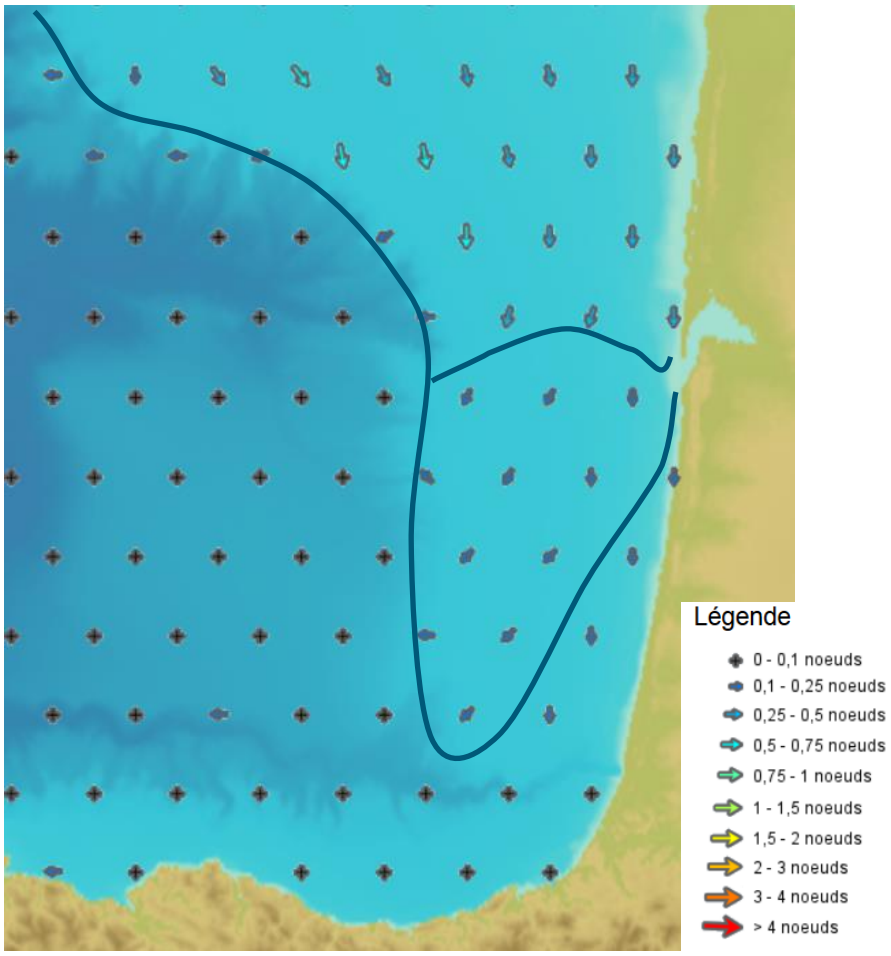

Nautical chart

Figure 65. Tidal currents 35' after high tide at Saint-Jean-de-Luz – Spring tide: model on the top, nautical SHOM chart on the bottom

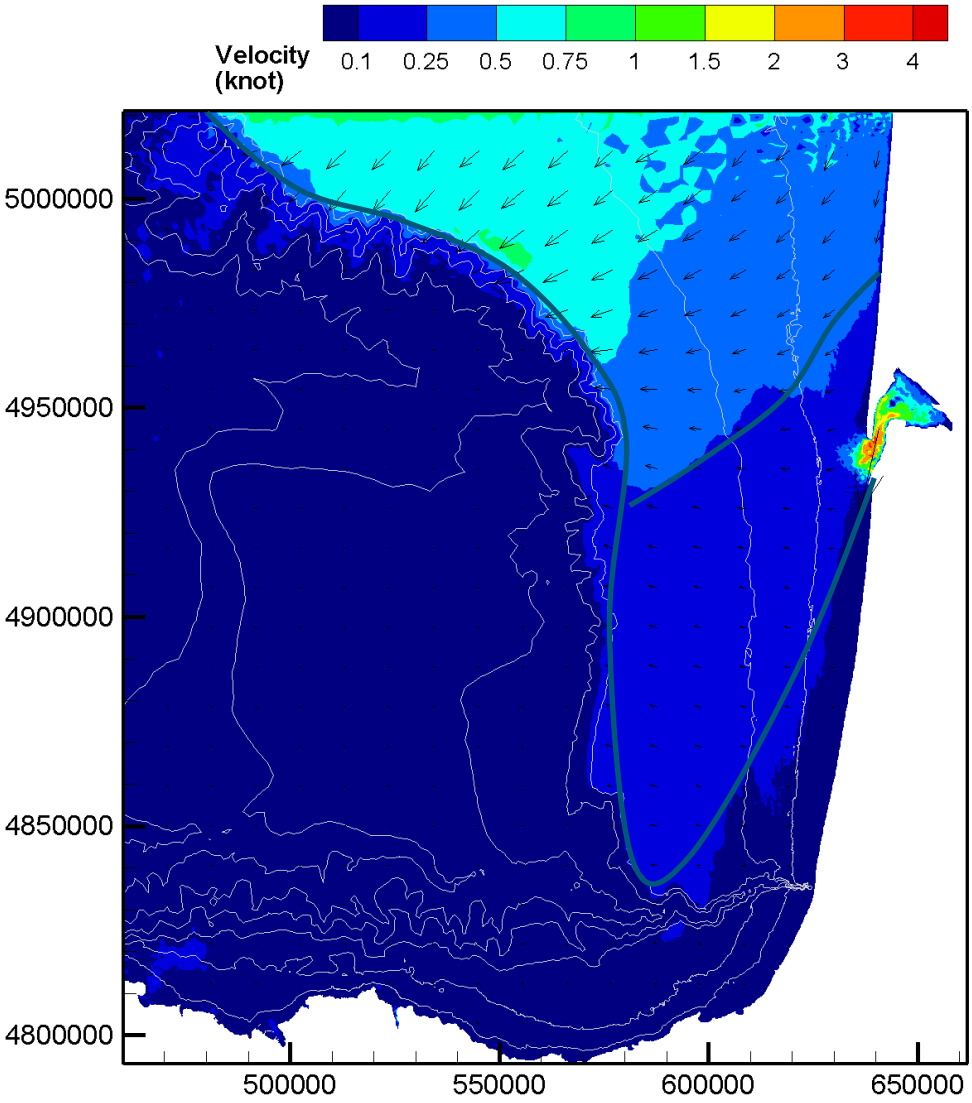
Velocity
(knot)
0.1
0.25
0.5
0.75
1
1.5
2
3
4
5000000
4950000
4900000
4850000
4800000
500000
550000
600000
650000
Model

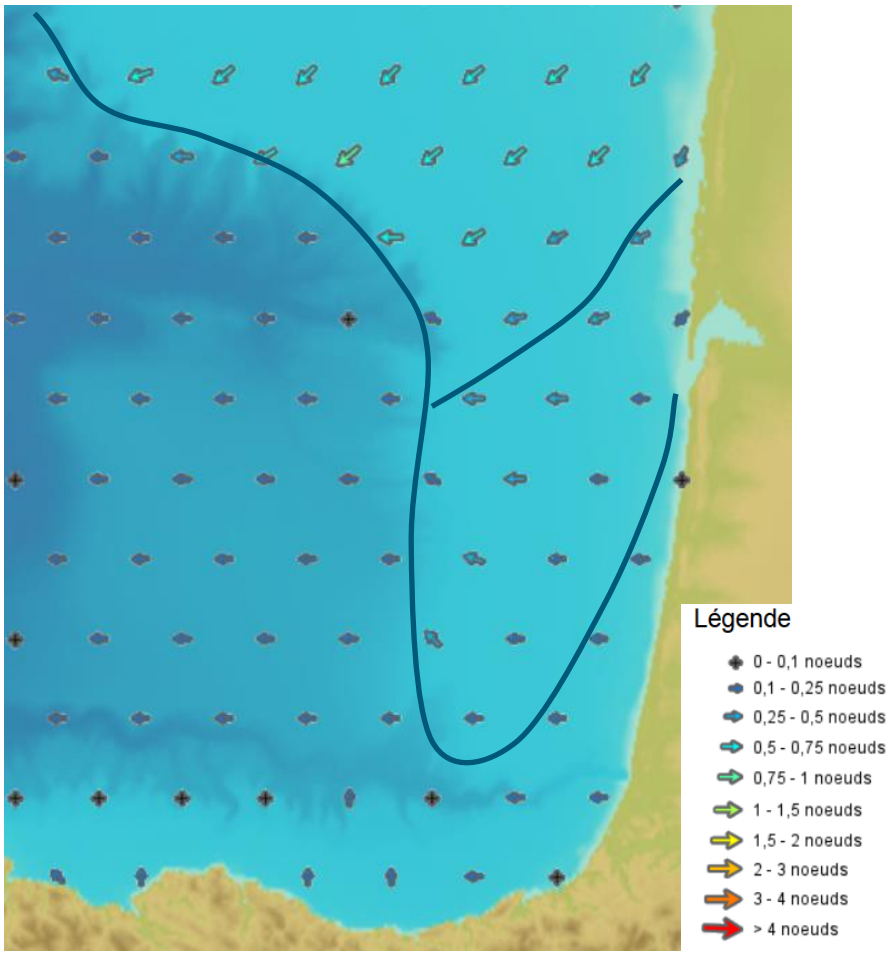

Nautical chart

Figure 66. Tidal currents 3h35' after high tide at Saint-Jean-de-Luz – Spring tide: model on the top, nautical SHOM chart on the bottom

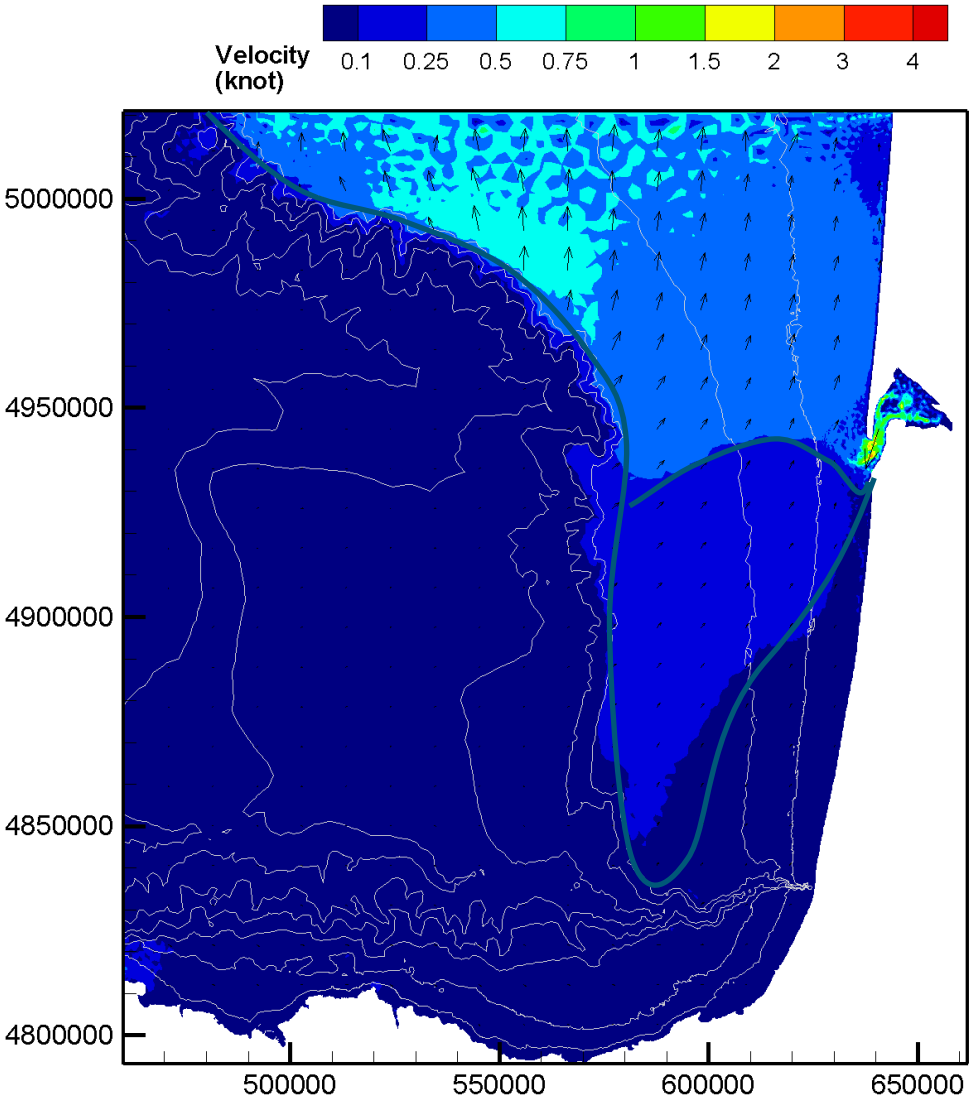
Velocity
(knot)
0.1
0.25
0.5
0.75
1
1.5
2
3
4
5000000
4950000
4900000
4850000
4800000
500000
550000
600000
650000
Model

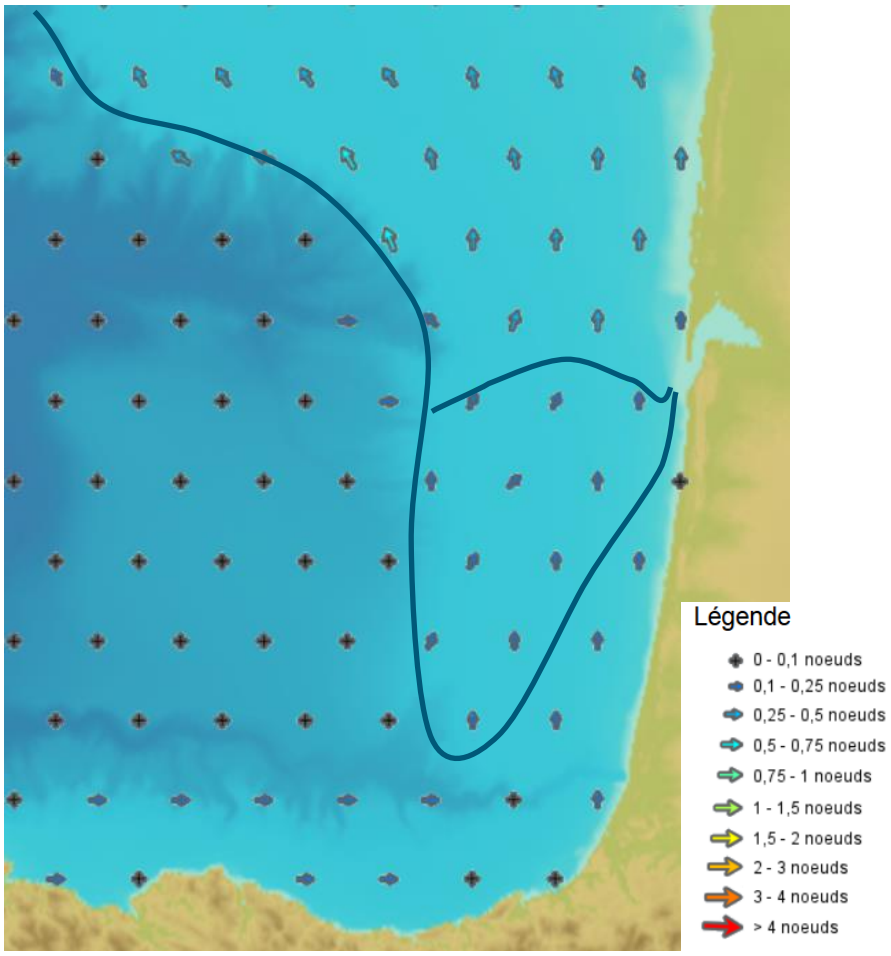

Nautical chart

Figure 67. Tidal currents 6h35' after high tide at Saint-Jean-de-Luz – Spring tide: model on the top, nautical SHOM chart on the bottom

Tidal currents are very low offshorer the continental shelf and along the Spanish coast. They are typically higher on the continental shelf along the French coast, with :

- a North-north-east to east direction during the ebb;
- a North to North-North-West direction at low tide ;
- a South to South-South-West direction at high tide;
- a West to South-West direction during the flow.

The tidal currents (intensity and direction) are correctly represented by the model.

5.4.3. Conclusion

The calibration of the model with respect to sea level is very good. Tidal current, intensity and direction are correctly represented by the model. Along the Spanish coast, tidal currents are very low and near the surface the meteorological conditions and the general oceanic circulation will predominate. The calibration of the model with respect to tidal current can therefore be considered satisfactory.

5.5. MODEL EXPLOITATION

5.5.1. Methodology

After validation, the model was run over a 19 years period in order to provide time series of sea level and depth-averaged currents. Surface and bottom current intensities were computed using a power law applied to the 2D-averaged velocity. According to bibliographic research carried out, different power laws can be applied.

In Ref. [8], the tidal current velocity throughout the water column is given by the following empirical formula:

$$U(z) = \left(\frac{z}{0.32h}\right)^{\frac{1}{7}} \bar{U} \quad for\ 0 < z < 0.5h \qquad \text{(Eq. 1)}$$

$$U(z) = 1.07\bar{U} \quad for\ 0.5h < z < h$$

Where $\bar{U} =$ depth-averaged current velocity and $h =$ water depth. This equation has been compared with a wide variety of in-situ measurement in various conditions. The fit is good with 96% of the date lying within 10% of the curve.

In their article (Ref. [9]), Lewis et al. characterised the velocity profile at tidal-stream energy sites always using the power law $U(z) = \left(\frac{z}{\beta h}\right)^{\frac{1}{\alpha}} \bar{U}$ but varying the α (power law) and β (bed roughness) coefficients. The analysis conditions are not the same as for our study (they focus on areas of strong tidal current) but nevertheless, their results show that the power law permits the correct representation of the vertical velocity profile, except near the surface (see Figure 68).

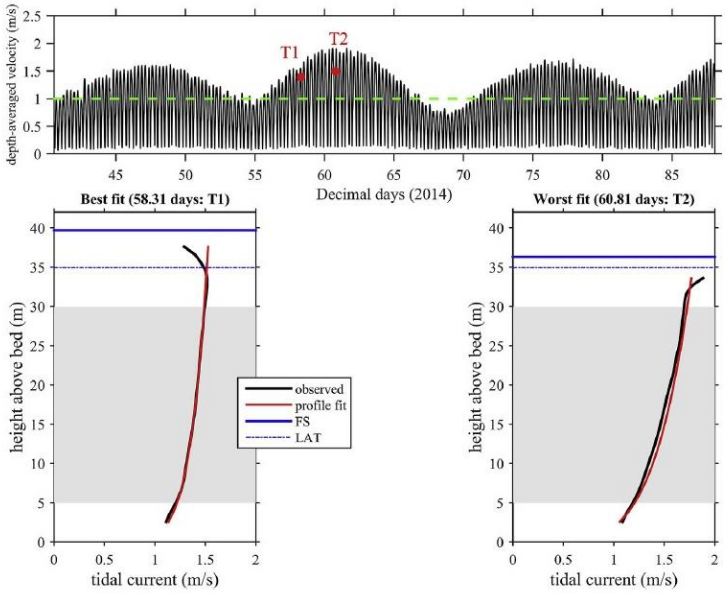

Fig. 3. The depth-averaged velocity time-series (top panel) measured at site A. Two examples (T1 and T2) of the velocity profile fit are shown in the bottom panels: Best fit (T1) with an AES of 0.00 m^2/s on the left hand bottom panel, and the least-accurate profile fit (T2) with an AES of 0.03 m^2/s on the right hand bottom panel. The free surface (FS) is shown in the velocity profiles (bottom panels), and grey shaded area indicating the maximum potential swept tidal turbine area, assumed as 5 m above the bed and 5 m below the Lowest Astronomical Tide (LAT).

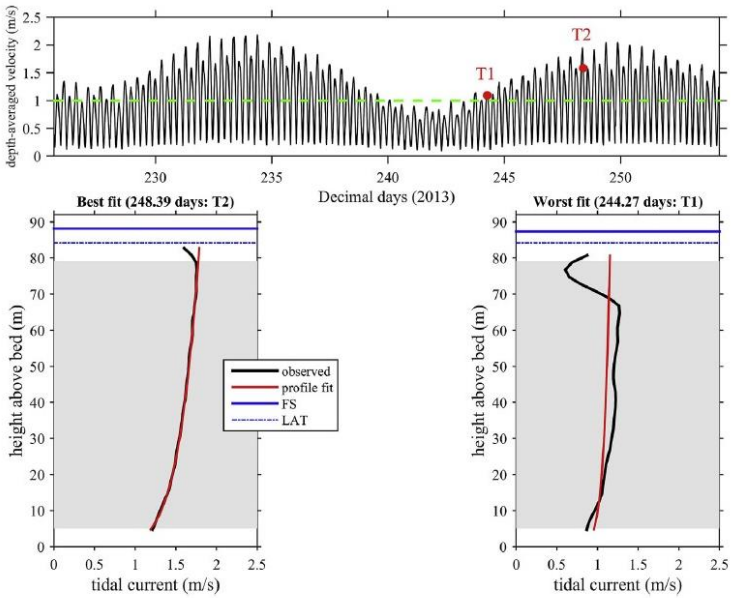

Fig. 4. The depth-averaged velocity time-series (top panel) and velocity profile fit examples for the site B; the least-accurate profile fit (T1) with an AES of 2.35 m^2/s, and the best profile fit (T2) with an AES of 0.00 m^2/s. Potential swept area is shown as grey shaded area in bottom panels and the green line in the top panel shows 1 m/s, above which velocity profile fits are analysed. (For interpretation of the references to colour in this figure legend, the reader is referred to the web version of this article.)

Figure 68. Examples of fit between power law and measurement – Ref. [5]

Figure 69 presents velocity profiles for conditions representative of the study along the studied area (depth-averaged velocity of 0.1 m/s and a water depth of 30 m) for different power laws.

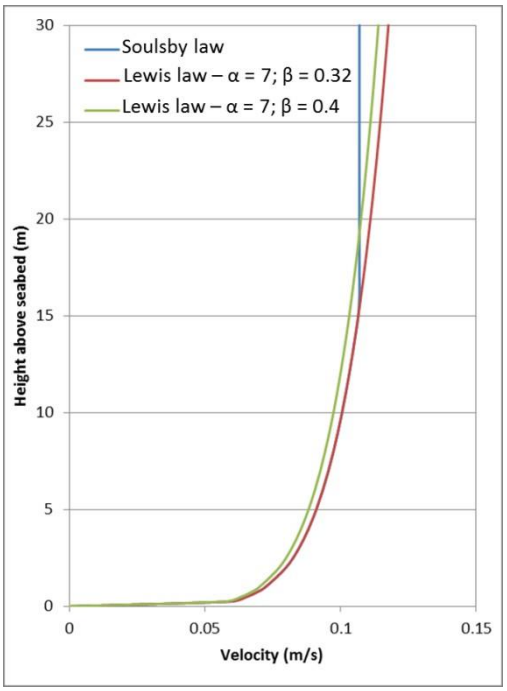

Figure 69. Velocity profiles for conditions representatives of the study area

The difference of intensity of velocity at the surface between the blue and red lines is in the order of 10%.

In agreement with Red Penguin Associates and INELFE, the red line (Lewis Law - α=7, β = 0.32) was used in the model. The slight overprediction of the results in consequence of the selected power law adds a degree of conservatism to the study outputs.

5.5.2. Outputs

The analysis of water levels and currents was carried out at the same points as for the wave propagation study as shown in Figure 70.

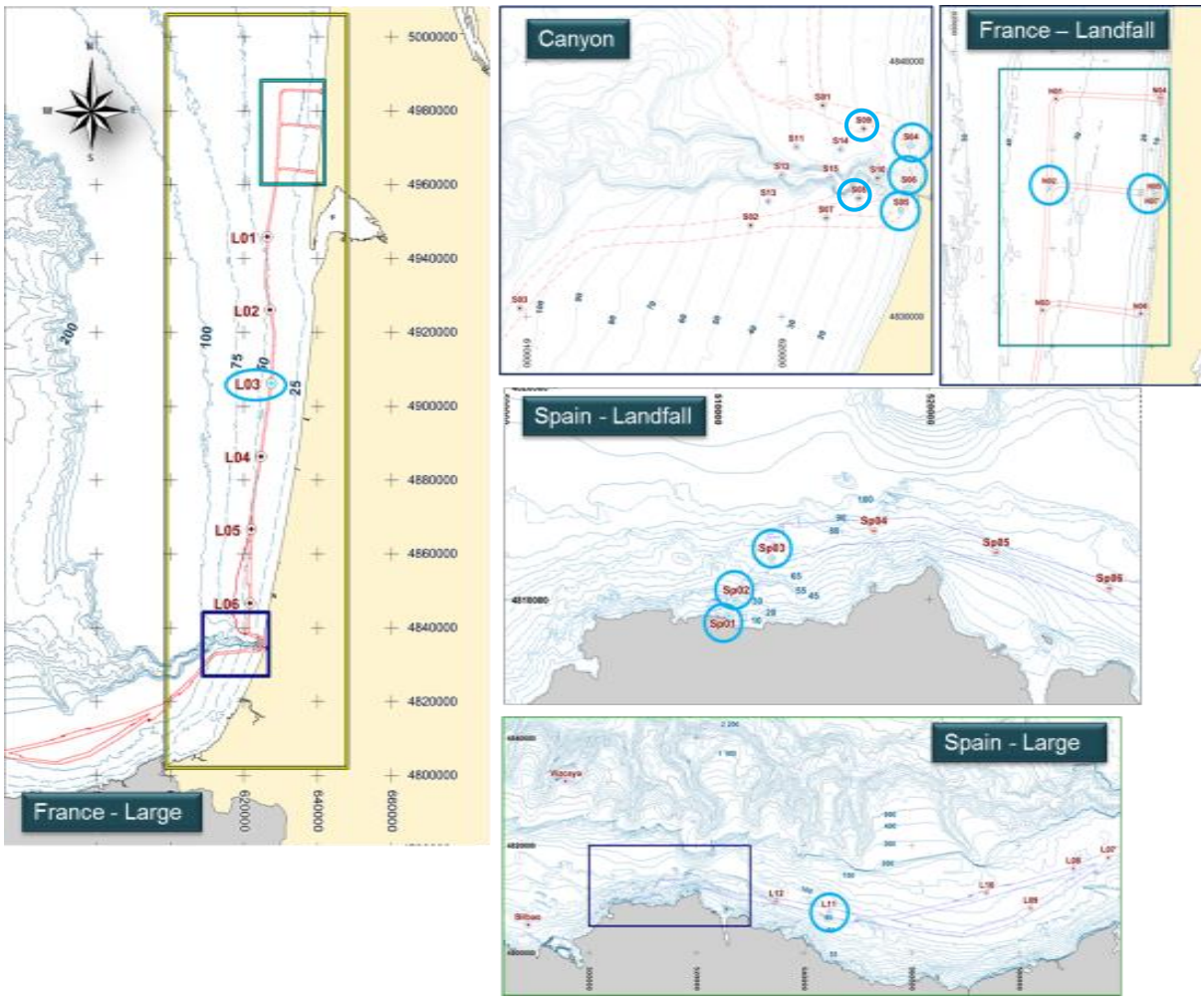

Figure 70. Output locations – Water levels / Current analyse

5.5.3. Water levels – results

5.5.3.1. Methodology

The extreme sea levels were assessed using a joint probability method that is described in detail in Ref. [10]. It consists first of extrapolating the extreme surges (positive and negative) following the methodology used for extrapolating extreme wave heights (see section 3.5.1.2.1). The distribution of the extreme surge peaks is included in the full distribution of surges. The astronomical tide is modelled by its empirical distribution over a saros period (18 years and 10 days), during which it is considered that the full range of astronomical tide conditions are observed. Then, the distributions of astronomical tide and surges are combined by a convolution operation in order to get the distribution of sea level, from which the distribution of extreme sea level peaks is derived.

5.5.3.2. Results – French coast

The results of the extrapolation of extreme surges and sea levels at the analysis points along the French coast are provided in Table 19 and Table 20.

The extreme sea levels are consistent along the probable cable route, varying between 2.46 and 2.52 m for the 1-year return period and 2.71 to 2.79 m for the 100-year return period. The extreme water levels are the highest in front of the landfall (points N02, N05, N07) and offshore (points L03).

The conclusions about the extreme surges are similar with values slighly higher in front of the landfall and offshore than around the canyon.

Table 19 - Results of statistical extrapolation of extreme surges - France

Return period (year)	Storm surge (m) *90% confidence interval*				
	L03	**N02**	**N05**	**N07**	
1	0.44	0.42	0.45	0.44	
	0.43-0.46	*0.41-0.43*	*0.43-0.46*	*0.43-0.46*	
10	0.55	0.52	0.55	0.55	
	0.51-0.58	*0.48-0.56*	*0.51-0.58*	*0.51-0.58*	
100	0.62	0.60	0.62	0.62	
	0.54-0.72	*0.51-0.71*	*0.54-0.72*	*0.54-0.72*	
Return period (year)	**Storm surge (m)** *90% confidence interval*				
	S04	**S05**	**S06**	**S08**	**S09**
1	0.39	0.39	0.39	0.39	0.39
	0.38-0.40	*0.38-0.40*	*0.38-0.40*	*0.38-0.40*	*0.38-0.40*
10	0.47	0.47	0.47	0.47	0.47
	0.44-0.50	*0.44-0.50*	*0.44-0.50*	*0.44-0.50*	*0.44-0.50*
100	0.55	0.55	0.54	0.55	0.55
	0.47-0.66	*0.46-0.66*	*0.46-0.65*	*0.46-0.66*	*0.46-0.66*

Table 20 - Results of statistical extrapolation of extreme sea levels - France

Return period (year)	Sea level (m MSL) *90% confidence interval*			
	L03	**N02**	**N05**	**N07**
1	+ 2.51	+ 2.52	+ 2.51	+ 2.51
	2.51-2.51	*2.52-2.52*	*2.51-2.51*	*2.51-2.51*
10	+ 2.67	+ 2.67	+ 2.67	+ 2.67
	2.67-2.67	*2.67-2.67*	*2.67-2.67*	*2.67-2.67*
100	+ 2.79	+ 2.79	+ 2.80	+ 2.80
	2.79-2.80	*2.79-2.79*	*2.79-2.81*	*2.79-2.81*

Return period (year)	Sea level (m MSL) *90% confidence interval*				
	S04	**S05**	**S06**	**S08**	**S09**
1	+ 2.46	+ 2.47	+ 2.46	+ 2.47	+ 2.47
	2.46-2.46	*2.47-2.47*	*2.46-2.46*	*2.47-2.47*	*2.47-2.47*
10	+ 2.60	+ 2.61	+ 2.60	+ 2.60	+ 2.61
	2.60-2.60	*2.61-2.61*	*2.60-2.60*	*2.60-2.61*	*2.61-2.61*
100	+ 2.71	+ 2.71	+ 2.71	+ 2.71	+ 2.71
	2.71-2.71	*2.71-2.72*	*2.71-2.71*	*2.71-2.71*	*2.71-2.72*

5.5.3.3. Results – Spanish coast

The results of the extrapolation of extreme surges and sea levels at the analysis points along the Spanish coast are provided in the Table 21 and Table 22.

The extreme sea levels are consistent along the spanish probable route cable: around 2.42 m for the 1-year return period and 2.66 m for the 100-year return period. These values are slightly lower than along the french coastline.

Table 21 - Results of statistical extrapolation of extreme surges - Spain

Return period (year)	Storm surge (m) *90% confidence interval*			
	L11	**Sp01**	**Sp02**	**Sp03**
1	0.38	0.38	0.38	0.39
	0.37-0.40	*0.38-0.40*	*0.38-0.40*	*0.38-0.40*
10	0.47	0.47	0.47	0.47
	0.44-0.50	*0.44-0.50*	*0.44-0.50*	*0.44-0.51*
100	0.54	0.55	0.54	0.55
	0.49-0.61	*0.47-0.66*	*0.47-0.65*	*0.47-0.66*

Table 22 - Results of statistical extrapolation of extreme sea levels - Spain

Return period (year)	Sea level (m MSL) *90% confidence interval*			
	L11	**Sp01**	**Sp02**	**Sp03**
1	+ 2.43	+ 2.42	+ 2.42	+ 2.42
	2.43-2.43	*2.42-2.42*	*2.42-2.42*	*2.42-2.42*
10	+ 2.56	+ 2.55	+ 2.55	+ 2.56
	2.56-2.56	*2.55-2.55*	*2.55-2.55*	*2.56-2.56*
100	+ 2.67	+ 2.66	+ 2.66	+ 2.66
	2.67-2.67	*2.66-2.66*	*2.66-2.66*	*2.66-2.67*

5.5.4. Current - results

For each analysis point, the currents have been studied 1 m below the surface and 1 m above the sea bottom as described in the previous section. Time series plots and currents roses for total currents and astronomical tidal currents are presented in APPENDIX 11.

All the analyses lead to the followings remarks:

- **Offshore from the French coast** (point L03), the near surface current speeds do not exceed 0.3 m/s. Most of the time the total current remains lower than 0.15 m/s and the current directions are variable. As observed during the calibration phase (Figure 64, Figure 65, Figure 66, Figure 67), the tidal currents remain weak (less than 0.15 m/s) as a consequence the residual currents are predominant. Due to the weak intensities, the mean tidal direction is difficult to derive. Near the seabed, the intensities are lower and do not exceed 0.15 m/s ; residual currents are predominant.
- In front of the **French landfall**, the influence of the tide is more visible with tidal current intensities higher than 0.15 m/s and total currents intensities higher than 0.35 m/s near surface. Offshore (point N02 - Figure 71), the 2 main directions are North-north-east and South-south-west both near surface and sea bottom. As we approach the coastline, the main direction rotates slightly to become North/South (point N05) for the 2 studied depths.
- Around the **canyon**, the total directions are directed alternately towards North and South for the 5 points (point S04, S05, S06, S08 and S09). The weakest total current appears at the head of the canyon (point S06) where the intensity is lower than 0.3 m/s near surface and 0.25 m/s above the sea bottom. The flow coming from the west is deviated by the canyon features towards the south; thus the total current is stronger to the south of the canyon (point S05 - Figure 72, point S08) where it can be higher than 0.35 m/s.
- **Offshore from the Spanish coast** (point L11 - Figure 73), the tidal currents are weak (less than 0.05 m/s near surface and less than 0.04 m/s above the seabed). Below the surface, the total currents remains higher than 0.3 m/s only 1% of the time. The main current direction is towards the South-East and less frequently towards the North-West.
- In front of the **Spain landfall**, offshore, the total direction (for the 2 studied depths) is mainly directed towards the East (point Sp03) and turns in direction East-South-East as the coast approaches (point Sp02). At the closest point to the coast (Sp01), 2 main directions appear (East-South-East and West-North-West). The intensity remains lower than 0.3 m/s near the sea bottom and can exceed 0.35 m/s close to the surface. The main part of the signal is due to residual currents.

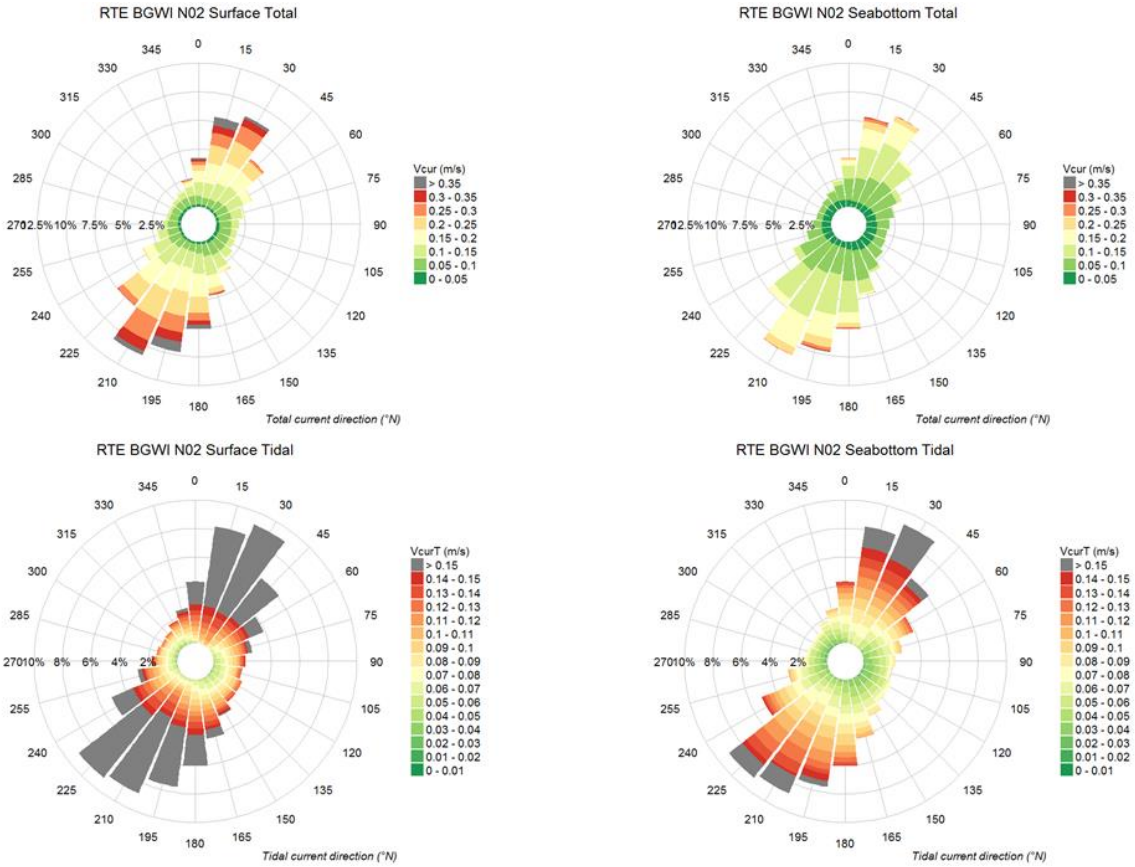

Figure 71. Point N02 – Offshore French landfall – Current roses 1 m below surface (left) and 1 m above the seabottom (right)

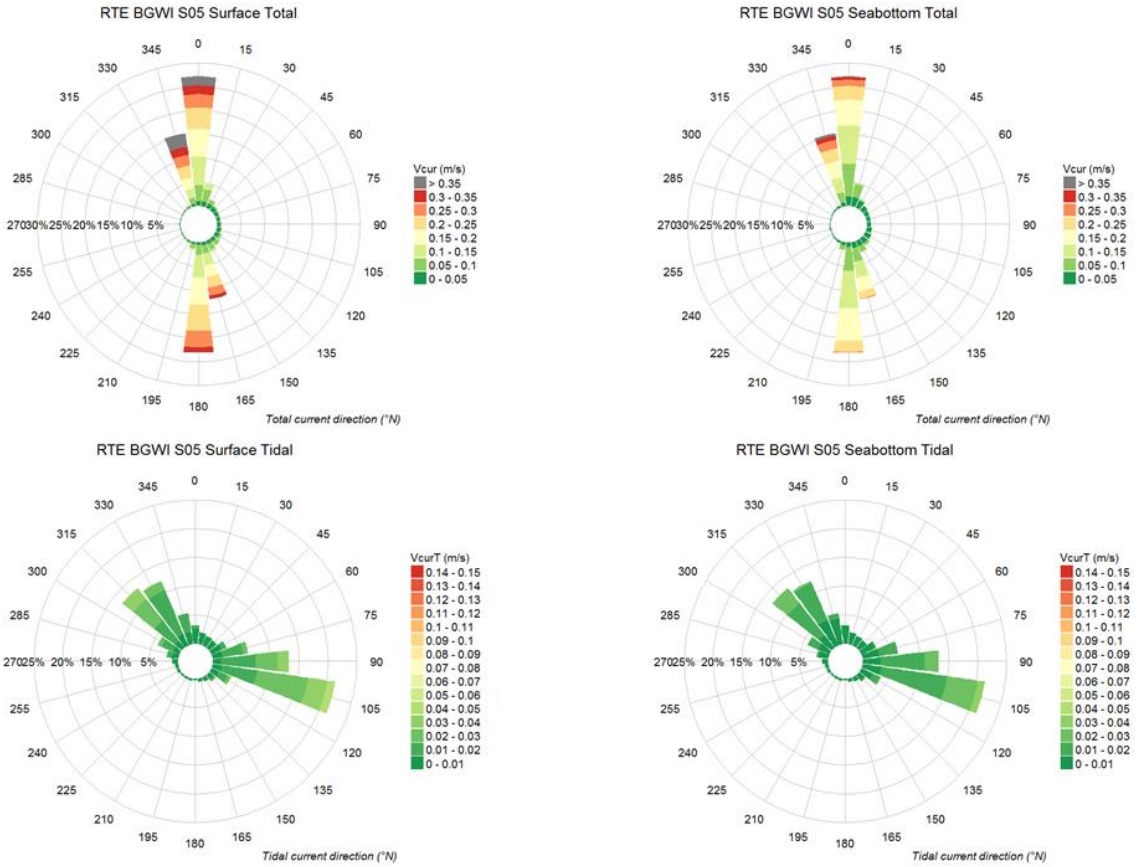

Figure 72. Point S05 – South of the canyon – Current roses 1 m below surface (left) and 1 m above the seabottom (right)

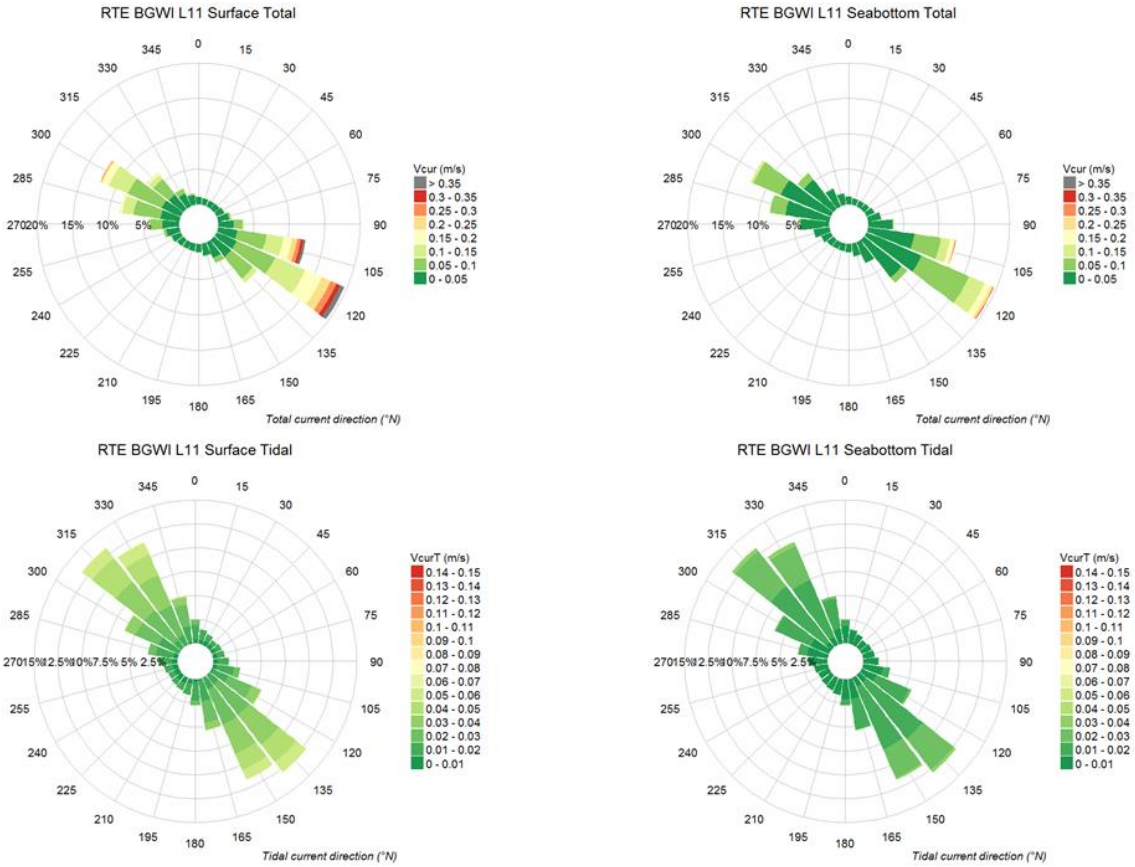

Figure 73. Point L11 – Spain - offshore – Current roses 1 m below surface (left) and 1 m above the seabottom (right)

oOo

6. PROPERTIES OF THE SEA WATER: TEMPERATURE AND SALINITY

6.1. PREAMBLE

Sea water is mainly composed of pure water (95%), salts and dissolved gas (N2, O2, CO2). Even if the total concentration of dissolved salts varies spatially, the proportion of main components remains almost stable (Figure 74).

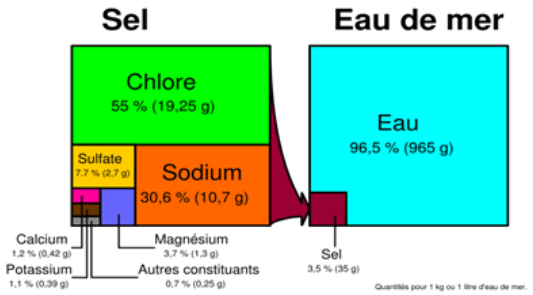

Anions		Cations	
Chlore Cl^-	18,9799	Sodium Na^+	10,5561
Sulfate SO_4^{--}	2,6486	Magnésium Mg^{++}	1,2720
Bicarbonate HCO_3^-	0,1397	Calcium Ca^{++}	0,4001
Brome Br^-	0,0646	Potassium K^+	0,3800
Fluor F^-	0,0013	Strontium Sr^{++}	0,0135

Figure 74. Sea water – composition (Salinity = 35)

The horizontal variations of the water properties are weaker than the vertical variations. The distribution of temperature, salinity and density evolves strongly according to the latitude (North-South) and the depth.

The ocean temperature varies between -1.9°C (≈ freezing temperature of sea water) and 30°C. Mean temperature of the global ocean is 4°C. As for salinity, near surface and the coast, the temperature can be lower or higher than the mean value (solar radiations). Throughout the water column and according to the region, thermoclines (water layers of strong temperature gradient) can appear permanently or seasonally (Figure 75).

The mean salinity of the global ocean is 34.78. At the surface (influence of atmospherical conditions), in the closed seas (Mediterranean basin, Black Sea, Red Sea…) and in coastal areas, the salinity can be lower or higher than the mean value. Salinity does not vary greatly with depth: below 100m, it is between 34.4 and 34.7. In the Atlantic Ocean, the mean salinity is around 36.5.). Throughout the water column and according to the region, haloclines (water layers of vertical strong salinity gradient) can appear permanently or seasonally. Generally, it is linked to the presence of the thermocline.

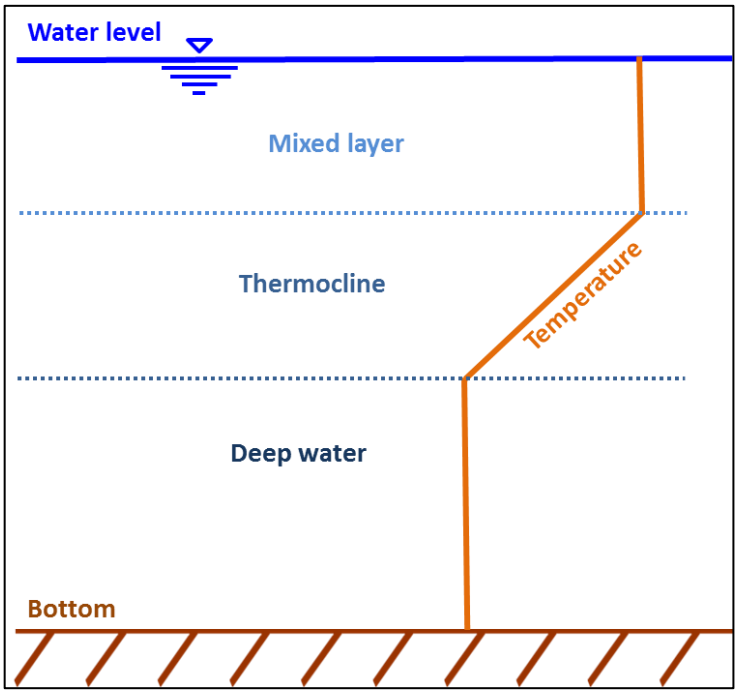

Figure 75. ***Vertical temperature profile scheme***

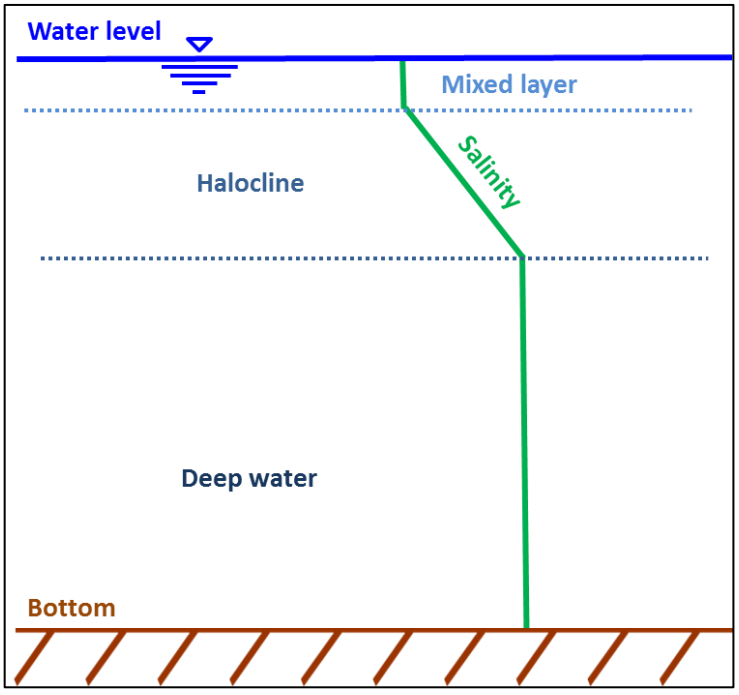

Figure 76. ***Vertical salinity profile scheme***

6.2. DATA SOURCES

The properties of the sea water are characterized by the sea temperature and salinity analyses presented in the present chapter and in the APPENDIX 12.

The sea temperature and the salinity values come from the global re-analyze GLORYS2V3 (Ref.[7]) which provides 3D daily mean fields of temperature and salinity. This modelling is based on a global ocean model and data assimilation. The horizontal resolution is 1/4° and the vertical resolution is 75 levels.

The sea temperature and salinity values are extracted in 5 locations along the possible cable route from 1993 to 2014.

6.3. OUTPUT LOCATIONS

Considering the source resolution, the 5 output points are located as shown in Figure 77:

- One point along the proposed cable route, about 10 km in front of the French landfall area (point TS01);
- One point along the cable between the French landfall area and the Capbreton canyon, 10 km offshore (point TS02);
- One point in the canyon area (point TS03);
- One point along the proposed cable route, about 10 km offshore the Spanish coast (point TS04);
- One point along the proposed cable route, about 5 km in front of the Spanish landfall area (point TS05).

The coordinates of the analysed points are specified in Table 23.

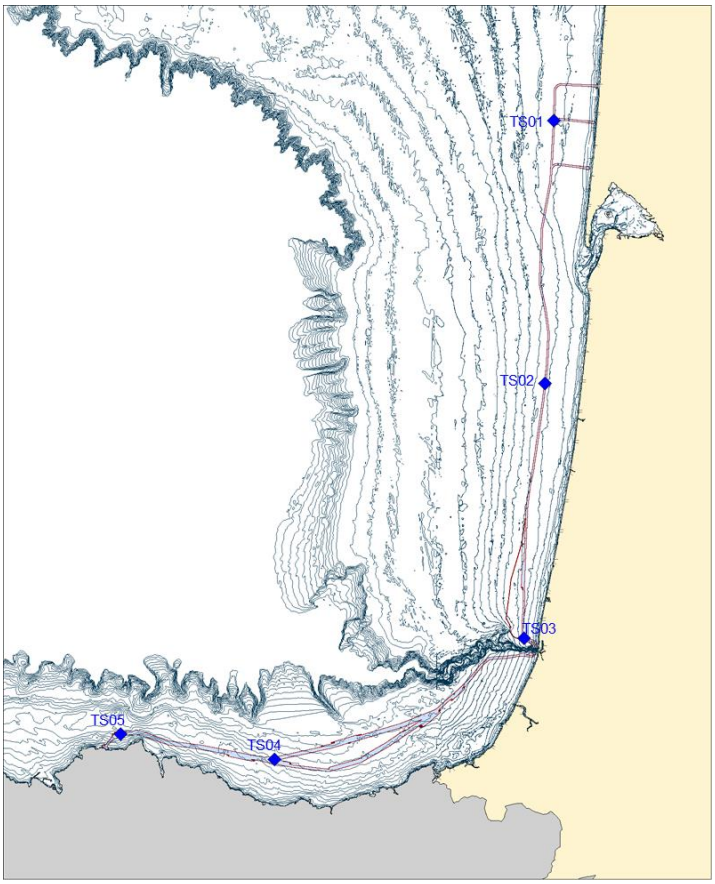

Figure 77. Temperature/salinity analysis - Output location

Table 23 – Coordinates (WGS84 - UTM30N) of the output points

Point	X	Y	Z (m MSL)	Area
TS01	629 605.100	4 975 975.450	-36	Large / Landfall - France
TS02	627 278.940	4 906 189.420	-47	Large - France
TS03	621 638.230	4 838 416.040	-41	Canyon
TS04	514 587.320	4 812 882.840	-108	Large - Spain
TS05	555 425.140	4 806 162.730	-87	Landfall - Spain

6.4. TEMPERATURE ANALYSIS

For each point, the followings analyses have been performed for both temperature and salinity:

- Minimum, maximum and mean throughout the water column during the entire period of extraction (1993-2014);
- Monthly minimum, maximum and mean throughout the water column;

Figure 78 presents the minimum temperatures (green colors), the mean temperatures (red colors) and the maximum temperatures (blue colors) throughout the water column and between 1993 and 2014. The main conclusions are summarised below:

- The **mean** temperature is fairly homogeneous along the possible cable route (maximum of 1°C of difference between the points near the surface and 0.5°C at -36 m).
- Close to the surface, the **mean** temperature varies between 15.8°C (Point TS01) and 16.7°C (Point TS05) whereas they are around 14°C at -36 m MSL;
- The **minimum** temperatures are globally higher along the Spanish coast (points TS04 and TS05) than offshore the French coast. Near the surface, they vary between 8.4°C (TS01) and 11.2°C (TS04).
- The vertical temperature profile remains homogeneous throughout the water column: point TS03 (10.5 / 11°C - canyon), point TS04 (≈11 / 11.2°C – Spanish coast) and point TS05 (10.5 / 11.5 °C - Spanish coast);
- The **maximum** vertical temperature profiles are heterogeneous for each point with a decrease of the temperature with depth and a difference of more than 7°C between the surface and the bottom. The mixing layer (top layer) is thin.
- Close to the surface, the **maximum** temperature varies between 25.7°C (Point TS04) and 26.8°C (Point TS03) whereas they are between 19.8°C (TS02) and 21.7°C (TS04) at -36 m MSL;
- The temperatures appear cooler along the French coast (TS01 and TS02) than along the Spanish coast.

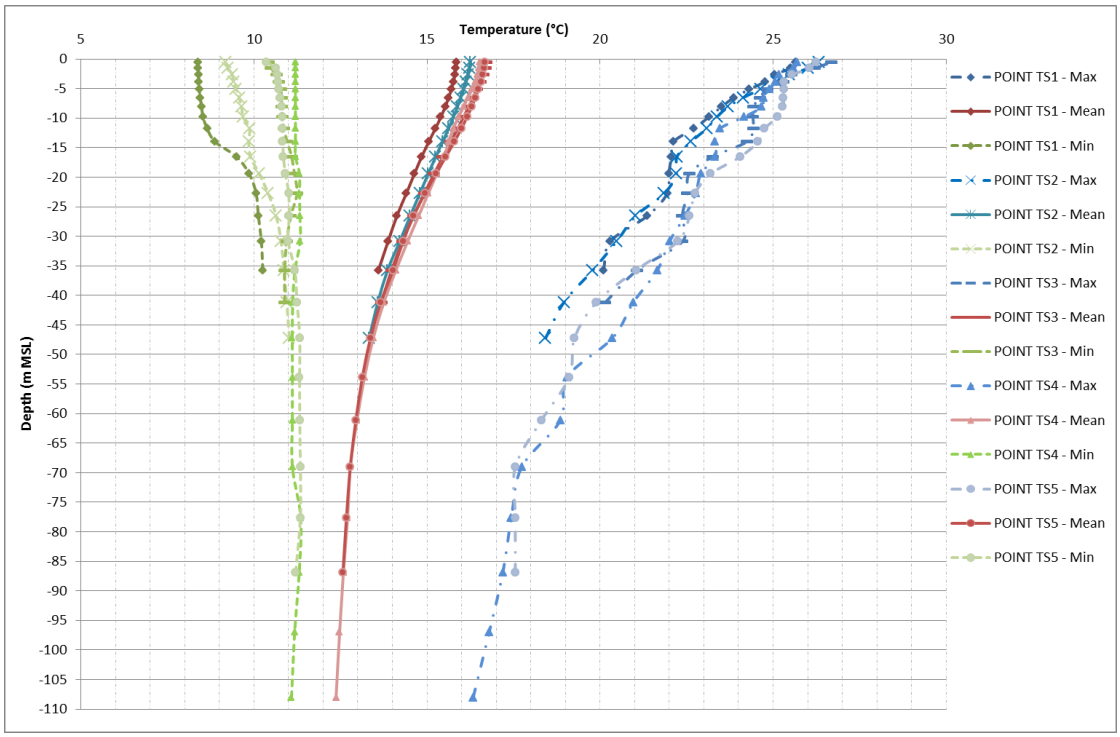

Figure 78. Temperature – Maximum, Minimum, Mean along the water column (1993-2014)

The monthly mean,minimum and maximum temperature are presented for each point in APPENDIX 12.

For each point, the main conclusions are proposed hereafter:

<u>POINT TS01 (French landfall):</u>

- The **mean** temperature profiles are clearly subject to strong seasonal variability:
  - From November to February (winter), the vertical temperature profiles are homogeneous with water cooler in the bottom layers. The difference of temperature between the surface and the bottom is up to 1°C in December;
  - From April (spring season), the temperature profile begins to change with an increase of the near surface temperature; the top layers (mixing layer) become warmer than those of the bottom. This temperature gradient increases until August where the mean surface temperatures can reach 21.5 °C and the bottom ones are around 14°C. The thermocline (layer of temperature gradient) is thick along the vertical;
  - In the surface layers, the temperatures vary between 10.8°C in February and 21.5°C in August. In the bottom layers, the temperatures are lower than 12°C in March/April and reach almost 16°C in October.
- The same seasonal trend is observed for the **maximum and minimum** temperature profiles. However, the thermocline is more marked in summer for the minimum temperature profiles with a homogeneous temperature from the surface to around -6 m MSL, then a decrease of the temperature and near the bottom an homogeneous layer again. The maximum temperatures decrease from the top to the bottom layers.

<u>POINT TS02 (French coast):</u>

- The variabilty of the temperature is the same than at Point TS01 with a similar seasonal variation;
- The vertical temperature profiles are consistent with Point TS01 except near the surface where the temperatures are slightly higher (almost 22°C in August and around 11.5°C in February for the mean temperature).

POINT TS03 (Canyon):

- The variabilty of the temperature is the same is at the previous point with a similar seasonal variation;
- The temperature is slightly higher for all the months, especially in the upper layers;
- Regarding the minimum and maximum temperature profiles, the depth of the upper level of the thermocline may vary according to the month by comparison to points TS02 and TS01. For example, in August, the upper limit of the thermocline is located around -1.5 m MSL at Point TS03 and -5 m MSL in Point TS02;
- In the surface layers, the mean temperatures vary between more than 12°C in February and 22.3°C in August. In the bottom layers, the temperatures are around 12.3°C in April and around15.8°C in October/November.

POINT TS04 (Spanish coast):

- The seasonal variability remains consistent with the other output points;
- In the surface layers, the mean temperatures are higher than 12°C in February and around 21.8°C in August. In the bottom layers, the temperatures vary between 12°C and around13.3°C;
- Even where the water depth reaches 100m MSL, the minimal temperatures in the bottom remain between 11 and 11.5°C which is in the same order of magnitude as points TS02 and TS03;
- However, the maximum temperatures are cooler near the bottom (13°C to around 16.3°C) than at the others points, which is to be expected, given the larger water depths.

POINT TS05 (Spanish landfall):

- The seasonal variability remains consistent with the other output points;
- In the surface layers, the mean temperatures are higher than 12°C in February and higher than 22°C in August. In the bottom layers, the temperatures vary between 12°C and around13.8°C;
- The minimal temperatures in the bottom remain between 11 and 11.5°C which is in the same order of magnitude as points TS02, TS03 and TS04. Near the surface, the minimal temperature is globally higher than at the others places and reaches 20°c in August;
- The maximum temperature varies between 13 and 16°C near the bottom as at point TS04.

6.5. SALINITY ANALYSIS

Figure 79 presents the vertical profiles for minimum (green), mean (red) and maximum (blue) salinity between 1993 and 2014. The main conclusions are summarised below:

- The maximum salinity profiles are homogeneous for each point and do not exceed 35.8;
- A decrease of the minimum and mean salinity in the upper layers of the water column clearly appears for the point TS01 located between the Gironde estuary and the Bassin d'Arcachon and the point TS02 near the Bassin d'Arcachon. It is worth noting that the freshwater influx can come from the Gironde river and various streams located in the bassin d'Arcachon;

- Close to the surface, the mean salinity varies between 33 (Point TS01) and 35.1 (Point TS04) whereas they are between 35.2 (TS01) and 35.4 (TS05) at -36 m MSL;
- The salinity appears higher along the Spanish coast (TS04 and TS05) where it is less affected by the fresh water supply, and where the water depth is deeper.

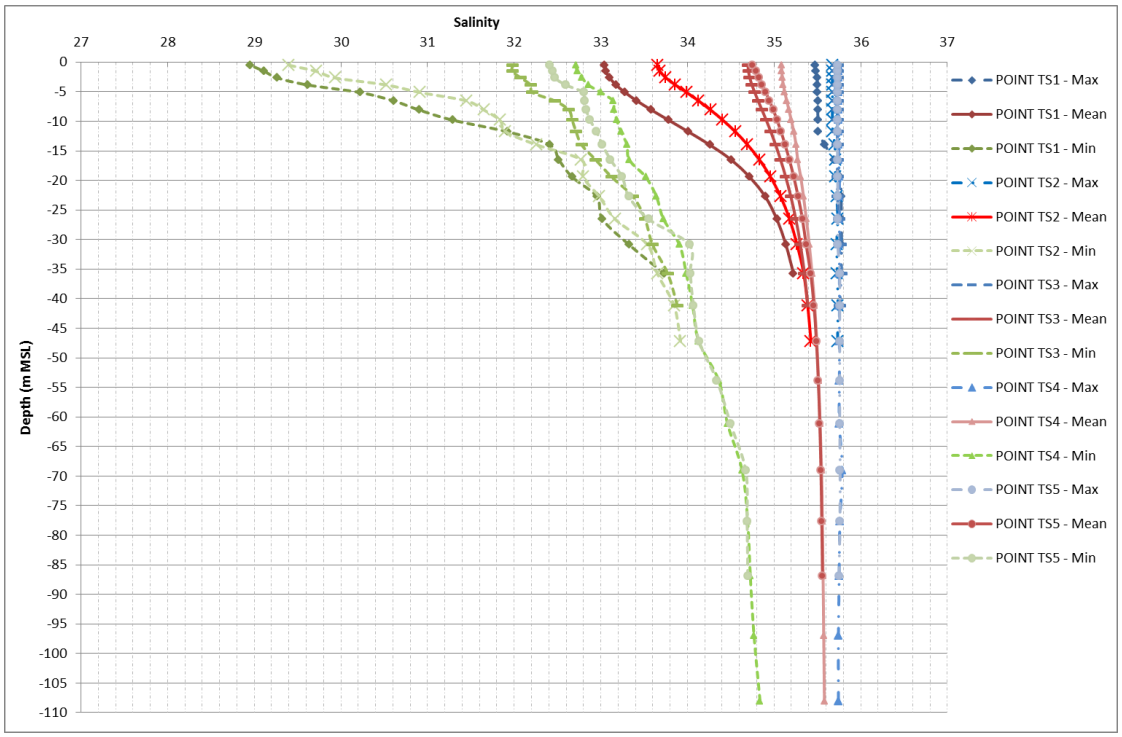

Figure 79. Salinity – Annual Maximum, Minimum, Mean along the water column (1993-2014)

The monthly mean,minimum and maximum salinity are presented for each point in APPENDIX 12 and the main conclusions drawn from the assessment are presented below:

For each point, the main conclusions are proposed hereafter:

POINT TS01 (French landfall):

- The water column can be divided into 2 parts: the top layers (mixing layer) where the mean salinity is different according to the months and the bottom layers where the mean salinity profiles are consistent from one month to another. A halocline is observed, with top level situated around -15m MSL;
- From September to January (autumn and beginning of winter), the mean vertical salinity profiles are slightly heterogeneous with values between 33.7 and 34.5 near the surface and 35 to 35.1 in the bottom (-36 m MSL);
- From March to July (spring and beginning of the summer), the mean salinity profiles are impacted by a strong decrease of salinity in the surface layers (from the surface to around 10 m depth – presence of a halocline). Here, the salinity drops to 31.5 in May and July whereas near the bottom the values of salinity are around 35.1 / 35.2. This decrease can be explained by the fresh water influx from the Gironde Estuary;
- February and August appear as “intermediate” months;
- The maximum salinity profiles show less differences near the surface (33.4 in July to 35.5 in November) than the mean profiles. The profiles become homogenous when the water depth is deeper (35.5 to 35.8 at -36 m MSL);
- The minimum salinity profiles are heterogeneous for each month.

POINT TS02 (French coast):

- The trend of the mean vertical salinity profiles is the same than for the point TS01: the mixing layer on the top of the water column and below -15 m MSL, homogeneous profiles;
- The mean salinity values vary between 32.6 and 35.8 at the surface and fluctuate around 35.2 below -36 m MSL;
- Unlike point TS01, the maximum vertical salinity profiles are homogeneous over depth and are similar for each month. The values are between 35.3 and 35.8 for the whole depth;
- The minimum salinity profiles are heterogeneous for each month especially in the top layers.

POINT TS03 (Canyon):

- Near the canyon, the behavior of the mean salinity profiles is different from points TS01 and TS02. The impact of the seasons is less clear and the profiles less contrasted according to the month;
- From November to February (winter), the vertical profiles are homogeneous (35.1 to 35.2);
- From April to September, the decrease of salinity near the surface appears (34 to 34.4) but it is less apparent than at point TS01 and TS02 whereas the bottom values remains similar to the other profiles (around 35.3);
- March and October are “intermediate” months;
- As point TS02, the maximum salinity profiles are homogeneous over depth and similar for each month. The values are between 35.2 and 35.8 for the whole depth.

POINT TS04 (Spanish coast):

- The salinity (mean, maximum and minimum) is globally higher than along the French coast (points TS01, TS02 and TS03) for all depths and months;
- The mean salinity values vary between 34.5 (August) and 35.5 (January) at the surface and fluctuate around 35.55 in the deep waters;
- The maximum salinity profiles display vertical homogeneity and show limited seasonal variability. The values are around 35.6 (surface) and 35.75 (bottom);
- The minimum salinity profiles are less heterogeneous than along the French coast.

POINT TS05 (Spanish landfall):

- The salinity (mean, maximum and minimum) is globally higher than along the French coast (points TS01, TS02 and TS03) for all depths and months; it is weaker than at point TS04 (Spanish coast) near the surface;
- The mean salinity values vary between 34.25 (May) and 35.25 (January) at the surface and fluctuate around 35.55 in the deep waters;
- The maximum salinity profilesdisplay vertical homogeneity and show limited seasonal variability. The values are around 35.5 / 35.6 (surface) and 35.7 (bottom).

oOo

REFERENCES

[1] http://www.geo.euskadi.eus/geograficos/batimetrias-marinas-pais-vasco-ano-2009/s69-geodir/es/

[2] http://geology.uprm.edu/MorelockSite/morelockonline/1_image/duxburyseafl.htm

[3] Mazas, F., Hamm, L., 2011. A multi-distribution approach to POT methods for determining extreme wave heights. *Coastal Engineering*, **58**, 385-394.

[4] Bernardara, P., Mazas, F., Kergadallan, X., Hamm, L., 2014. A two-step framework for over-threshold modelling of environmental extremes. Nat Hazards Earth Syst Sci 14, 635–647.

[5] Mazas, F., Garat, P., Hamm, L., 2014. Questioning MLE for the estimation of environmental extreme distributions. *Ocean Engineering* **92**, 44–54. doi:10.1016/j.oceaneng.2014.09.034

[6] https://www.aviso.altimetry.fr/fr/donnees/produits/produits-auxiliaires/maree-oceanique-fes/description-fes2012.html

[7] Barnier et al. 2006 – Impact of partial steps and momentum advection schemes in a global ocean circulation model at eddy permitting resolution. Ocean Dynamics, DOI 10.1007/s 10236-006-0082-1.

[8] Soulsby, 1997 – Dynamics of marine sands: A manual for practical applications. Thomas Telford.

[9] Lewis et al. 2017. Characteristics of the velocity profile at tidal-stream energy sites. Renewable Energy 114(2017) 258-272

[10] Mazas, F., Kergadallan, X., Garat, P., Hamm, L., 2014. Applying POT methods to the Revised Joint Probability Method for determining extreme sea levels. Coastal Engineering 91, 140–150.

APPENDIX 1
ROUTE POSITION

"Name"	"X" UTM 30 N WGS 84	"Y" UTM 30 N WGS 84
"1"	640936.83278021	4985288.2390413
"2"	640506.68006666	4985455.5749806
"3"	640506.79550848	4985457.5845715
"4"	640506.71305004	4985457.5745736
"5"	640508.37046474	4985507.634384
"6"	640004.44218228	4985524.5609387
"7"	640007.2375235	4985479.8300435
"8"	638842.66044189	4985531.8594531
"9"	629929.49645874	4985929.2985555
"10"	629920.55796352	4985729.51922
"11"	629720.69518947	4985735.0081028
"12"	629458.86489555	4976296.5492737
"13"	628534.87681296	4960074.6012042
"14"	626270.00725187	4947745.5307507
"15"	625669.17380725	4932767.8894061
"16"	627120.02186528	4925800.3076372
"17"	628028.27687695	4919489.2622322
"18"	627524.94229528	4910408.5605826
"19"	626493.34594463	4901235.5277269
"20"	623787.85969359	4882728.3148164
"21"	623004.47974794	4879381.9259641
"22"	622220.26697202	4873054.5438844
"23"	621382.78604194	4852337.9706827
"24"	621507.24881574	4848218.6691546
"25"	621037.26042841	4841651.2559325
"26"	621053.01823686	4839407.6526115
"27"	621373.63315477	4838091.7104677
"28"	623279.80848898	4837205.9007717
"29"	623277.16981881	4836683.897024
"30"	623294.65100872	4836676.4385422
"31"	622365.10522708	4836653.4832147
"32"	622383.34503466	4835718.3435596
"33"	622867.88733718	4834937.7524467
"34"	619942.97092358	4833968.3397678
"35"	618378.72601479	4833759.3922985
"36"	618363.84226583	4833870.8996015
"37"	616322.74018141	4833598.2550975
"38"	614044.73499036	4833509.5031627

"39"	612431.93030451	4833325.8005548
"40"	611609.5392695	4832841.4491431
"41"	610632.00267405	4831948.7008595
"42"	610556.14915237	4832031.7739502
"43"	610017.72025738	4831540.0940302
"44"	607020.21567644	4827761.0132511
"45"	603980.79746895	4824746.7068045
"46"	597150.99552224	4818695.1985714
"47"	588878.49241166	4815369.8254415
"48"	570295.17944729	4809910.6166476
"49"	556481.39475722	4806847.8700608
"50"	551555.86335469	4806574.885626
"51"	551459.60961422	4806594.0317288
"52"	551439.96801311	4806483.2642752
"53"	536273.88959603	4809501.2899648
"54"	527599.66544304	4810622.33178
"55"	519580.71379872	4813404.9353891
"56"	513074.19842348	4813078.8617605
"57"	511488.58853211	4811160.6722024
"58"	511575.35955164	4811089.0767754
"59"	510865.31814516	4810230.0916194
"60"	510505.20563307	4809729.2035737
"61"	510258.34154653	4809495.0512347
"62"	510100.5325784	4809226.4958984
"63"	510324.17636739	4809204.630349
"64"	510613.41584776	4809154.9904531
"65"	510733.09603187	4808963.939341
"66"	510949.86278673	4808794.9237436
"67"	511004.71414298	4809204.4803796
"68"	510981.13927414	4809567.1565579
"69"	510976.07632574	4809698.9697277
"70"	511182.19769561	4809985.6113826
"71"	511883.66342402	4810834.1886572
"72"	511970.36023095	4810762.4832526
"73"	513380.50680154	4812468.4260129
"74"	519490.65268732	4812774.6336852
"75"	527455.61878903	4810010.8062543
"76"	536172.71308652	4808884.2555604
"77"	551330.80952632	4805867.8095492

"78"	551311.07722092	4805756.932118
"79"	560280.80769594	4803971.9354489
"80"	569972.47008492	4802857.7222438
"81"	578327.60480119	4805201.3752
"82"	585830.67168882	4809536.0928808
"83"	595661.31778341	4816239.5984017
"84"	604562.41809636	4824126.3230818
"85"	607654.73339502	4827193.1688342
"86"	610646.86993132	4830965.3410195
"87"	611128.81479288	4831403.6917945
"88"	611057.38104375	4831482.9356646
"89"	611053.51374277	4831487.2047957
"90"	611982.82864077	4832335.9820295
"91"	612634.6131573	4832719.8638915
"92"	614092.39597039	4832885.8501055
"93"	616376.42062777	4832974.9419711
"94"	618446.60580503	4833251.4356916
"95"	618431.63959763	4833362.9329966
"96"	619998.8777479	4833572.2703866
"97"	623855.18701227	4833513.3023894
"98"	623895.97095815	4833524.3901325
"99"	623880.33683737	4833649.6446373
"100"	623890.85853469	4833652.5140532
"101"	624092.34574006	4833707.2329154
"102"	624407.83998867	4833852.7432972
"103"	624691.8598496	4834015.1302438
"104"	625151.59040664	4835414.3754315
"105"	625218.55490816	4835663.2747687
"106"	625247.27518385	4835921.572193
"107"	625247.25044631	4836181.4392978
"108"	625207.41477252	4836439.3368036
"109"	625132.34460605	4836688.7960269
"110"	625023.40875705	4836925.4078652
"111"	624885.61245302	4837140.1541542
"112"	624874.2331879	4837157.9405338
"113"	624970.2890281	4837234.614927
"114"	624802.38714654	4837430.245107
"115"	624593.90746521	4837613.8877271
"116"	624362.06730698	4837767.0065602

"117"	624111.26995272	4837886.4422494
"118"	623849.62931321	4837969.2553931
"119"	621709.4039345	4838403.2270594
"120"	621452.74378495	4839457.0125644
"121"	621437.42300625	4841638.3085679
"122"	621907.65876891	4848210.3208539
"123"	621783.08055329	4852335.8411162
"124"	622619.31636088	4873021.8205451
"125"	623398.82075971	4879311.510297
"126"	624181.21120404	4882653.710002
"127"	626890.144218	4901184.1981748
"128"	627923.71132543	4910375.1273879
"129"	628429.88247754	4919506.8286566
"130"	627514.17322263	4925869.5835363
"131"	626070.84537459	4932801.1226416
"132"	626668.53715254	4947701.1097924
"133"	628932.82125868	4960026.8909154
"134"	629182.62911163	4964412.0383314
"135"	636521.21614309	4963480.4579519
"136"	636527.08718423	4963479.6981066
"137"	638019.27990556	4963290.2966587
"138"	638012.98832636	4963240.7067526
"139"	638508.96761492	4963177.6995775
"140"	638515.25094828	4963227.3994612
"141"	639135.01685141	4963301.0244751
"142"	639146.00031601	4963400.3942486
"143"	638565.63305692	4963624.1287081
"144"	638571.92463612	4963673.7186142
"145"	638075.90411834	4963736.7257893
"146"	638069.61253914	4963687.1358832
"147"	636571.63948096	4963877.2771805
"148"	629205.42062526	4964812.3368518
"149"	629858.59868948	4976279.642715
"150"	629861.33630979	4976378.0526839
"151"	638225.55794647	4975528.3156454
"152"	638227.21536117	4975528.2356617
"153"	639537.58721578	4975395.0727666
"154"	639530.29788942	4975345.5628442
"155"	639838.38736985	4975314.2792119

"156"	640027.01930397	4975286.5048653
"157"	640034.22617188	4975336.0047897
"158"	640299.69288315	4975448.5118892
"159"	640314.26329002	4975547.4117584
"160"	640092.5325369	4975731.7142442
"161"	640099.82186326	4975781.104191
"162"	639900.11576025	4975810.5282019
"163"	639603.19939884	4975840.722056
"164"	639597.83135421	4975804.4794331
"165"	639595.91007248	4975791.2121336
"166"	638265.9955669	4975926.28464
"167"	629872.38574114	4976779.0210679
"168"	630114.8795302	4985520.6617323
"169"	638824.78345146	4985132.2507923
"170"	639994.40698978	4985080.0014275
"171"	639992.74132923	4985030.0615926
"172"	640492.72809811	4985007.8161206
"173"	640493.91549969	4985057.7459575
"174"	640932.33879507	4985188.3293776
"175"	640936.83278021	4985288.2390413
"176"	595258.46706033	4817018.3398911
"177"	589157.49055341	4814565.8690845
"178"	570507.18010414	4809087.0242874
"179"	556597.61993257	4806002.9820353
"180"	554902.0846909	4805909.0111628
"181"	560412.53505857	4804812.4243698
"182"	569903.74921856	4803721.22648
"183"	577995.07463827	4805990.9044936
"184"	585378.04904957	4810256.2262997
"185"	595137.87983335	4816911.44165
"186"	595258.46706033	4817018.3398911
"187"	625097.29152195	4836169.9616341
"188"	625060.7789234	4836406.1535579
"189"	624991.72822327	4836635.5068737
"190"	624891.54121507	4836853.1725685
"191"	624759.39331439	4837059.1306463
"192"	624756.32586031	4837063.9696613
"193"	624657.40046629	4836985.0157322
"194"	624517.02321299	4837148.5024549

"195"	624350.35820808	4837295.3825579
"196"	624164.88443233	4837417.8176366
"197"	623964.26304061	4837513.4181774
"198"	623749.2526506	4837581.4243349
"199"	623166.370409	4837699.6502704
"200"	623681.01828905	4837460.5089469
"201"	623676.32640364	4836515.06139
"202"	623664.22150422	4836520.1703501
"203"	624389.38578914	4835895.2275554
"204"	624342.1700847	4834725.3356835
"205"	623396.86649461	4834702.2803763
"206"	623409.80422431	4834695.9716605
"207"	621172.18717862	4833954.3726108
"208"	623804.85437868	4833914.1208039
"209"	623845.86920821	4833925.3185247
"210"	623861.503329	4833799.9540423
"211"	624040.91640919	4833848.7141173
"212"	624339.11912231	4833986.2361251
"213"	624567.33935489	4834116.6895717
"214"	625007.78288211	4835457.3466848
"215"	625070.756395	4835691.1690909
"216"	625097.26678441	4835929.8705039
"217"	625097.29152195	4836169.9616341

APPENDIX 2

HOMERE DATABASE

APPENDIX 3

FRENCH COAST - WAVE ANALYSIS

APPENDIX 4

FRENCH COAST
WAVE COLOUR MAPS

APPENDIX 5

FRENCH COAST
EXTREME WAVE ANALYSIS

APPENDIX 6

SPANISH COAST - WAVE ANALYSIS

APPENDIX 7

SPANISH COAST
WAVE COLOUR MAPS

APPENDIX 8

SPANISH COAST
EXTREME WAVE ANALYSIS

APPENDIX 9

WINDS – FRANCE

APPENDIX 10

WINDS – SPAIN

APPENDIX 11

CURRENTS

APPENDIX 12

TEMPERATURE AND SALINITY